Interplay of Nuclear and New Physics with Low-Energy Neutrino Sources

Vishvas Pandey (विश्वास पाण्डेय)

Fermi National Accelerator Laboratory

CETUP* 2025, Lead, South Dakota, June-July, 2025

Neutrino Sources and Physics Scope

✦ $E_\nu \approx$ 10s of MeV

- **Pion decay-at-rest neutrinos**

  (SNS at ORNL, LANSCE at LANL, MLF at JPARC, F2D2 at FNAL, ESS, ..)

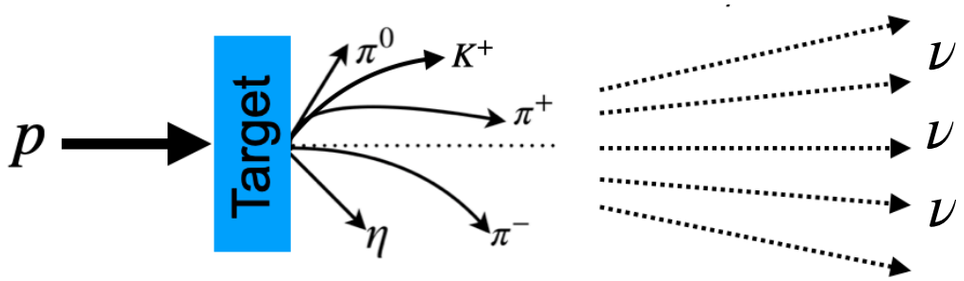

- **Core-collapse Supernova Neutrinos**

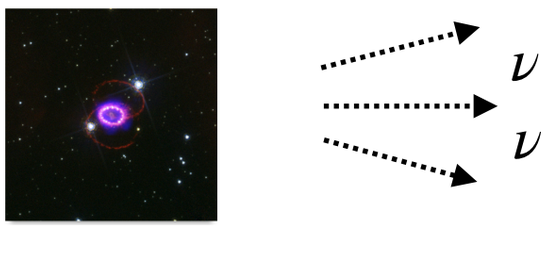

piDAR and Supernova Neutrino Energy Spectrum

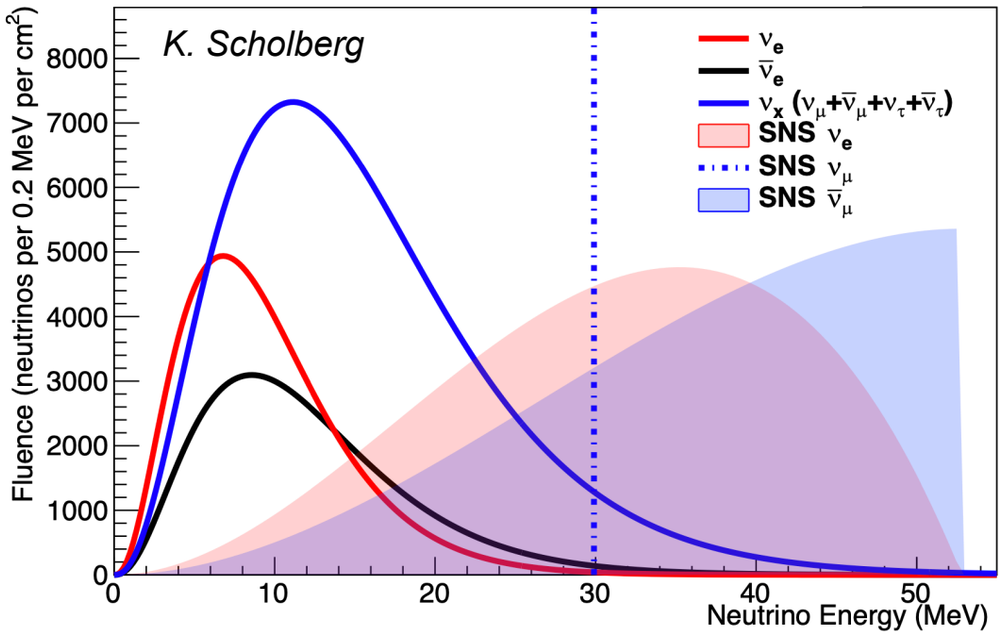

Neutrino Sources and Physics Scope

✦ $E_\nu \approx$ 10s of MeV

- **Pion decay-at-rest neutrinos**

  (SNS at ORNL, LANSCE at LANL, MLF at JPARC, F2D2 at FNAL, ESS, ..)

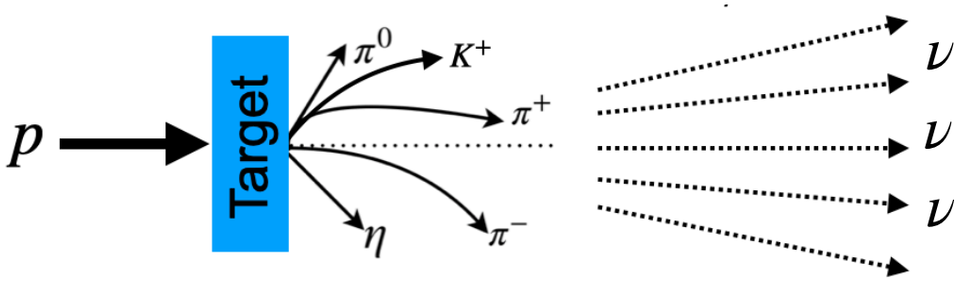

- **Core-collapse Supernova Neutrinos**

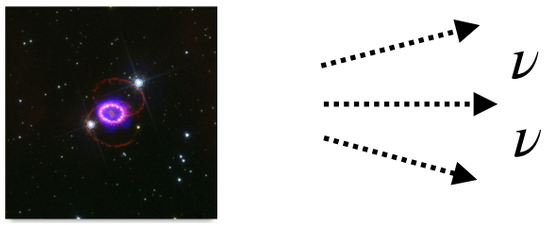

piDAR and Supernova Neutrino Energy Spectrum

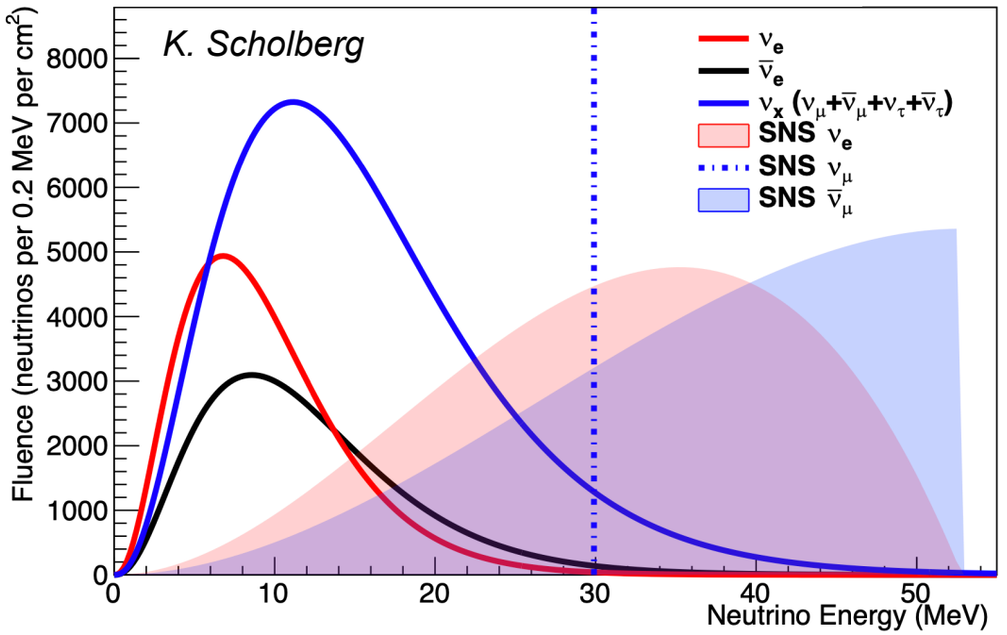

✦ 10s MeV scale physics in GeV scale ν beam

- **Pion decay-in-flight neutrinos**

  (BNB/NUMI/LBNF at FNAL, JPARC, …)

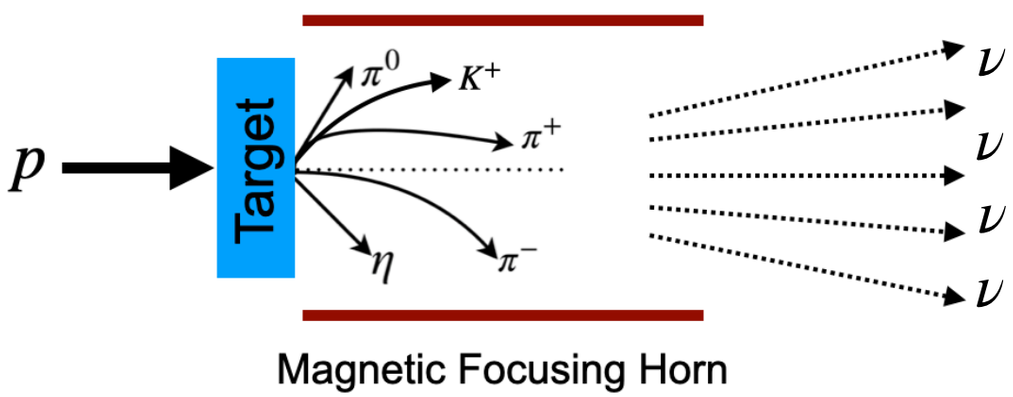

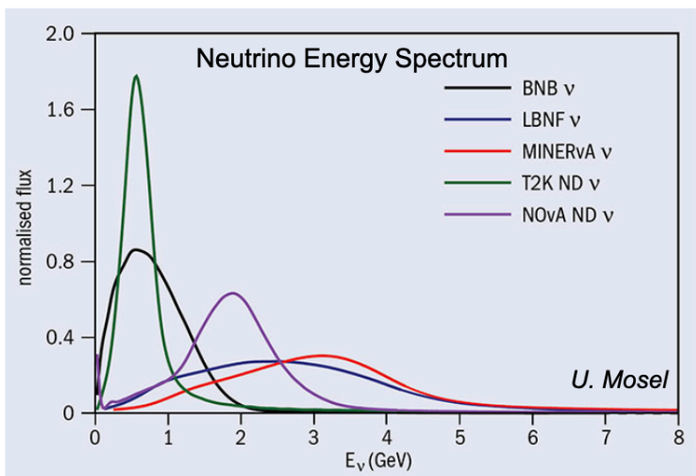

Kaon decay at rest

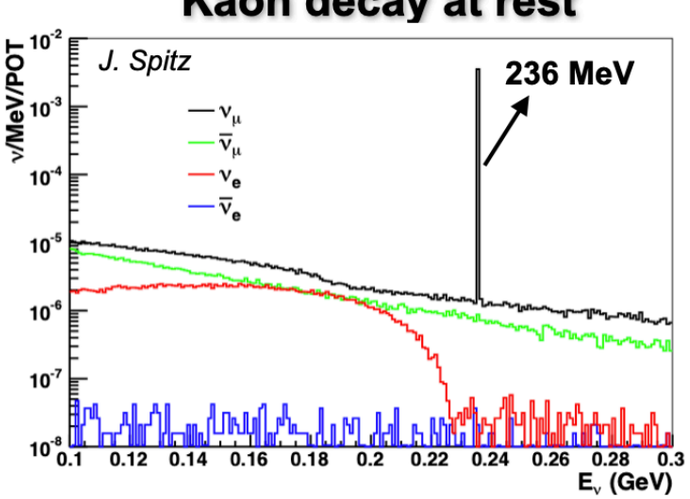

Neutrino Sources and Physics Scope

✦ $E_\nu \approx$ 10s of MeV

- **Pion decay-at-rest neutrinos**

  (SNS at ORNL, LANSCE at LANL, MLF at JPARC, F2D2 at FNAL, ESS, ..)

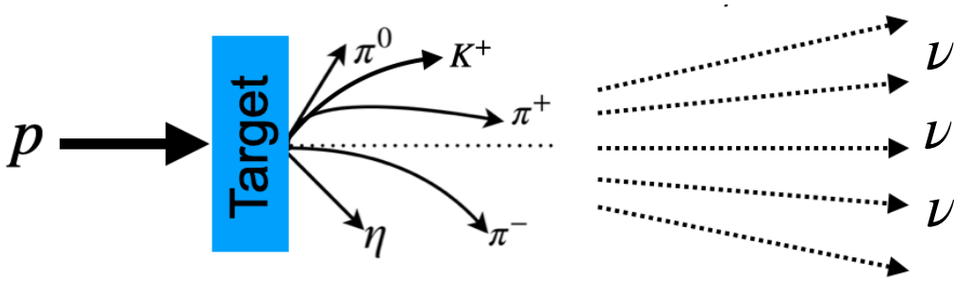

- **Core-collapse Supernova Neutrinos**

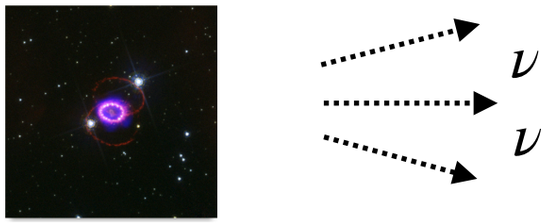

piDAR and Supernova Neutrino Energy Spectrum

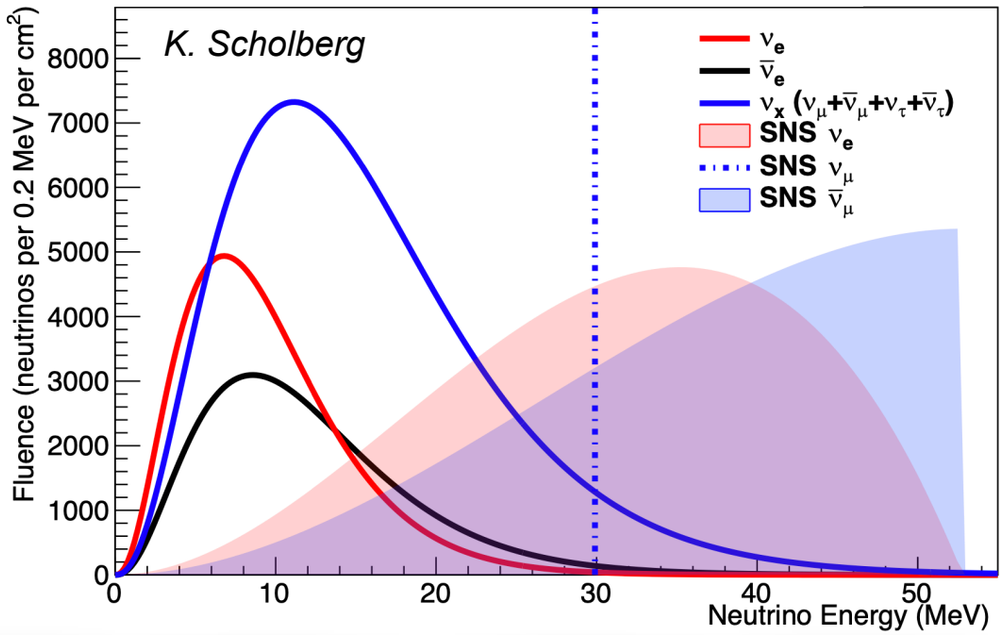

Neutrino physics, SM precision test, astrophysics, nuclear physics, BSM physics

✦ 10s MeV scale physics in GeV scale ν beam

- **Pion decay-in-flight neutrinos**

  (BNB/NUMI/LBNF at FNAL, JPARC, …)

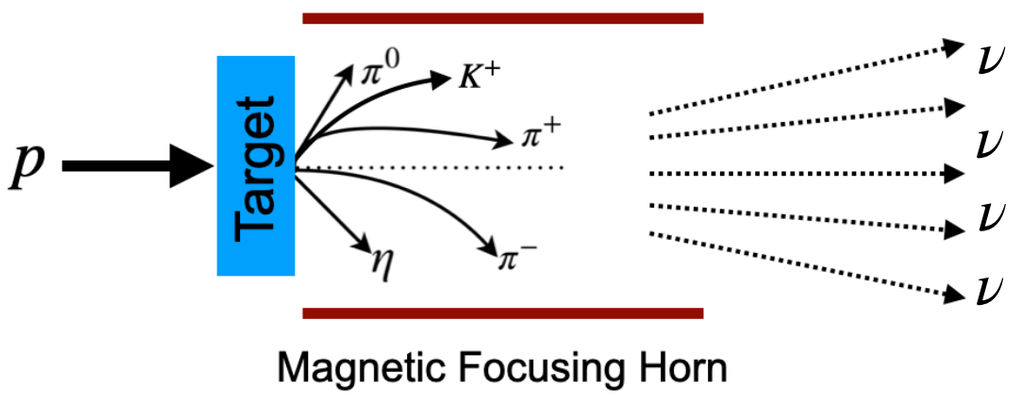

Magnetic Focusing Horn

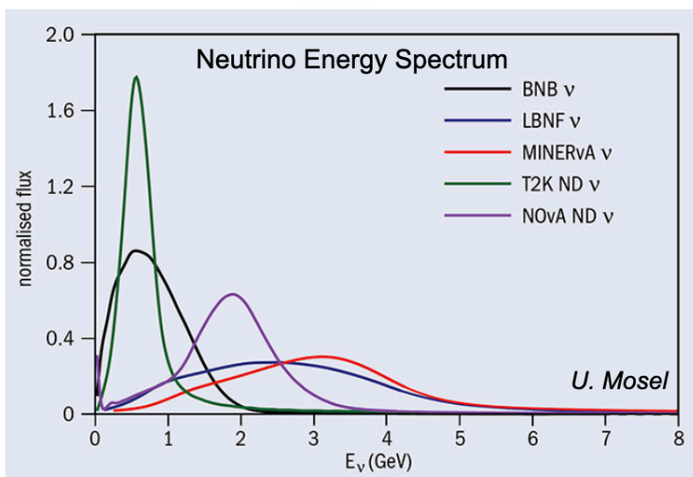

Kaon decay at rest

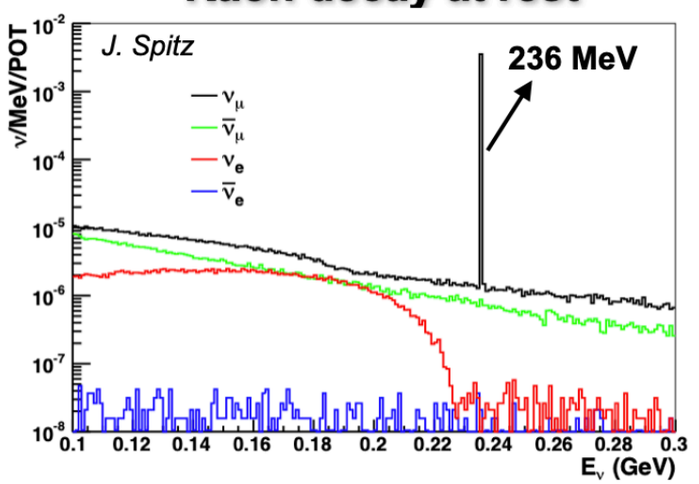

Neutrino Sources and Physics Scope

■ The Fermilab Facility for Dark Sector Discovery (F2D2)

arxiv:2311.09915 [hep-ex]

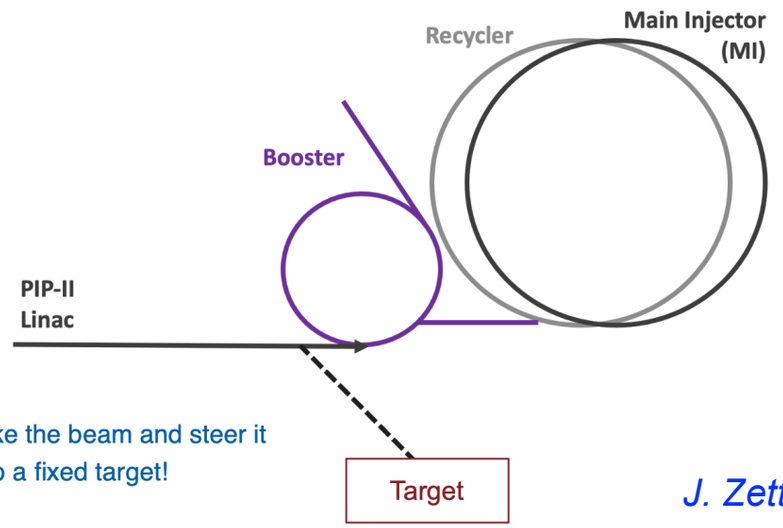

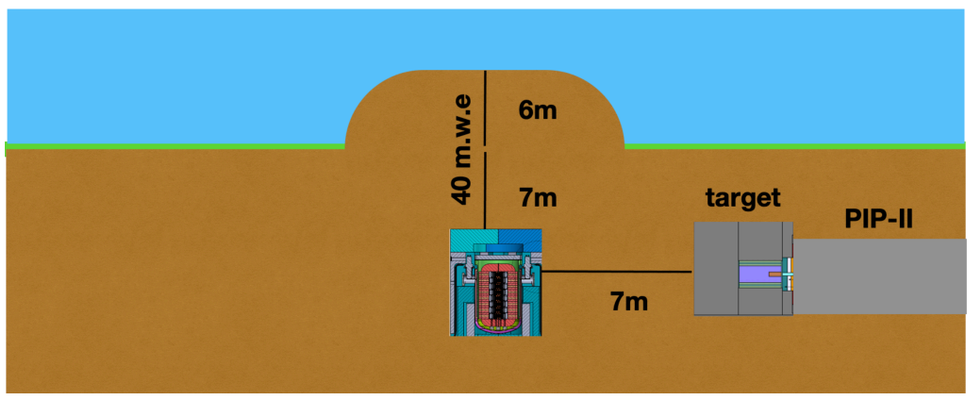

Potential future upgrade: bunch the available beam via an accumulator ring.

J. Zettlemoyer

- **Also a prolific pion decay-at-rest neutrino facility!**

Fermilab Facility for Dark Sector Discovery (F2D2) Task Force Report

M. Toups, N. Dhanaraj, S. Dixon, S. Ganguly, M. Hedges, J. Eldred, J. Estrada,
G. Krnjaic, K. Lynch, V. Pandey, M. Strait, N. Tran, J. Williams, and J. Zettlemoyer
Fermi National Accelerator Laboratory, Batavia, IL 60510, USA

W. Asztalos
Illinois Institute of Technology, Chicago, IL 60616, USA

B. Batell
University of Pittsburgh, Pittsburgh, PA 15260, USA

S. Gori
University of California, Santa Cruz, Santa Cruz, CA 95064, USA

K.J. Kelly
Texas A&M University, College Station, TX 77840, USA

J. Yu
Department of Physics, University of Texas, Arlington, TX 76019, USA

Y.-T. Tsai
SLAC National Accelerator Laboratory, Menlo Park, CA, 94025, USA

(Dated: July 9, 2025)

Neutrino Sources and Physics Scope

■ The Fermilab Facility for Dark Sector Discovery (F2D2)

arxiv:2311.09915 [hep-ex]

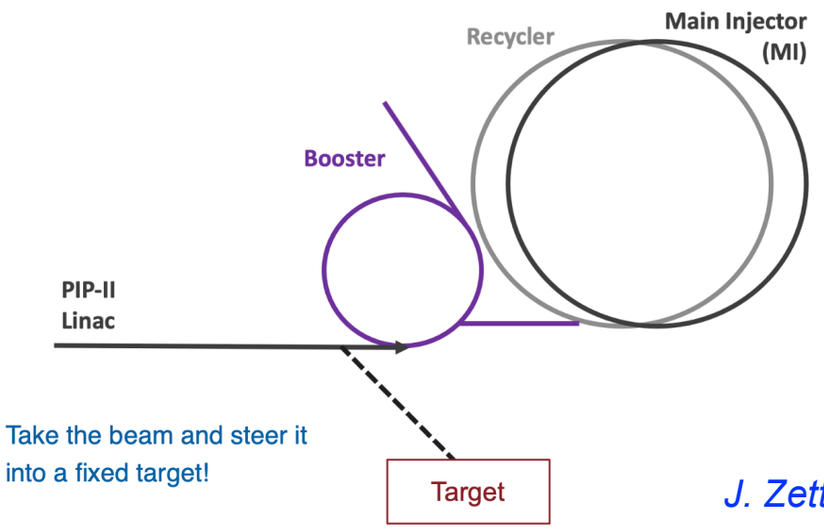

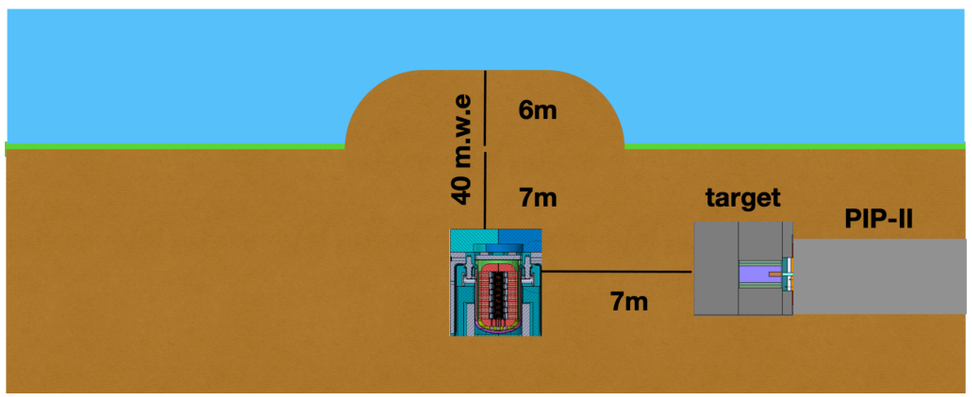

Potential future upgrade: bunch the available beam via an accumulator ring.

J. Zettlemoyer

- **Also a prolific pion decay-at-rest neutrino facility!**

■ Experimental Concepts:

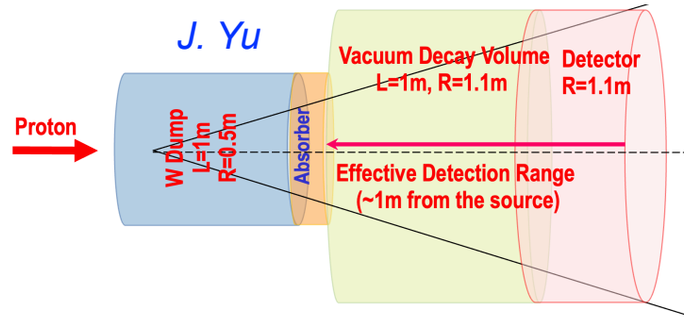

- **The DAMSA Experiment:** A table-top size at an extremely short baseline
  see Jae's talk last week

- **A Low-Threshold Skipper-CCD detector**

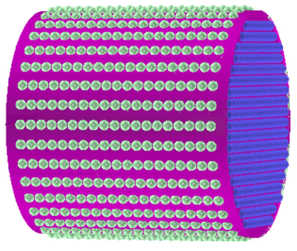

- **The PIP2-BD:** A 100 ton liquid argon (LAr) detector instrumented with 1200 photomultiplier tubes (PMTs)

- **A 100 ton LArTPC experiment:** size similar to SBND ≈ DUNE-ND-LAr

10s of MeV Neutrinos-Nucleus Scattering

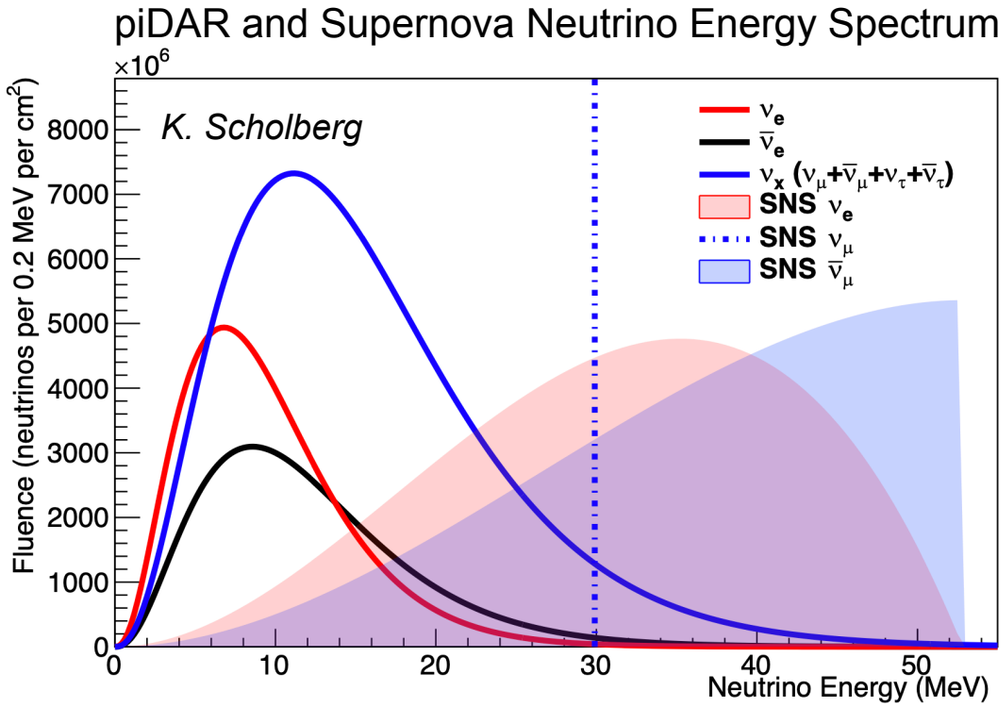

10s of MeV Neutrinos-Nucleus Scattering

Coherent elastic [CEvNS]

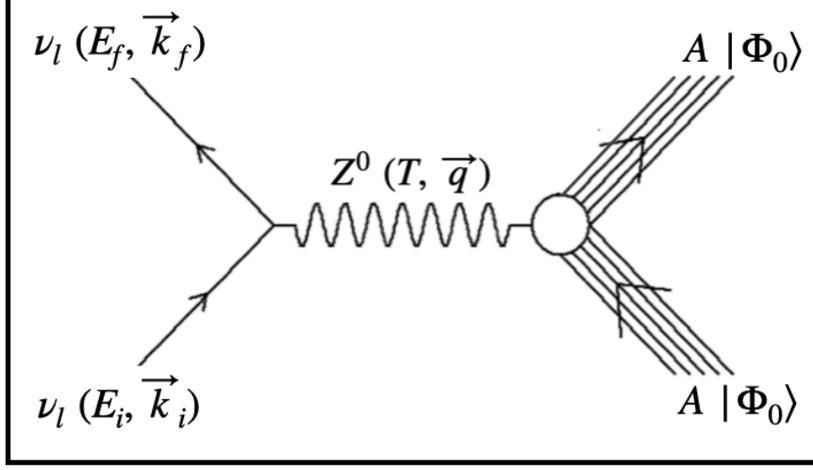

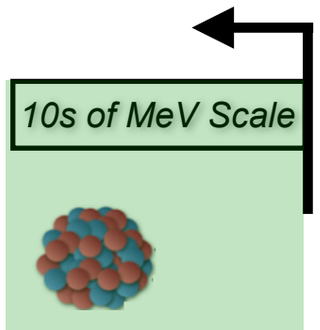

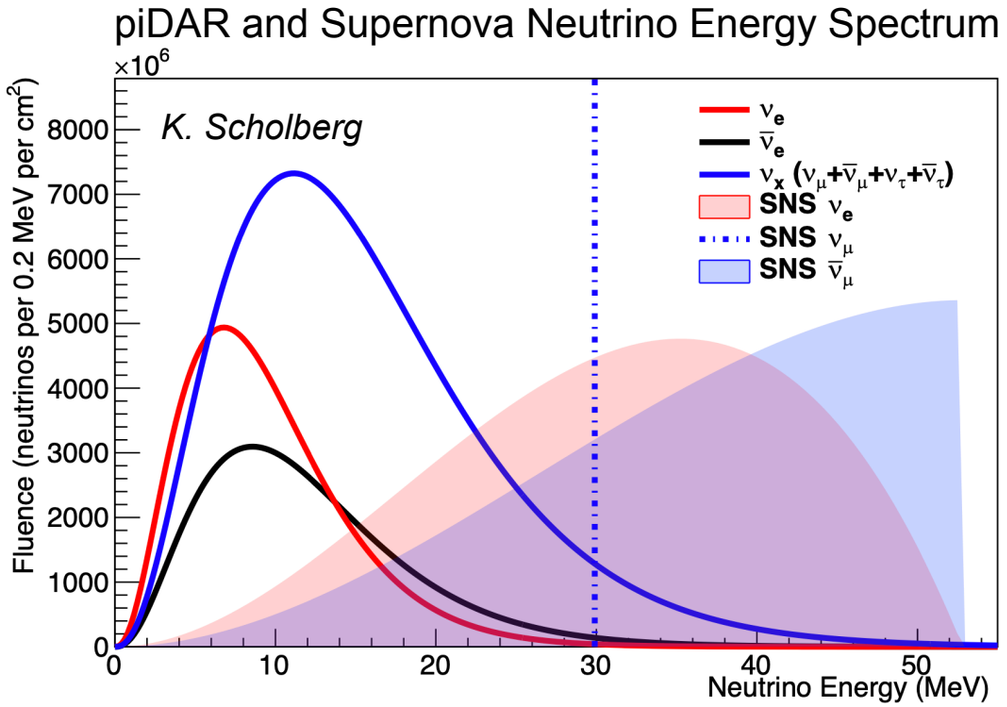

Inelastic CC/NC

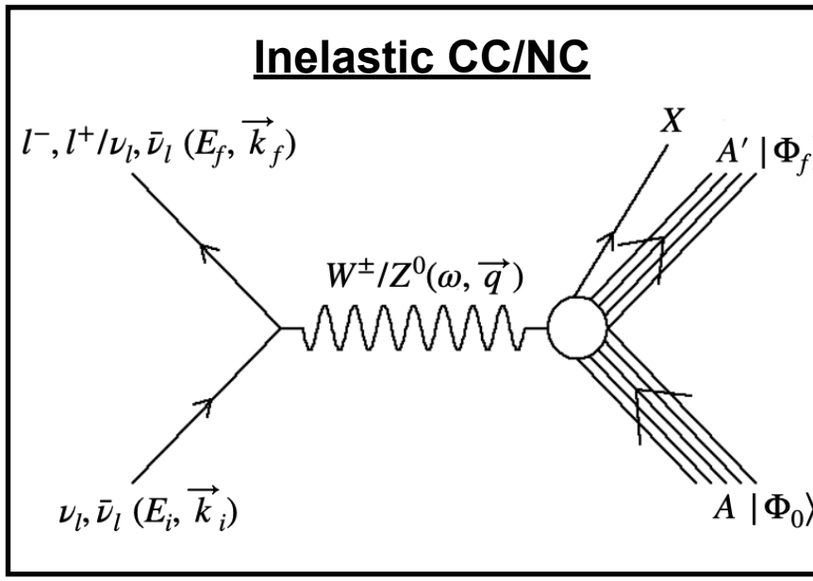

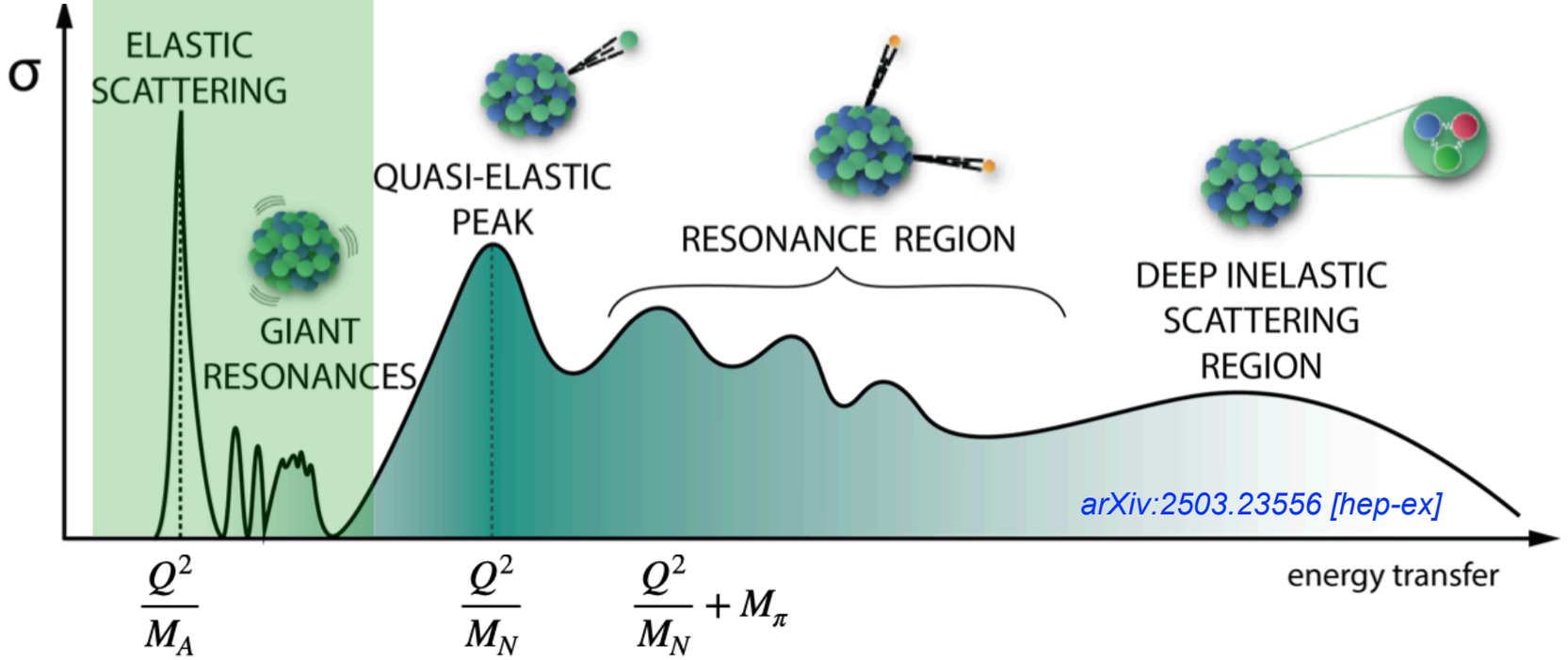

10s of MeV Neutrinos-Nucleus Scattering

Coherent elastic [CEvNS]

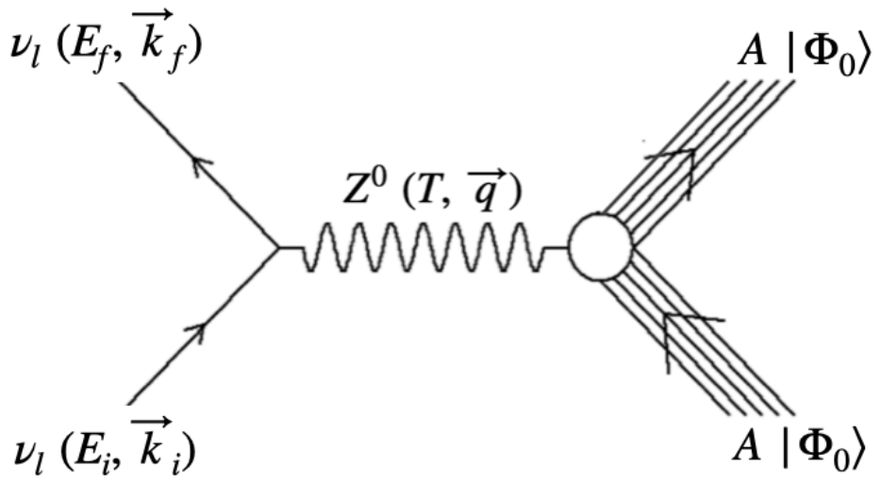

- Final state nucleus stays in its ground state
- Tiny recoil energy, large cross section
- Signal: keV energy nuclear recoil

Inelastic CC/NC

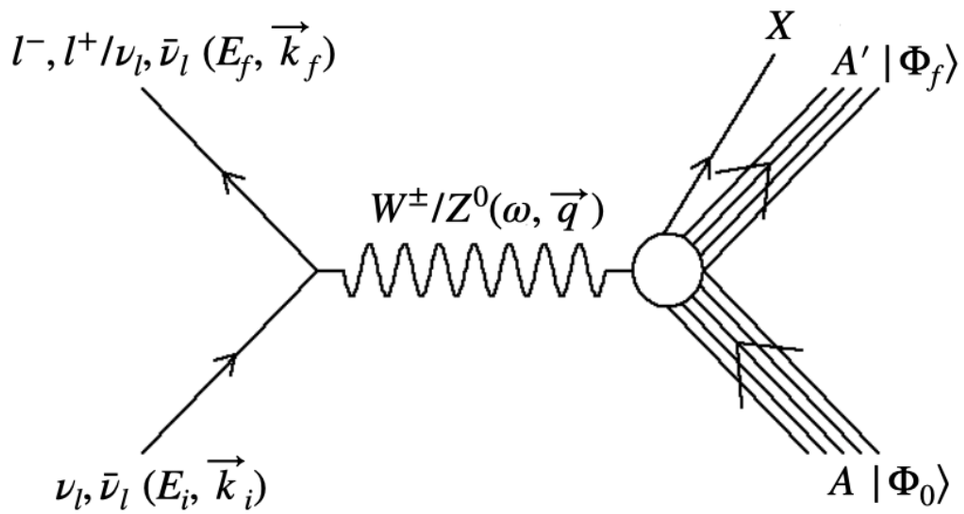

- Nucleus excites to states with well-defined excitation energy, spin and parity (J^{π})
- Followed by nuclear de-excitation into MeV energy gammas, including n, p or nuclear fragmentation emission.

10s of MeV Neutrinos-Nucleus Scattering

Coherent elastic [CEvNS]

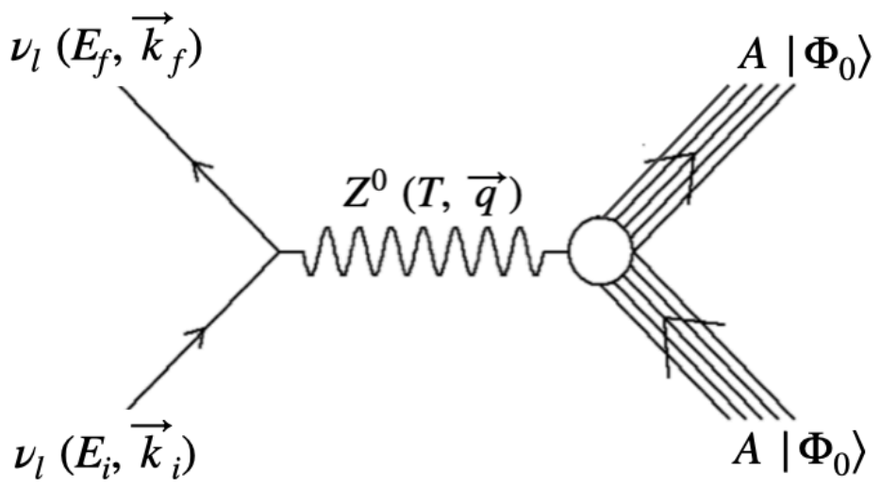

- Final state nucleus stays in its ground state
- Tiny recoil energy, large cross section
- Signal: keV energy nuclear recoil

Inelastic CC/NC

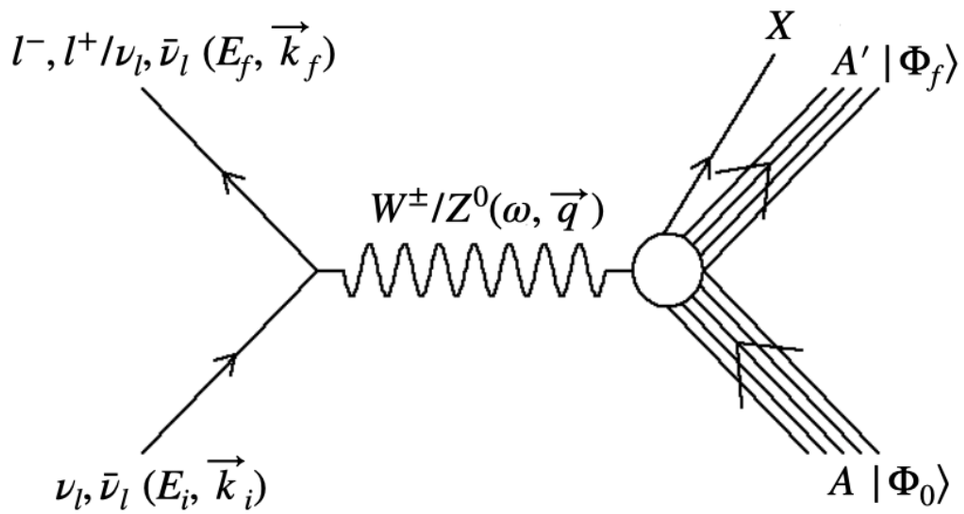

- Nucleus excites to states with well-defined excitation energy, spin and parity (J^{π})
- Followed by nuclear de-excitation into MeV energy gammas, including n, p or nuclear fragmentation emission.

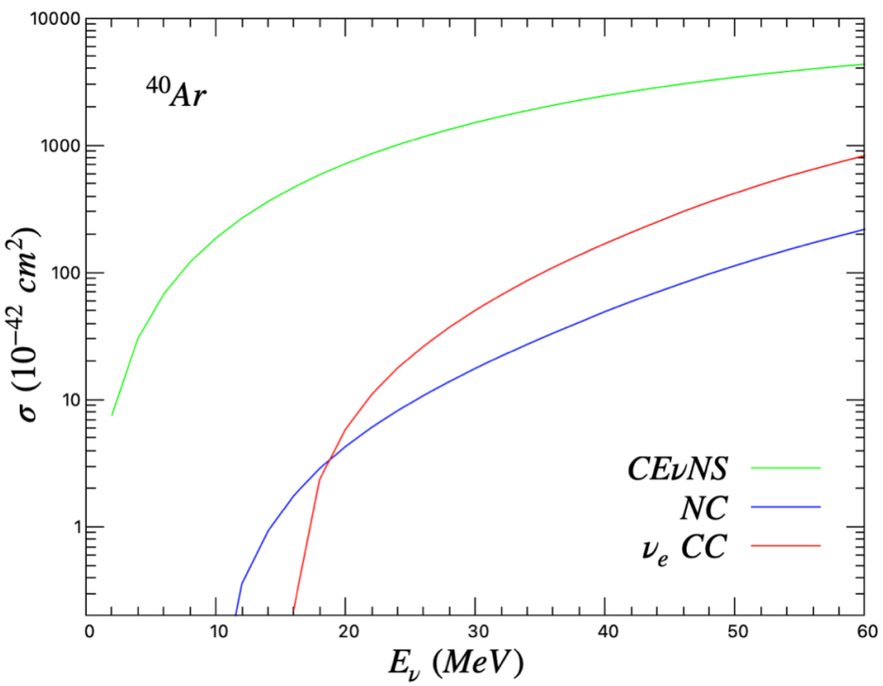

- At 10s of MeV, CEvNS cross section is significantly larger than inelastic ones.

V. Pandey, Prog. Part. Nucl. Phys., 104078 (2024)

10s of MeV Neutrinos-Nucleus Scattering

Coherent elastic [CEvNS]

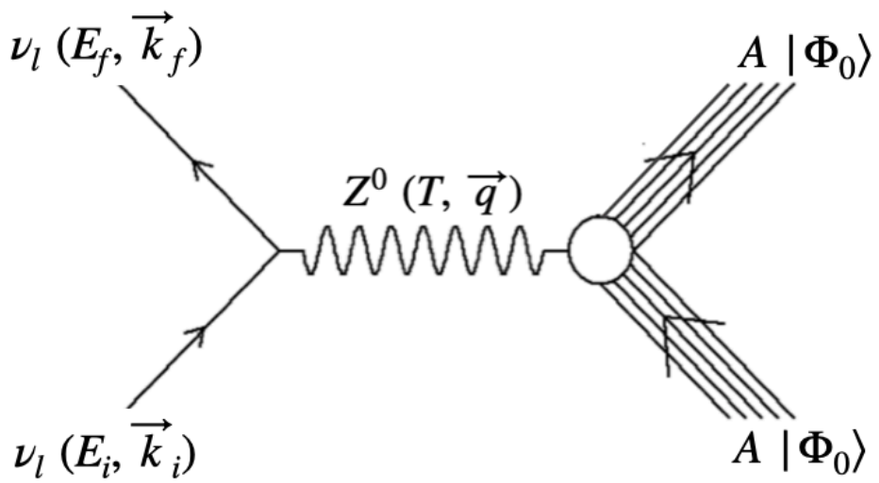

Inelastic CC/NC

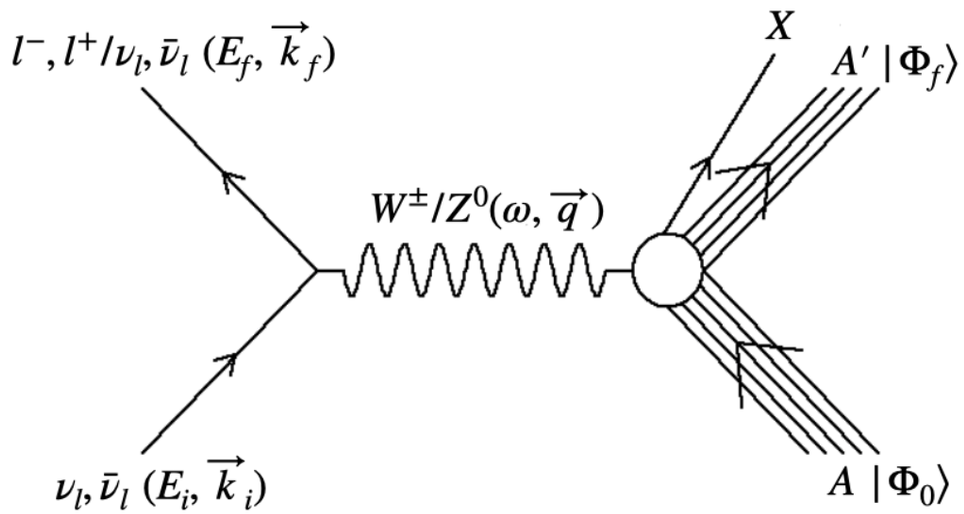

$$\sum_{fi} |\mathscr{M}|^2 \propto \frac{G_F^2}{2} L_{\mu\nu} W^{\mu\nu}$$

Leptonic Tensor: $L_{\mu\nu} = \sum_{fi} (\mathscr{J}_{l,\mu})^\dagger \mathscr{J}_{l,\nu}$ Hadronic Tensor: $W^{\mu\nu} = \sum_{fi} (\mathscr{J}_n^\mu)^\dagger \mathscr{J}_n^\nu$

10s of MeV Neutrinos-Nucleus Scattering

Coherent elastic [CEvNS]

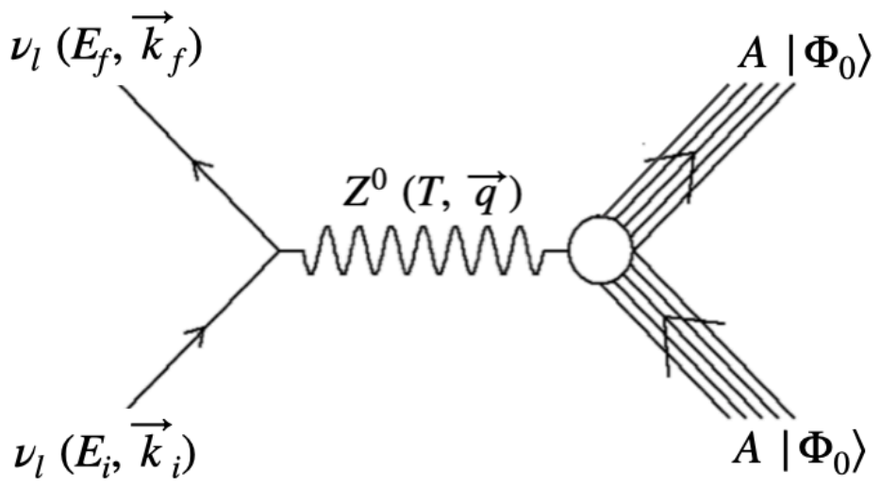

Inelastic CC/NC

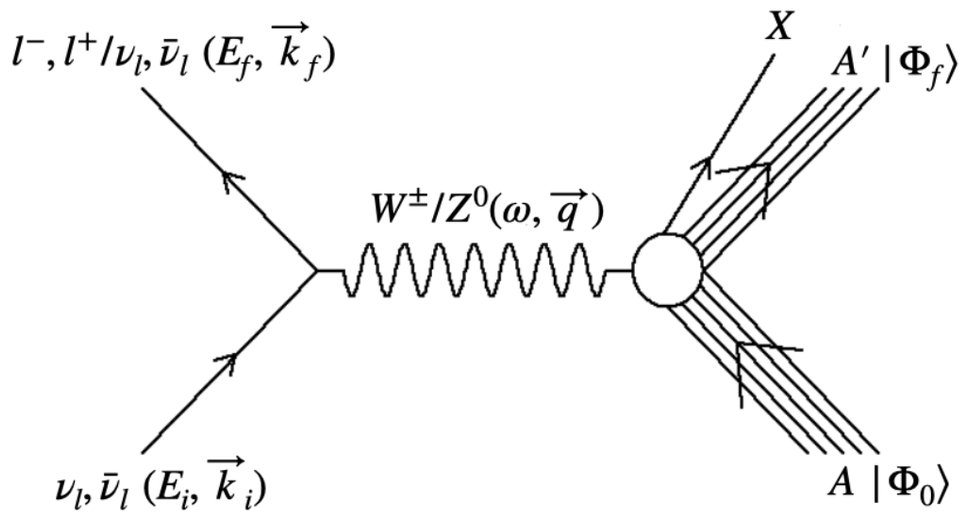

$$\sum_{fi} |\mathscr{M}|^2 \propto \frac{G_F^2}{2} L_{\mu\nu} W^{\mu\nu}$$

Leptonic Tensor: $L_{\mu\nu} = \sum_{fi} (\mathscr{J}_{l,\mu})^\dagger \mathscr{J}_{l,\nu}$

Hadronic Tensor: $W^{\mu\nu} = \sum_{fi} (\mathscr{J}_n^\mu)^\dagger \mathscr{J}_n^\nu$

Transition Amplitude: $\mathscr{J}_n^\mu = \langle \Phi_0 | \hat{J}_n^\mu(q) | \Phi_0 \rangle$

Transition Amplitude: $\mathscr{J}_n^\mu = \langle \Phi_f | \hat{J}_n^\mu(q) | \Phi_0 \rangle$

Neutrino-Nucleus Interactions: Many-Body QM Problem

- Nucleus is a complex many-body quantum mechanical system
- Nucleons bound in the nucleus subject to various nuclear effects
- Fermi momentum, Pauli blocking, multi-body nucleon correlation, intra-nuclear hadronic interaction, …

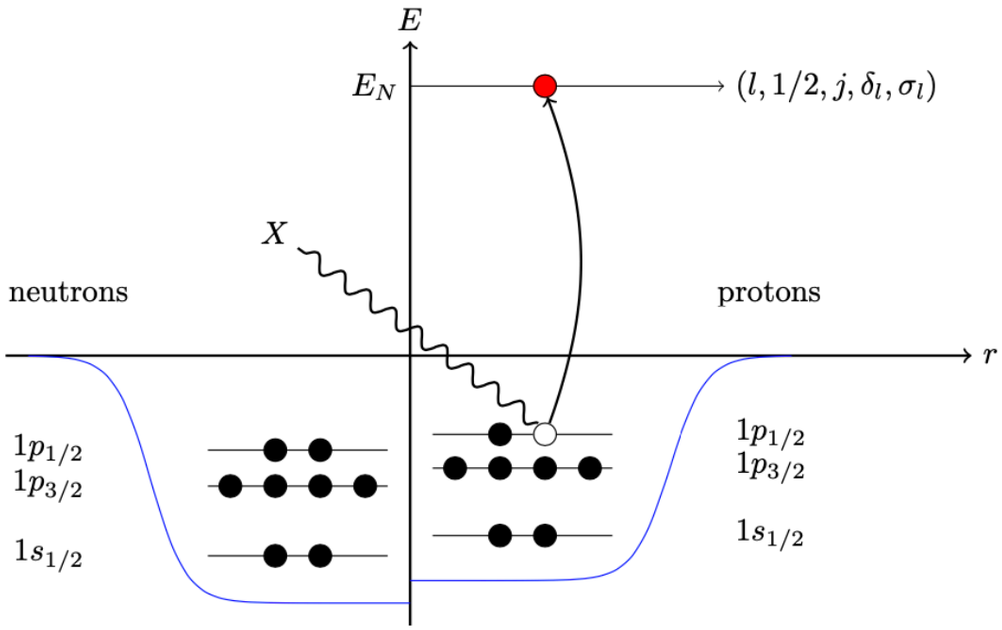

JLab Hall A, Phys. Rev. D 105, 112002 (2022)

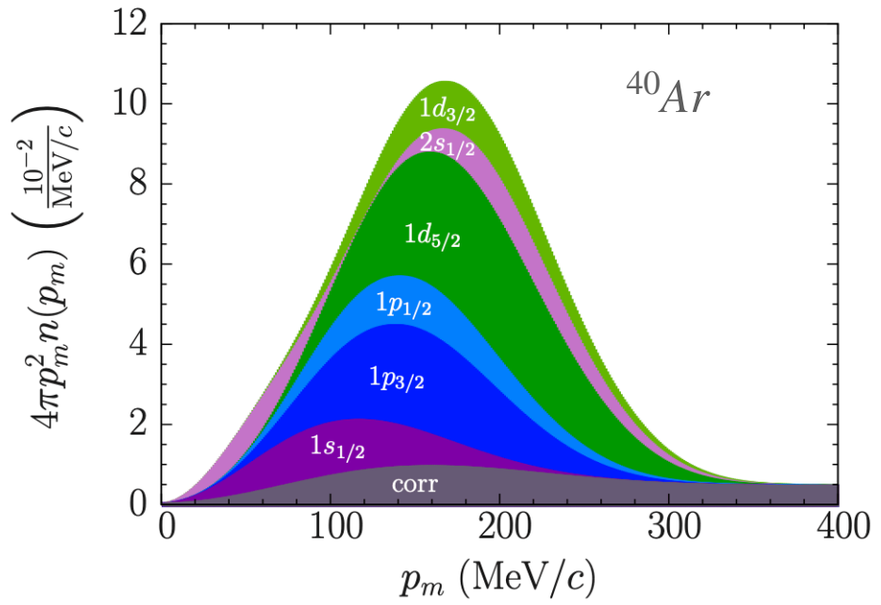

Neutrino-Nucleus Interactions: Many-Body QM Problem

The Nuclear Many-body Problem

- In the low-energy regime, quark and gluons are confined within hadrons and the effective degrees of freedoms are nucleons and pions

  - Nuclear Many-body Hamiltonian

$$H = \sum_i \frac{\mathbf{p}_i^2}{2m} + \sum_{i<j} v_{ij} + \sum_{i<j<k} V_{ijk} + \dots$$

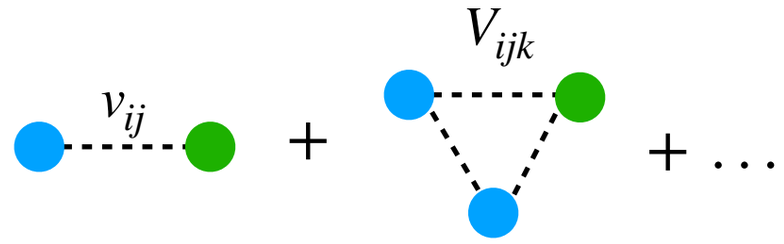

v_{ij} and V_{ijk} are two- and three-nucleon potential operators

  - The interactions of nuclei with external electroweak probes is mediated by charge and current operators that are consistent with the nuclear interactions.

Nuclear Current Operators:

$$J^\mu = \sum_i j_i^\mu + \sum_{i<j} j_{ij}^\mu + \dots$$

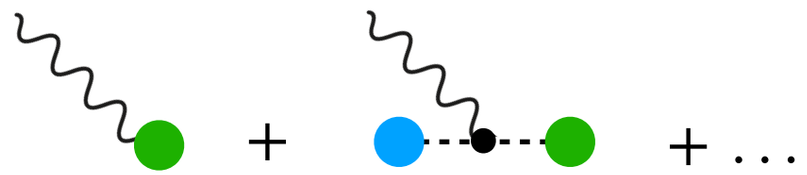

one and two-body contributions

- The response functions contain all nuclear-dynamics information

$$R(\omega, \mathbf{q}) = \sum_f \langle \Psi_0 | J^\dagger | \Psi_f \rangle \langle \Psi_f | J | \Psi_0 \rangle \delta(\omega - E_f + E_0)$$

Neutrino-Nucleus Interactions: HF-CRPA Approach

- Nuclear ground state described as a many-body quantum mechanical system where nucleons are bound in an effective nuclear potential.
- Solve Hartree-Fock (**HF**) equation with a Skyrme (**SkE2**) nuclear potential to obtain single–nucleon wave functions for the bound nucleons in the nuclear ground state.
- Add the influence of long-range correlations between the nucleons is introduced through the continuum Random Phase Approximation (CRPA) on top of the HF-SkE2 approach.

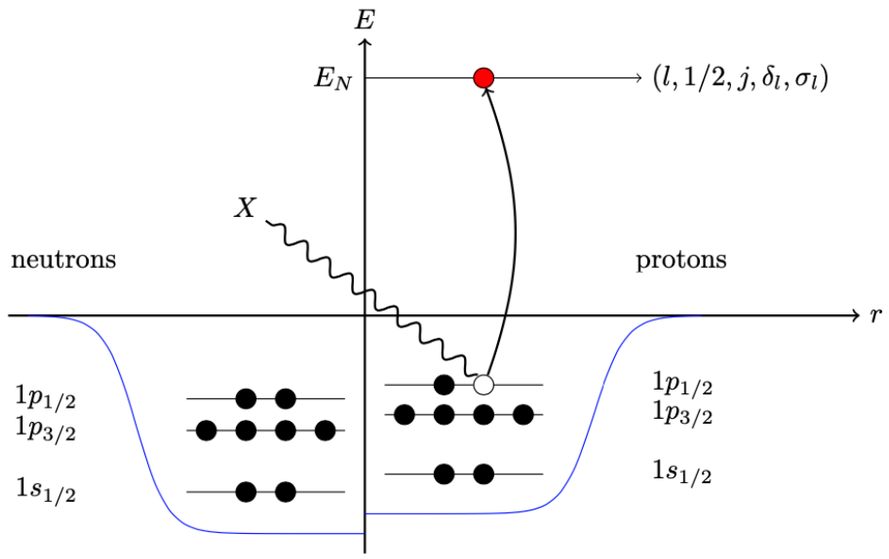

- The local RPA-polarization propagator is obtained by an iteration to all orders of the first order contribution to the particle-hole Green's function.

$$\Pi^{(RPA)}(x_1, x_2; E_x) = \Pi^{(0)}(x_1, x_2; E_x) + \frac{1}{\hbar} \int dx dx' \, \Pi^0(x_1, x; E_x) \times \tilde{V}(x, x') \, \Pi^{(RPA)}(x', x_2; E_x)$$

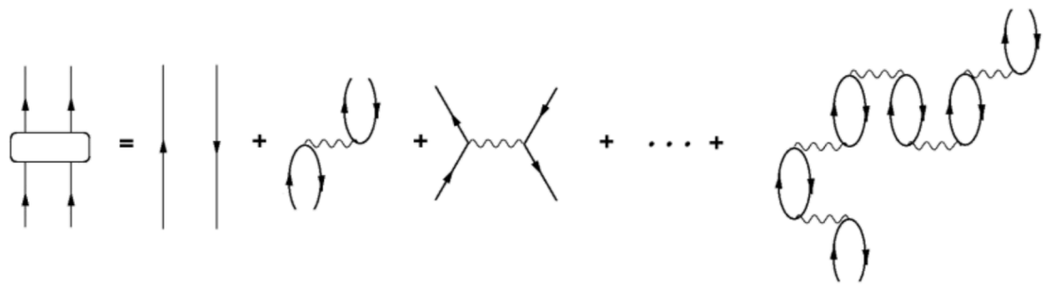

Neutrino-Nucleus Interactions: HF-CRPA Approach

- **Cross section**

$$\left(\frac{d^2\sigma}{d\omega_\nu d\Omega}\right)_\nu = \frac{G_F^2\ \cos^2\theta_c}{(4\pi)^2}\left(\frac{2}{2J_i+1}\right)\varepsilon_f\kappa_f\ \times\ \zeta^2\left(Z',\varepsilon_f,q_\nu\right)\ \left[\sum_{J=0}^{\infty}\sigma^J_{CL,\nu}+\sum_{J=1}^{\infty}\sigma^J_{T,\nu}\right]$$

$$\sigma^J_{CL,\nu} = \left[v^{\mathcal{M}}_\nu R^{\mathcal{M}}_\nu + v^{\mathcal{L}}_\nu R^{\mathcal{L}}_\nu + 2\ v^{\mathcal{ML}}_\nu R^{\mathcal{ML}}_\nu\right]$$

$$\sigma^J_{T,\nu} = \left[v^T_\nu R^T_\nu \pm 2\ v^{TT}_\nu R^{TT}_\nu\right]$$

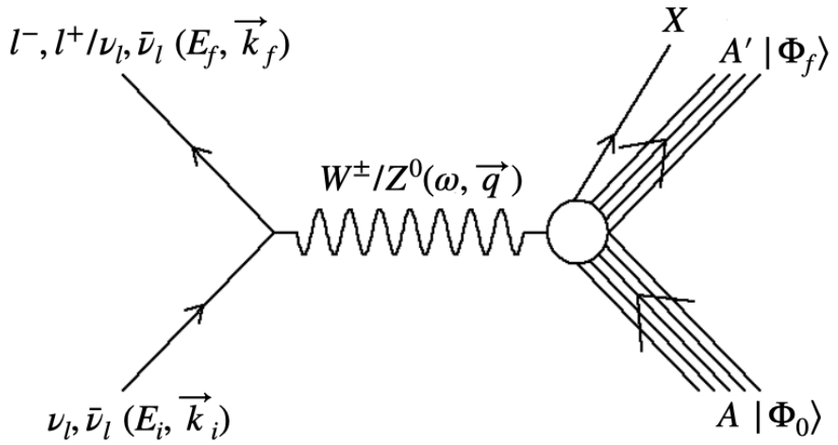

- **Leptonic Coefficients**

$$v^{\mathcal{M}}_\nu = \left[1+\frac{\kappa_f}{\varepsilon_f}\cos\theta\right] \qquad v^{\mathcal{L}}_\nu = \left[1+\frac{\kappa_f}{\varepsilon_f}\cos\theta-\frac{2\varepsilon_i\varepsilon_f}{|\vec{q}|^2}\left(\frac{\kappa_f}{\varepsilon_f}\right)^2\sin^2\theta\right]$$

$$v^{\mathcal{ML}}_\nu = \left[\frac{\omega}{|\vec{q}|}\left(1+\frac{\kappa_f}{\varepsilon_f}\cos\theta\right)+\frac{m_l^2}{\varepsilon_f|\vec{q}|}\right] \qquad v^T_\nu = \left[1-\frac{\kappa_f}{\varepsilon_f}\cos\theta+\frac{\varepsilon_i\varepsilon_f}{|\vec{q}|^2}\left(\frac{\kappa_f}{\varepsilon_f}\right)^2\sin^2\theta\right]$$

$$v^{TT}_\nu = \left[\frac{\varepsilon_i+\varepsilon_f}{|\vec{q}|}\left(1-\frac{\kappa_f}{\varepsilon_f}\cos\theta\right)-\frac{m_l^2}{\varepsilon_f|\vec{q}|}\right],$$

- **Response Functions**

$$R^{\mathcal{M}}_\nu = |\langle J_f||\widehat{\mathcal{M}}^\nu_J(|\vec{q}|)||J_i\rangle|^2 \qquad R^{\mathcal{L}}_\nu = |\langle J_f||\widehat{\mathcal{L}}^\nu_J(|\vec{q}|)||J_i\rangle|^2$$

$$R^{\mathcal{ML}}_\nu = \mathcal{R}\left[\langle J_f||\widehat{\mathcal{L}}^\nu_J(|\vec{q}|)||J_i\rangle\langle J_f||\widehat{\mathcal{M}}^\nu_J(|\vec{q}|)||J_i\rangle^*\right]$$

$$R^T_\nu = \left[|\langle J_f||\widehat{\mathcal{T}}^{mag,\nu}_J(|\vec{q}|)||J_i\rangle|^2+|\langle J_f||\widehat{\mathcal{T}}^{el,\nu}_J(|\vec{q}|)||J_i\rangle|^2\right]$$

$$R^{TT}_\nu = \mathcal{R}\left[\langle J_f||\widehat{\mathcal{T}}^{mag,\nu}_J(|\vec{q}|)||J_i\rangle\langle J_f||\widehat{\mathcal{T}}^{el,\nu}_J(|\vec{q}|)||J_i\rangle^*\right]$$

- **Multipole Operators**

$$\widehat{\mathcal{M}}_{JM}(\kappa) = \int d\vec{x}\ \left[j_J\ (\kappa r)\ Y^M_J\ (\Omega_x)\right]\ \hat{J}_0(\vec{x})$$

$$\widehat{\mathcal{L}}_{JM}(\kappa) = \frac{i}{\kappa}\int d\vec{x}\ \left[\vec{\nabla}\left(j_J\ (\kappa r)\ Y^M_J\ (\Omega_x)\right)\right]\ \cdot\ \widehat{\vec{J}}(\vec{x})$$

$$\widehat{\mathcal{T}}^{el}_{JM}(\kappa) = \frac{1}{\kappa}\int d\vec{x}\ \left[\vec{\nabla}\ \times\ \left(j_J\ (\kappa r)\ \vec{\mathcal{Y}}^M_{J,J}\ (\Omega_x)\right)\right]\ \cdot\ \widehat{\vec{J}}(\vec{x})$$

$$\widehat{\mathcal{T}}^{mag}_{JM}(\kappa) = \int d\vec{x}\ \left[j_J\ (\kappa r)\ \vec{\mathcal{Y}}^M_{J,J}\ (\Omega_x)\right]\ \cdot\ \widehat{\vec{J}}(\vec{x})$$

10s of MeV Inelastic Neutrino-Nucleus Scattering: HF-CRPA Model

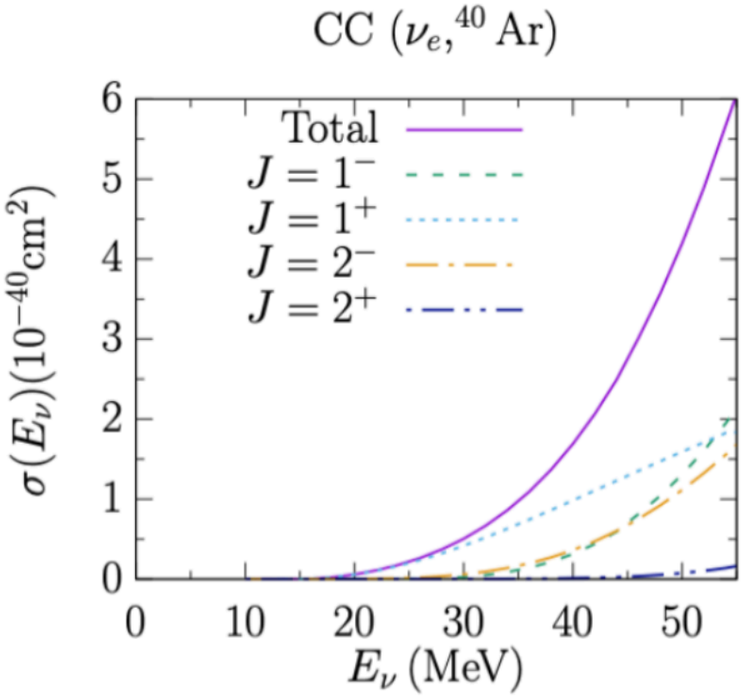

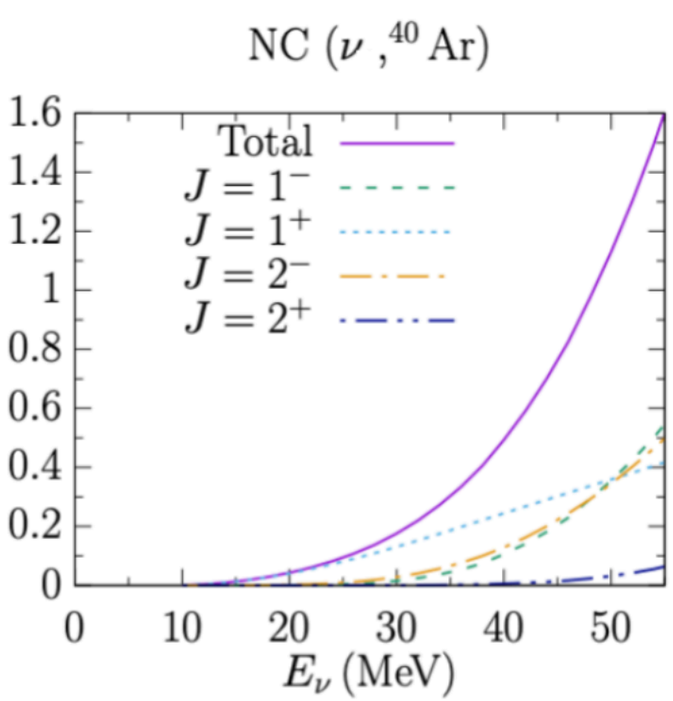

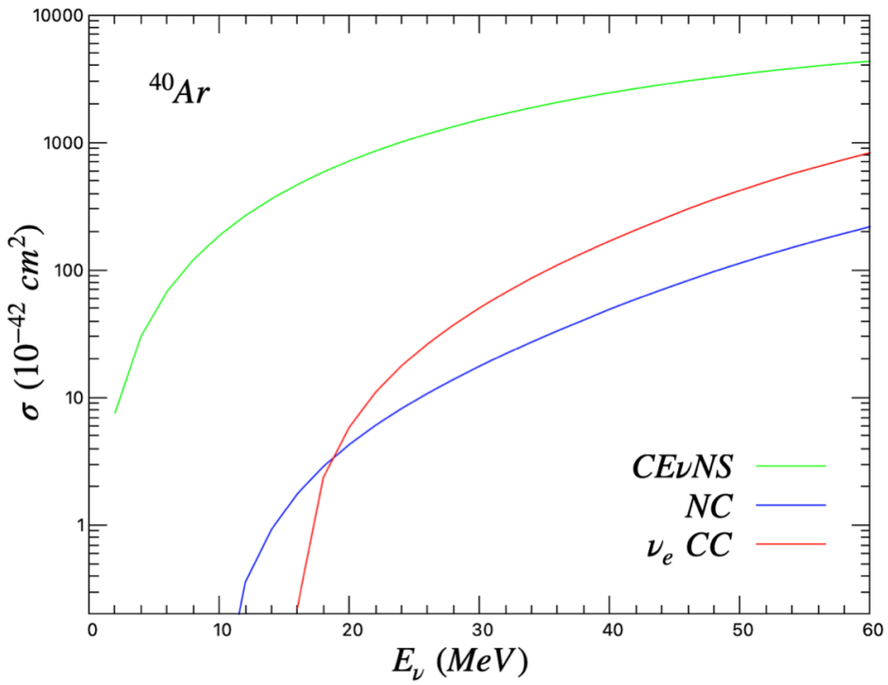

q = 95 [MeV/c], Q^2 = 0.009 [(GeV/c)^2] **q = 121 [MeV/c], Q^2 = 0.015 [(GeV/c)^2]**

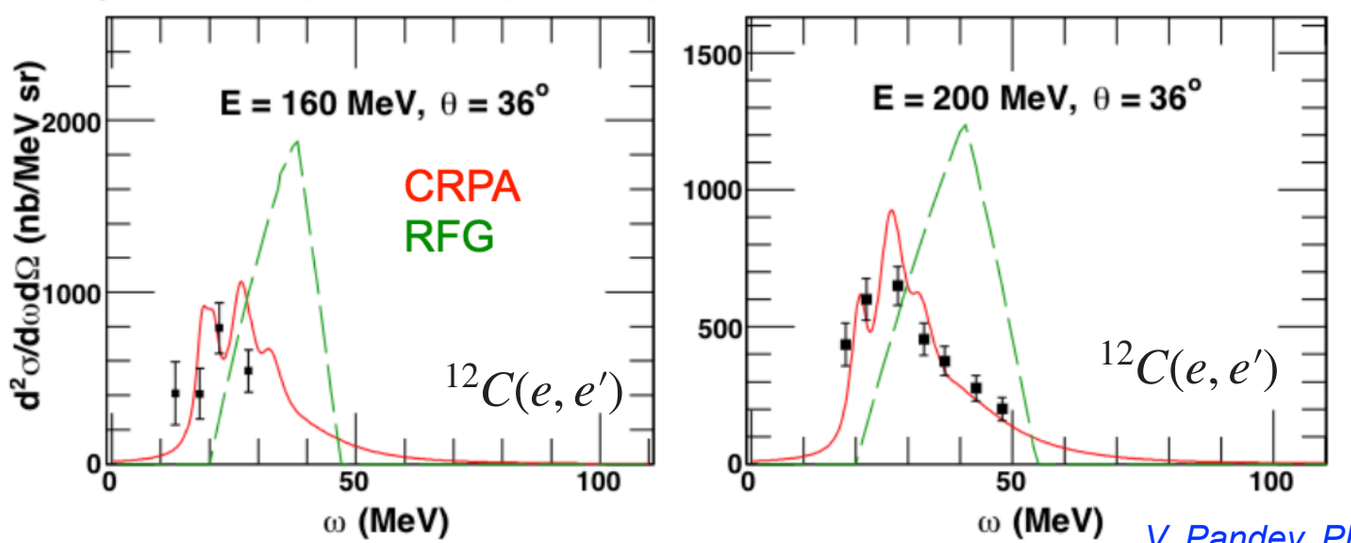

V. Pandey, PhD thesis (2016)

N. Van Dessel, V. Pandey, H. Ray and N. Jachowicz, Universe 9, 207 (2023)

V. Pandey, Prog. Part. Nucl. Phys., 104078 (2024)

V. Pandey, N. Jachowicz, T. Van Cuyck, J. Ryckebusch, M. Martini, Phys. Rev. C92, 024606 (2015)

10s of MeV Inelastic Neutrino-Nucleus Scattering: Supernova Neutrinos

- DUNE relies on ν_e CC inelastic neutrino-nucleus scattering process to detect neutrinos from **core-collapse supernova.**

- The inelastic neutrino-nucleus cross sections are quite poorly understood. There are very few existing measurements, none at better than the 10% uncertainty level. As a result, the uncertainties on the theoretical calculations of, e.g., neutrino-argon cross sections are not well quantified at all at these energies.

No measurements on Argon yet

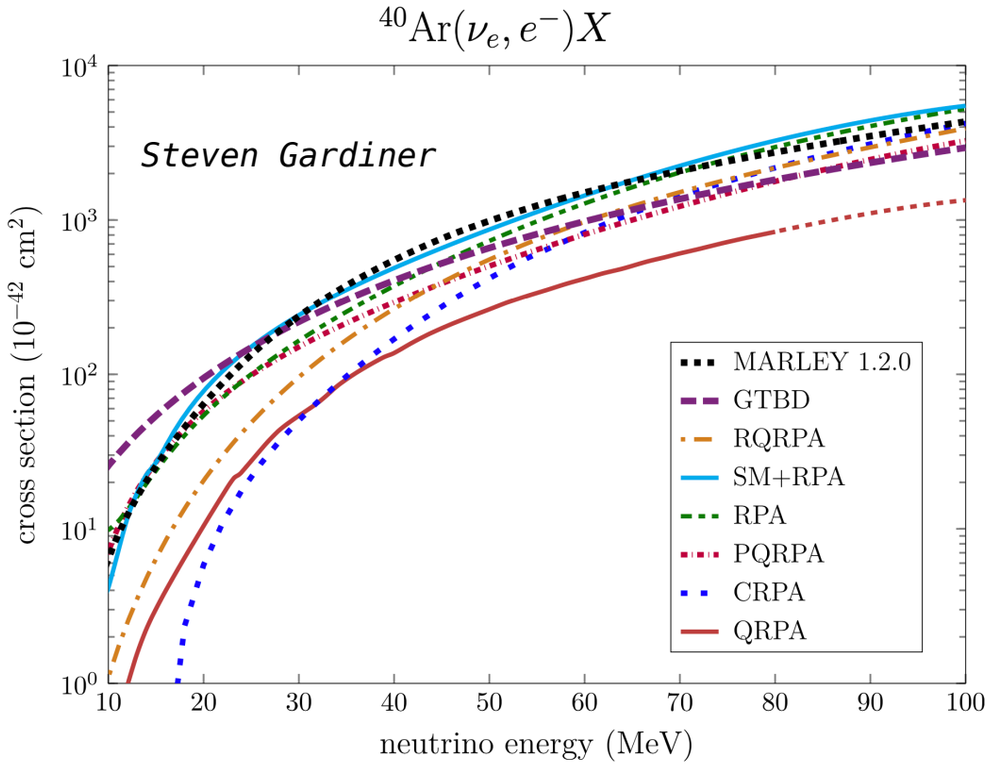

Past measurements on Carbon

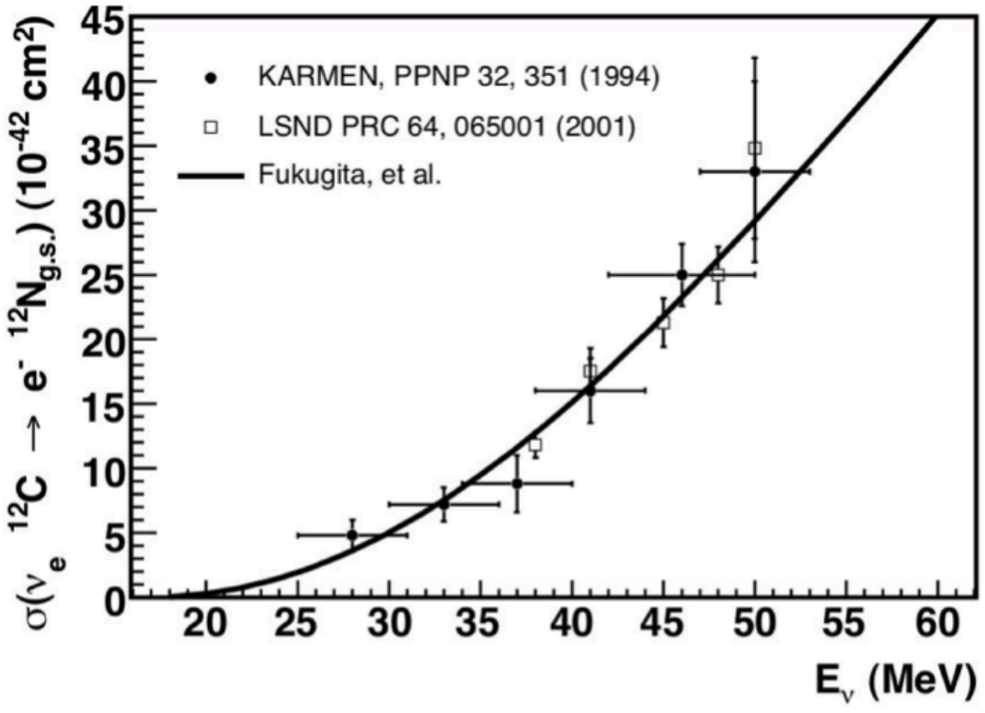

Rev. Mod. Phys. 84,1307 (2012)

Fermilab

10s of MeV Inelastic Neutrino-Nucleus Scattering: Supernova Neutrinos

- DUNE relies on ν_e CC inelastic neutrino-nucleus scattering process to detect neutrinos from **core-collapse supernova.**

- The inelastic neutrino-nucleus cross sections are quite poorly understood. There are very few existing measurements, none at better than the 10% uncertainty level. As a result, the uncertainties on the theoretical calculations of, e.g., neutrino-argon cross sections are not well quantified at all at these energies.

Reaction Channel	Experiment	Measurement (10^{-42} cm^2)
$^{12}\mathrm{C}(\nu_e, e^-)^{12}\mathrm{N}_{\mathrm{g.s.}}$	KARMEN	$9.1 \pm 0.5(\mathrm{stat}) \pm 0.8(\mathrm{sys})$
	E225	$10.5 \pm 1.0(\mathrm{stat}) \pm 1.0(\mathrm{sys})$
	LSND	$8.9 \pm 0.3(\mathrm{stat}) \pm 0.9(\mathrm{sys})$
$^{12}\mathrm{C}(\nu_e, e^-)^{12}\mathrm{N}^*$	KARMEN	$5.1 \pm 0.6(\mathrm{stat}) \pm 0.5(\mathrm{sys})$
	E225	$3.6 \pm 2.0(\mathrm{tot})$
	LSND	$4.3 \pm 0.4(\mathrm{stat}) \pm 0.6(\mathrm{sys})$
$^{12}\mathrm{C}(\nu_\mu, \nu_\mu)^{12}\mathrm{C}^*$	KARMEN	$3.2 \pm 0.5(\mathrm{stat}) \pm 0.4(\mathrm{sys})$
$^{12}\mathrm{C}(\nu, \nu)^{12}\mathrm{C}^*$	KARMEN	$10.5 \pm 1.0(\mathrm{stat}) \pm 0.9(\mathrm{sys})$
$^{56}\mathrm{Fe}(\nu_e, e^-)\ ^{56}\mathrm{Co}$	KARMEN	$256 \pm 108(\mathrm{stat}) \pm 43(\mathrm{sys})$
$^{127}\mathrm{I}(\nu_e, e^-)^{127}\mathrm{Xe}$	LSND	$284 \pm 91(\mathrm{stat}) \pm 25(\mathrm{sys})$
$^{127}\mathrm{I}(\nu_e, e^-)\mathrm{X}$	COHERENT	$920^{+2.1}_{-1.8}$
$^{nat}\mathrm{Pb}(\nu_e, Xn)$	COHERENT	– –

V. Pandey, Prog. Part. Nucl. Phys., 104078 (2024)

TABLE III. Flux-averaged cross-sections measured at stopped pion facilties on various nuclei. Experimental data gathered from the LAMPF [89], KARMEN [90–93], E225 [94], LSND [95–97], and COHERENT [98, 99] experiments. Table adapted from the Ref. [9].

10s of MeV Inelastic Neutrino-Nucleus Scattering: MARLEY

- MARLEY (Model of Argon Reaction Low Energy Yields) is a dedicated low-energy neutrino event generator developed by Steven Gardiner to simulate tens-of-MeV neutrino-nucleus interactions on argon.

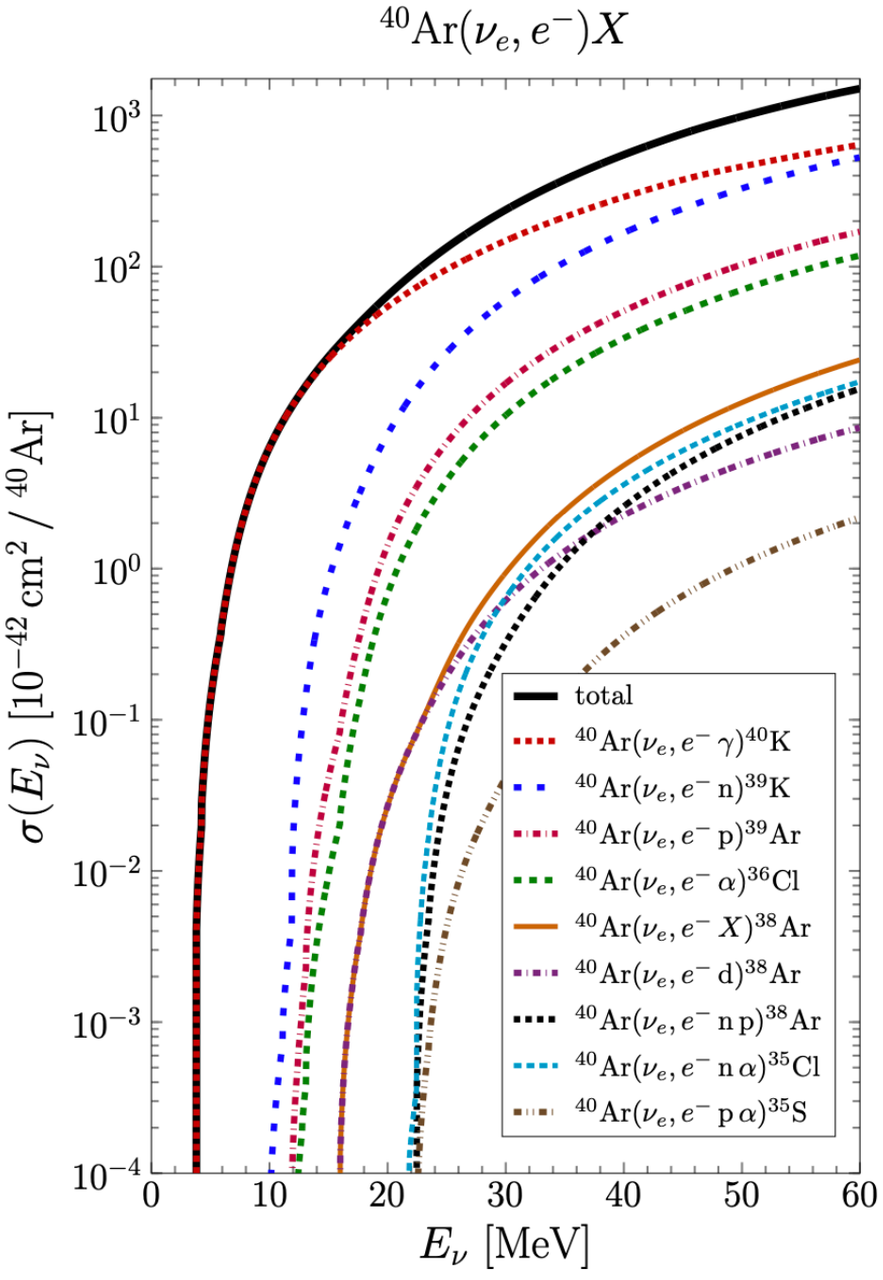

S. Gardiner, Phys. Rev. C 103, 044604 (2021)

I. Inclusive scattering on the nucleus:

Allowed approximation (long–wavelength ($q \to 0$) and slow nucleons ($p_N/m_N \to 0$) limit), Fermi and Gamow-Teller matrix elements:

II. Nuclear de-excitation:

For bound nuclear states, the de-excitation gamma rays are sampled using tables of experimental branching ratios.

For unbound nuclear states, MARLEY simulates the competition between gamma-ray and nuclear fragment emission using the Hauser-Feshbach statistical model.

10s of MeV Inelastic Neutrino-Nucleus Scattering: CRPA and MARLEY

- **CRPA and MARLEY**
  - **Allowed and forbidden transitions**

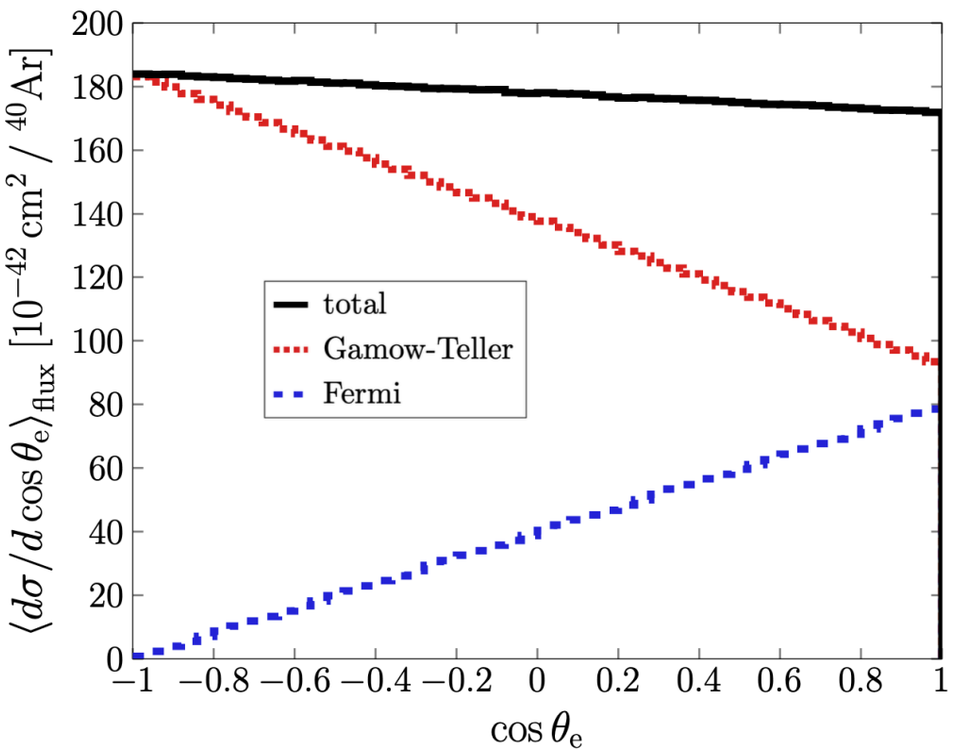

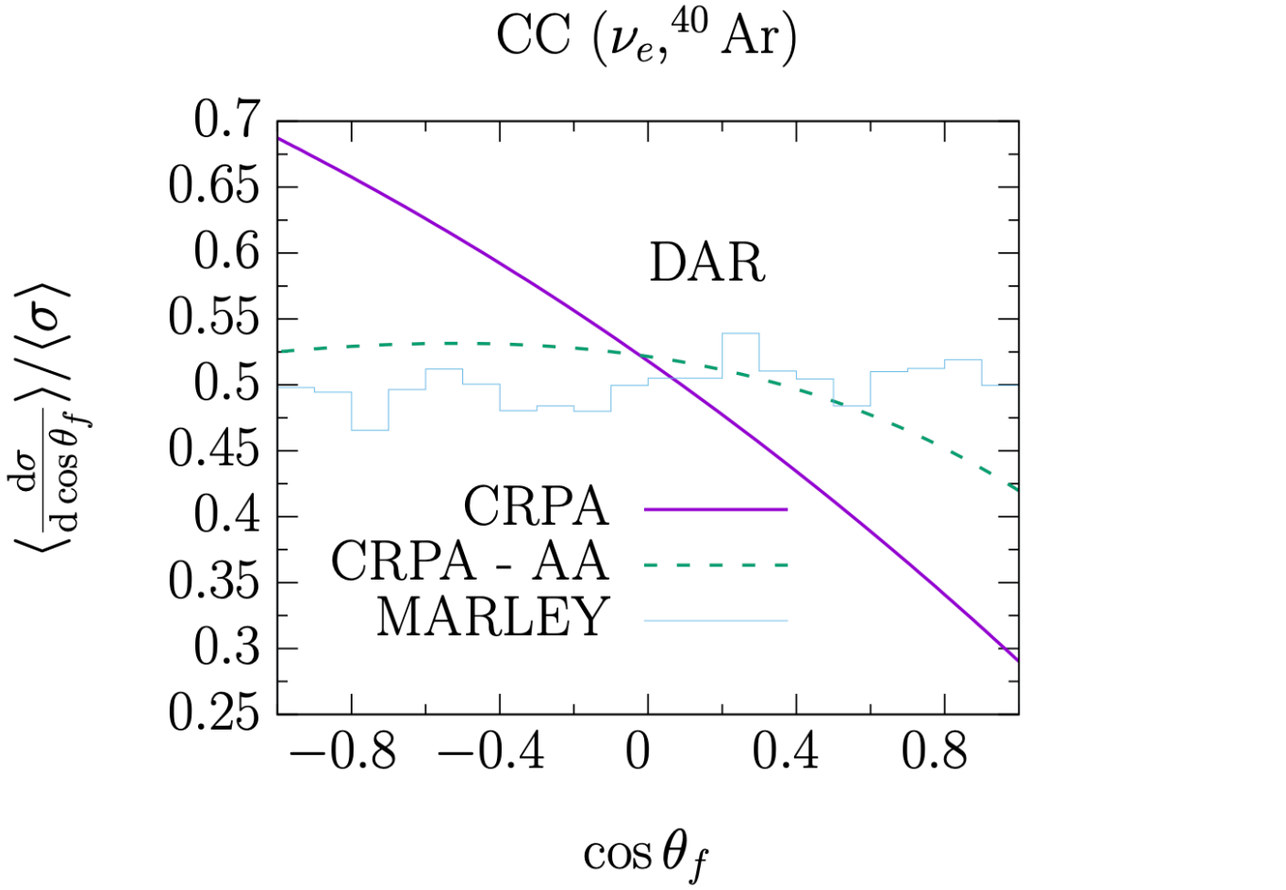

- MARLEY (used in DUNE): Allowed approximation (long–wavelength $(q \to 0)$ and slow nucleons $(p_N/m_N \to 0)$ limit)
  Fermi and Gamow-Teller matrix elements predicts a nearly flat angular distribution.

- CRPA: includes full multipole expansion of nuclear matrix element (allowed as well as forbidden transitions), predict more backwards strength.

MARLEY: S. Gardiner, Phys. Rev. C 103, 044604 (2021)

10s of MeV Inelastic Neutrino-Nucleus Scattering: CRPA and MARLEY

- **Electron angular distribution is important for Supernova pointing capability**

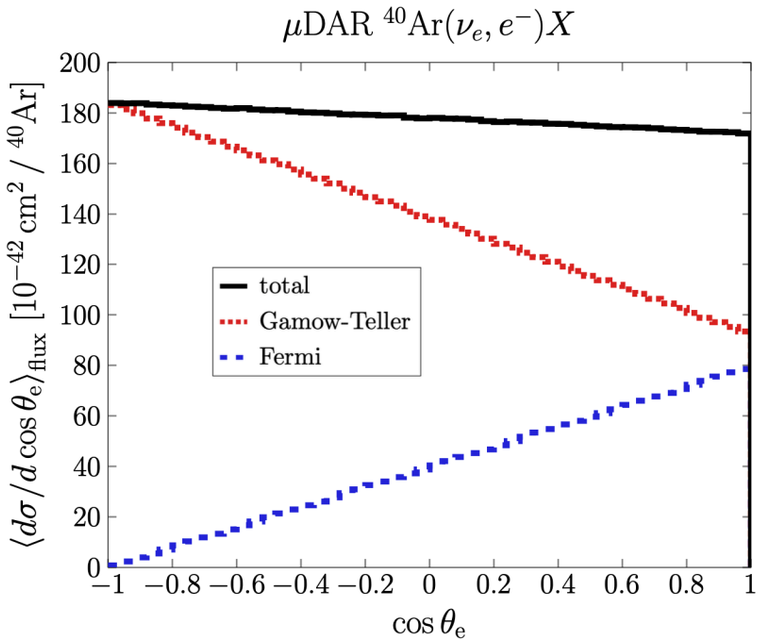

- The information about the incoming neutrino direction is preserved in the final-state electron's angular distribution.
- CC scattered electron angular distribution will enable DUNE's capability for supernova pointing and enabling multi-messenger exploration.

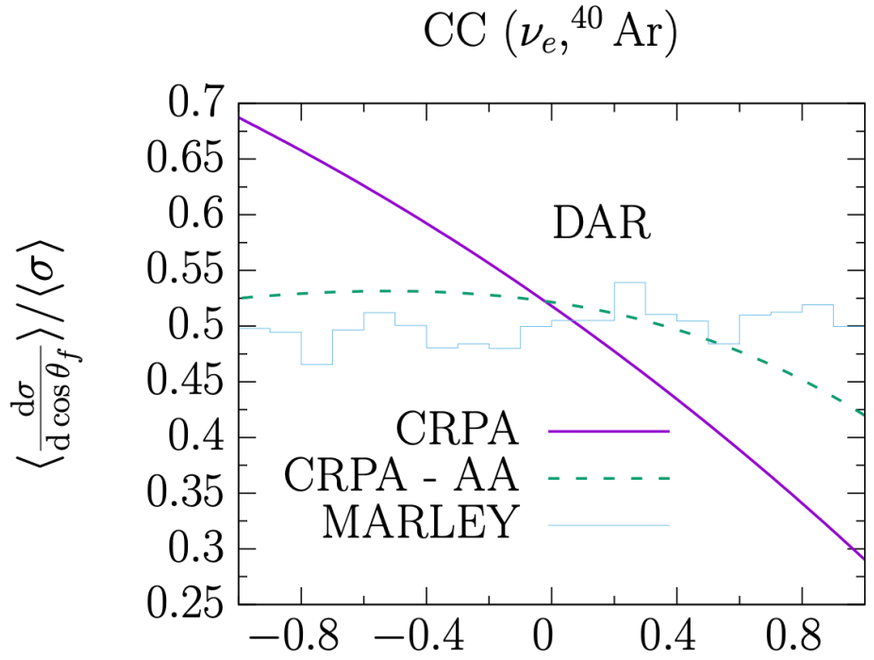

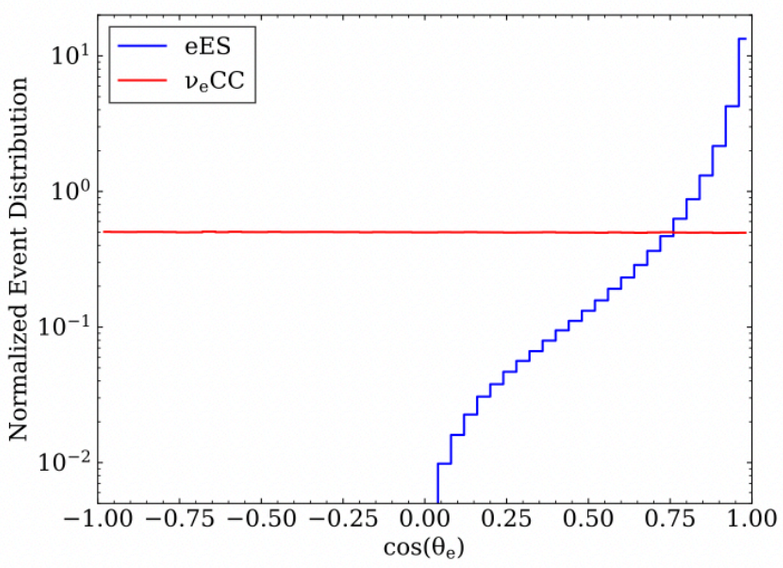

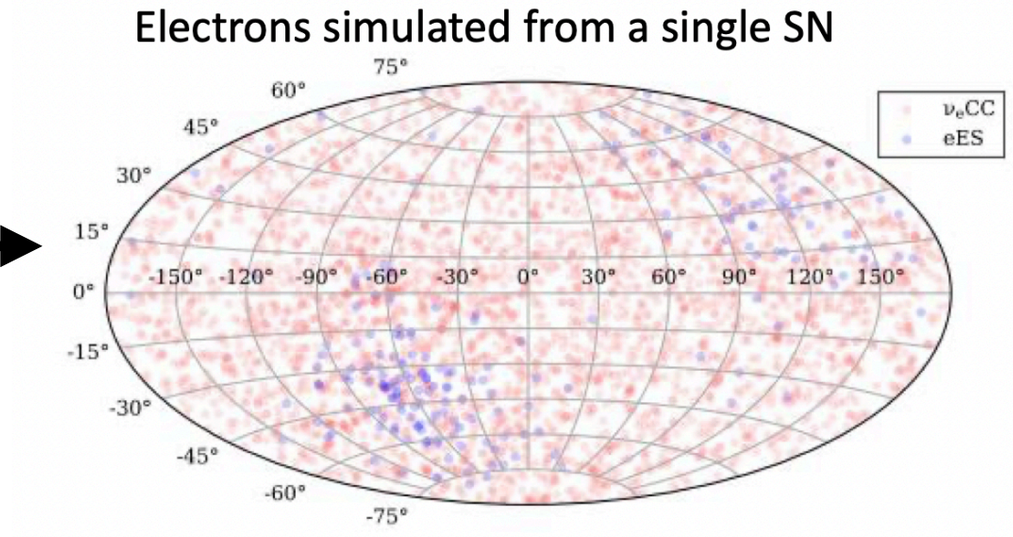

Channel	Events "GKVM" model
$\nu_e + ^{40}\mathrm{Ar} \to e^- + ^{40}\mathrm{K}^*$	3350
$\overline{\nu}_e + ^{40}\mathrm{Ar} \to e^+ + ^{40}\mathrm{Cl}^*$	160
$\nu_x + e^- \to \nu_x + e^-$	260
Total	3770

DUNE Collaboration, arXiv:2407.10339 [hep-ex]

10s of MeV Inelastic Neutrino-Nucleus Scattering: CRPA and MARLEY

- **CRPA implementation in MARLEY is on-going.**

S. Gardiner, P. B. Alzas, A. Nikolakopoulos, L. A. El-Haj, N. Jachowicz, V. Pandey, in preparation.

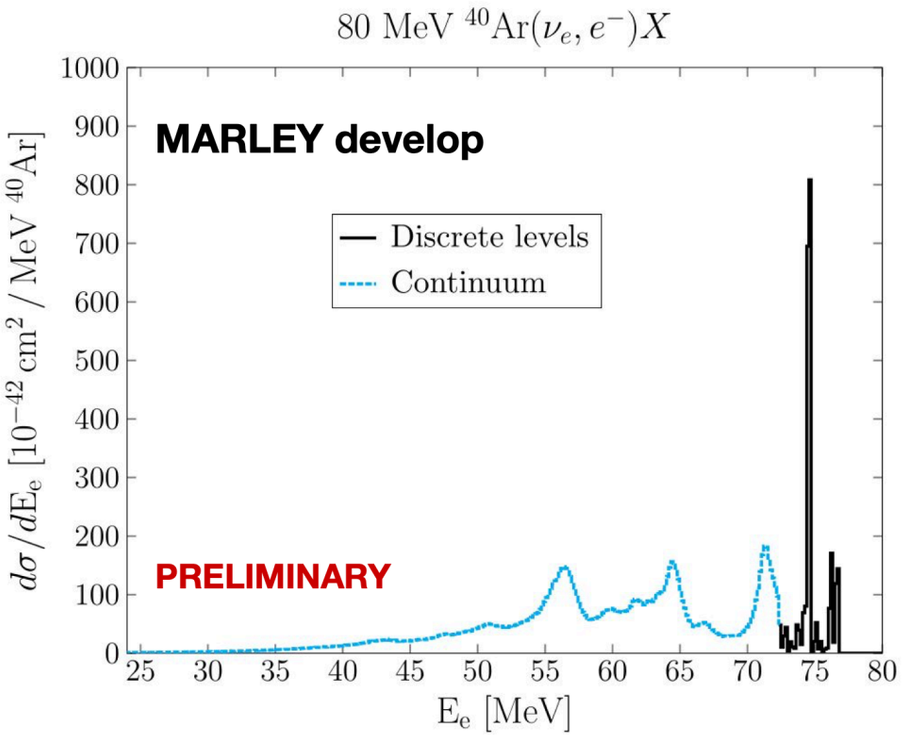

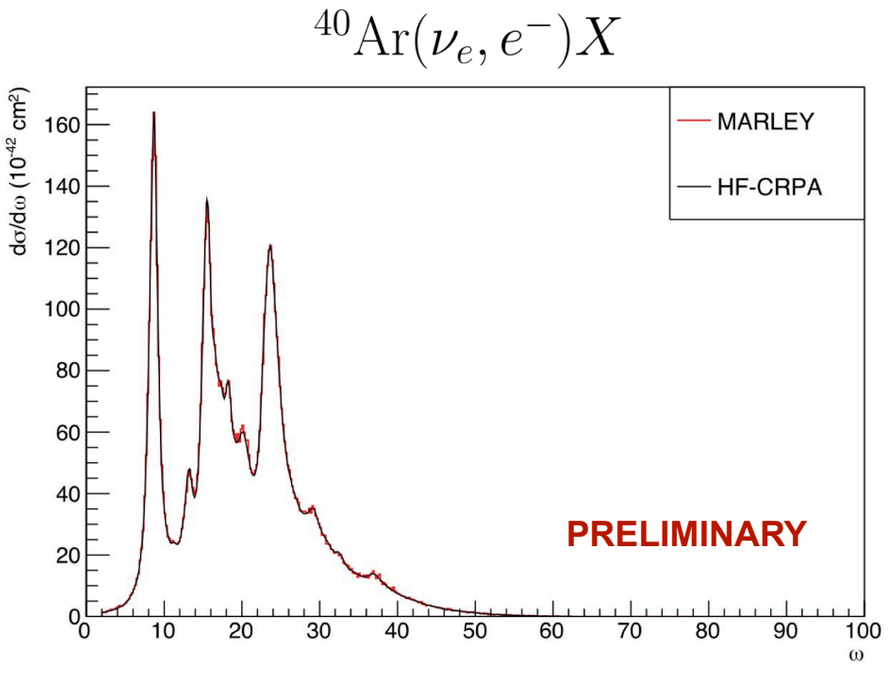

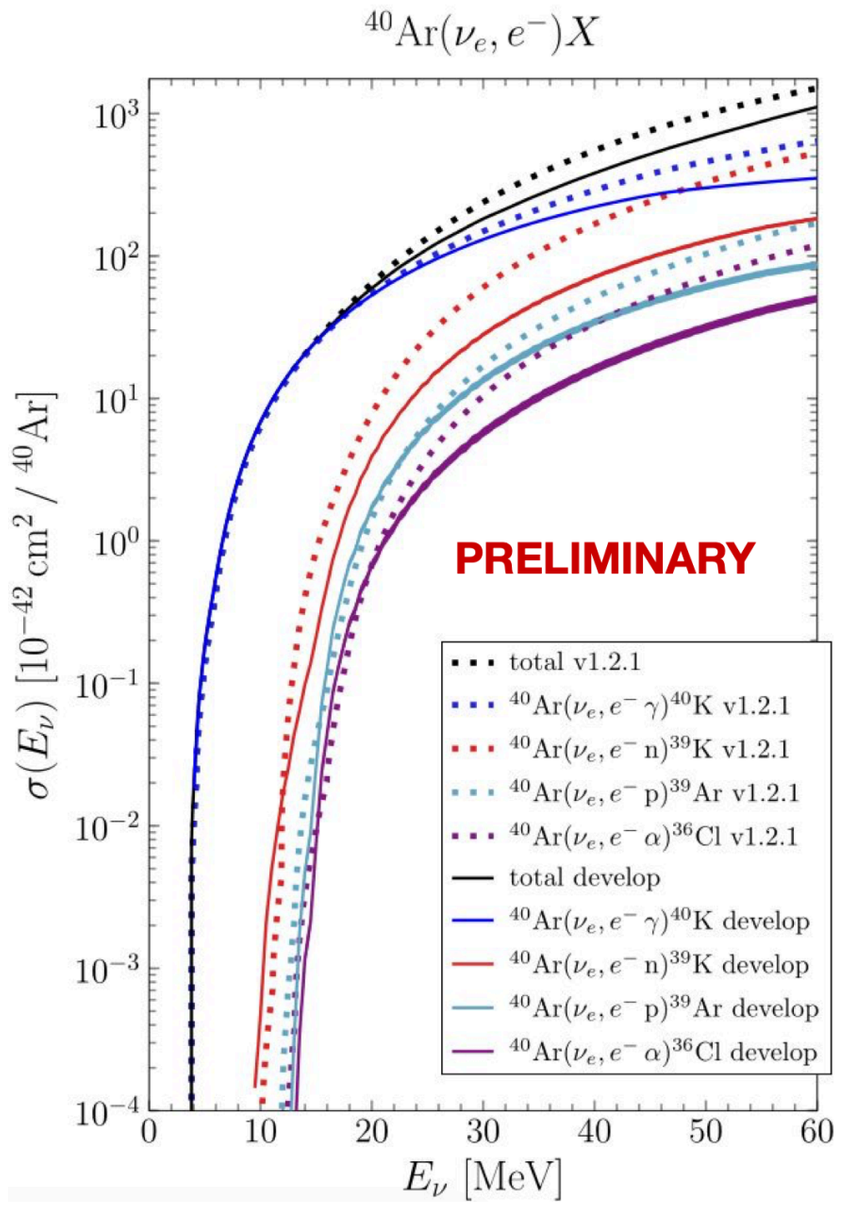

10s of MeV Inelastic Neutrino/DarkMatter-Nucleus Scattering

■ New theory improvements in-progress

- Adding ab-initio method's discrete states to CRPA's continuum

B. Dutta, B. Hu, N. Jachowicz, V. Pandey, M. Vanderpoorten, work in progress

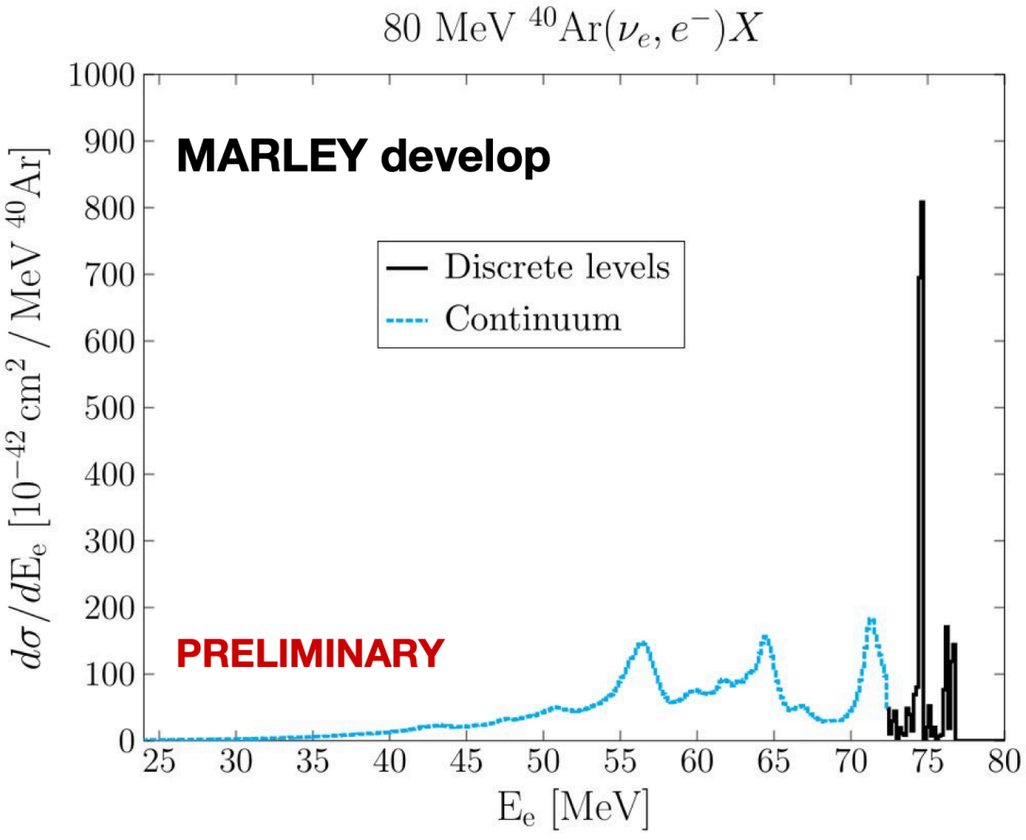

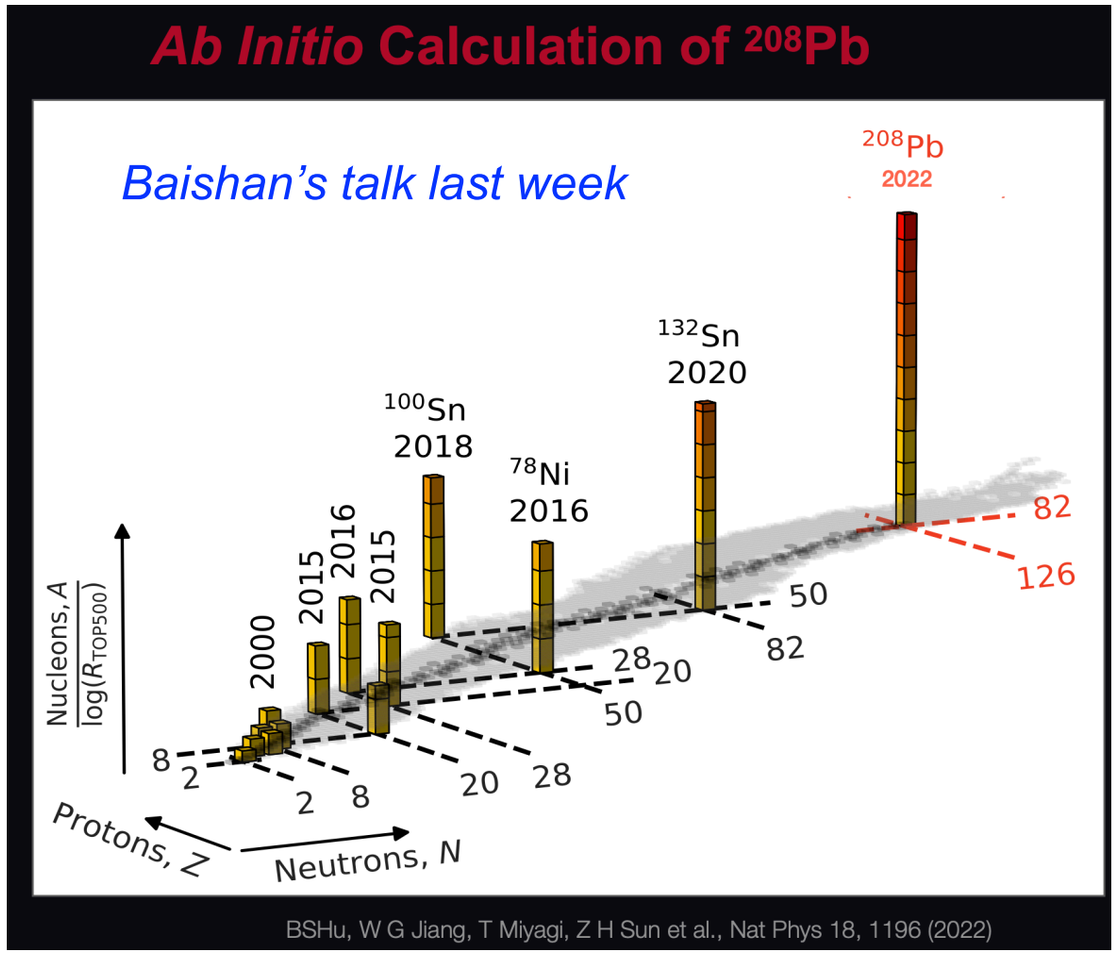

10s of MeV Inelastic Neutrino/DarkMatter-Nucleus Scattering

- **NC ν-nucleus $\rightarrow$ χ-nucleus scattering**

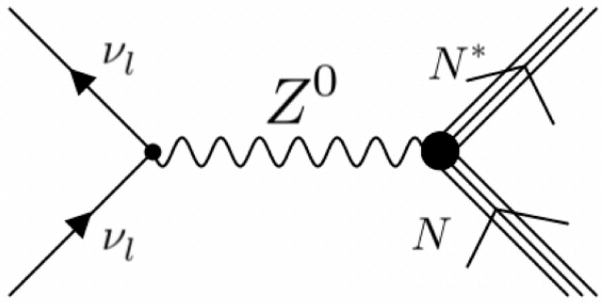

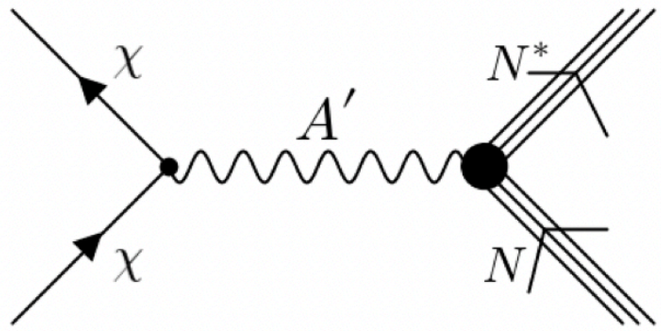

$$\pi^- + p \rightarrow n + A'$$
$$\pi^0 \rightarrow \gamma + A'$$
$$\eta^0 \rightarrow \gamma + A'$$
$$e^{\pm *} \rightarrow e^{\pm} + A'$$
$$A' \rightarrow \chi\bar{\chi}$$

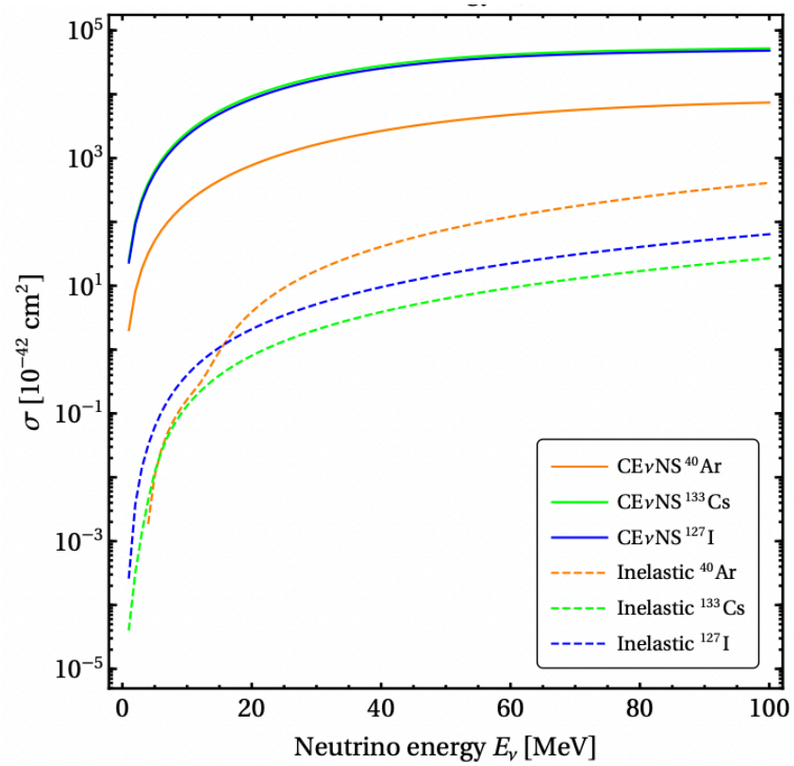

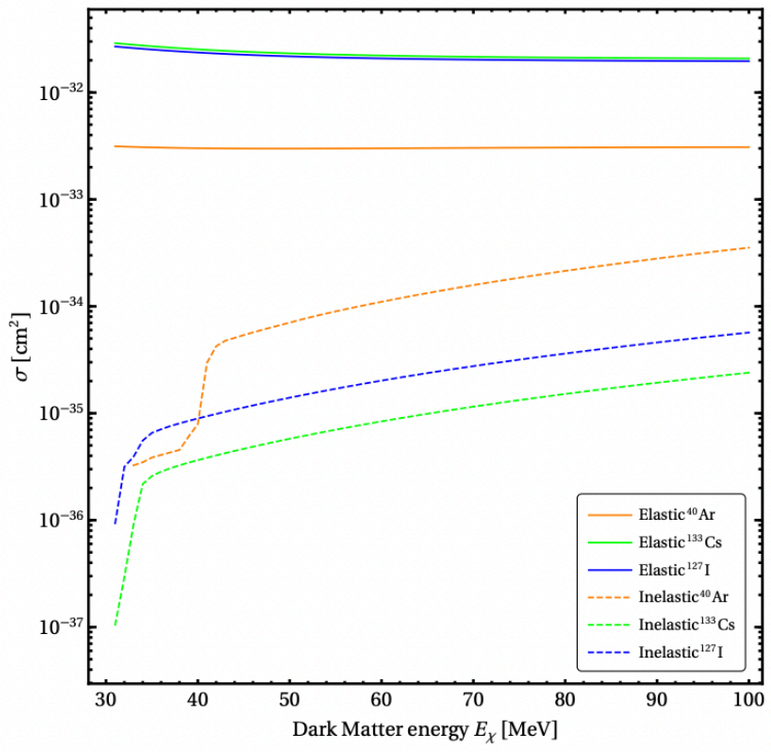

B. Dutta, W. C. Huang, J. L. Newstead, V. Pandey, Phys. Rev. D 106, 113006 (2022)

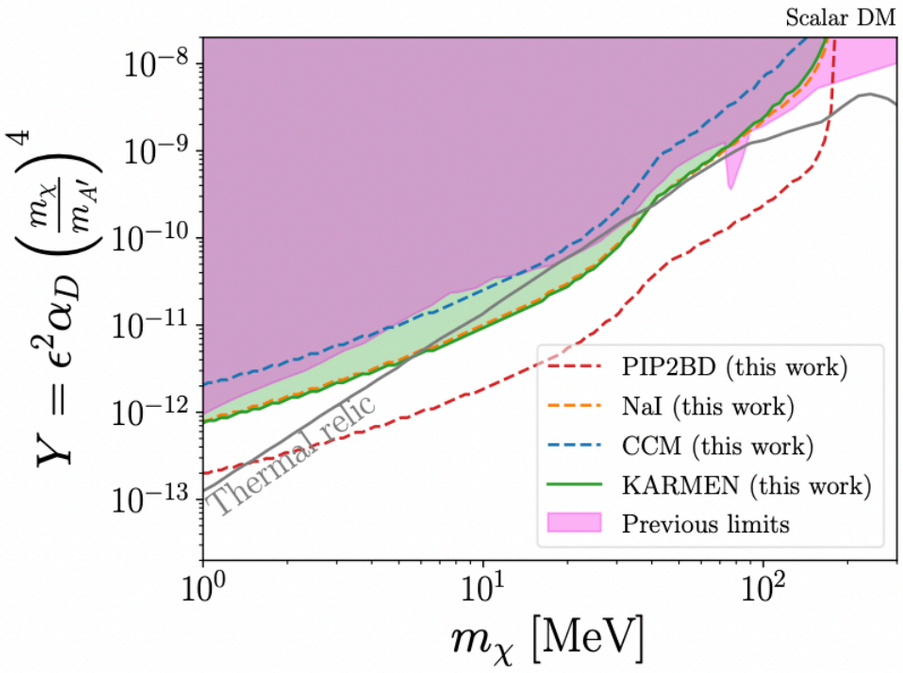

B. Dutta, W. C. Huang, J. L. Newstead, Phys. Rev. Lett. 131, 111801 (2023)

- Using ab-intio and CRPA together for DM scattering is expected to improve the sensitivities significantly

B. Dutta, B. Hu, N. Jachowicz, V. Pandey, M. Vanderpoorten, work in progress

10s of MeV Inelastic Neutrino-Nucleus Scattering: Measurements

✦ **CEvNS experiments at pion-decay at rest facilities are well suited to perform these measurements.**

- **Coherent CAPTAIN Mills (CCM) at LANL:** 10 ton LAr detector at Lujan center at LANL. Collected data in 2019, 2021, 2022 …

  ν_e CC cross section analysis is ongoing!

	Total events/year*
CEvNS	300.82
CC (ν_e)	57.25
NC	5.28

*6 months of running, at 23 m, for 5 tons. E_ν =30 MeV.

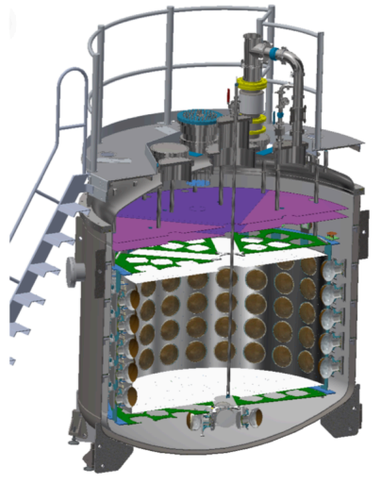

10s of MeV Inelastic Neutrino-Nucleus Scattering: Measurements

✦ **CEvNS experiments at pion-decay at rest facilities are well suited to perform these measurements.**

- **Coherent CAPTAIN Mills (CCM) at LANL:** 10 ton LAr detector at Lujan center at LANL.
  Collected data in 2019, 2021, 2022 …

  ν_e CC cross section analysis is ongoing!

	Total events/year*
CEvNS	300.82
CC (ν_e)	57.25
NC	5.28

*6 months of running, at 23 m, for 5 tons. E_ν =30 MeV.

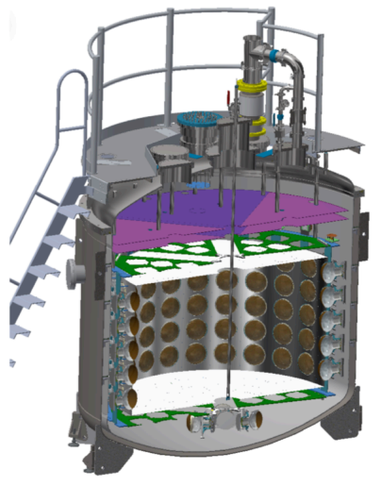

- **COHERENT at SNS:** COH-Ar-10 (24kg) LAr detector.
  COH-Ar-750 (750 kg) LAr detector is underway.

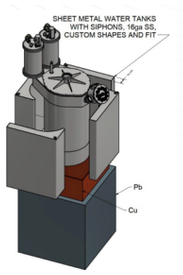

- **F2D2 at Fermilab**: Opportunity to measure these cross sections with ~100 ton scale LAr detectors at PIP-II Beam Stop Facility.

  arxiv:2311.09915 [hep-ex]

10s of MeV Neutrinos-Nucleus Scattering

Coherent elastic [CEvNS]

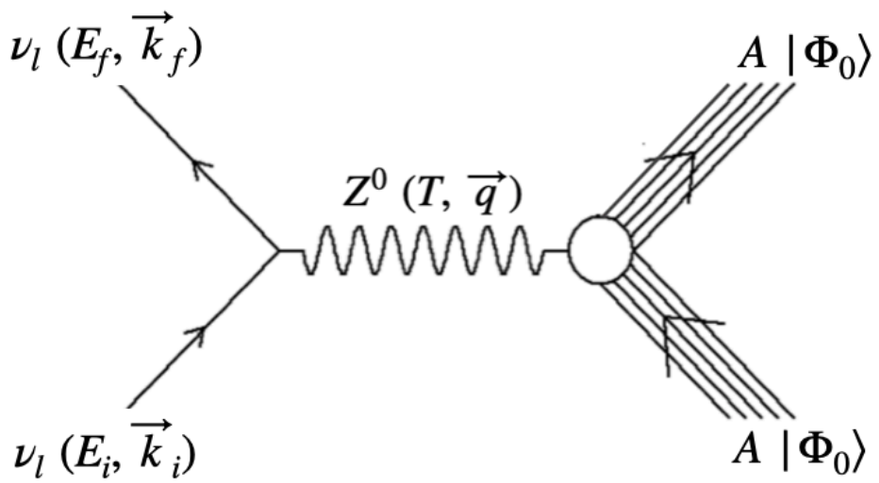

Inelastic CC/NC

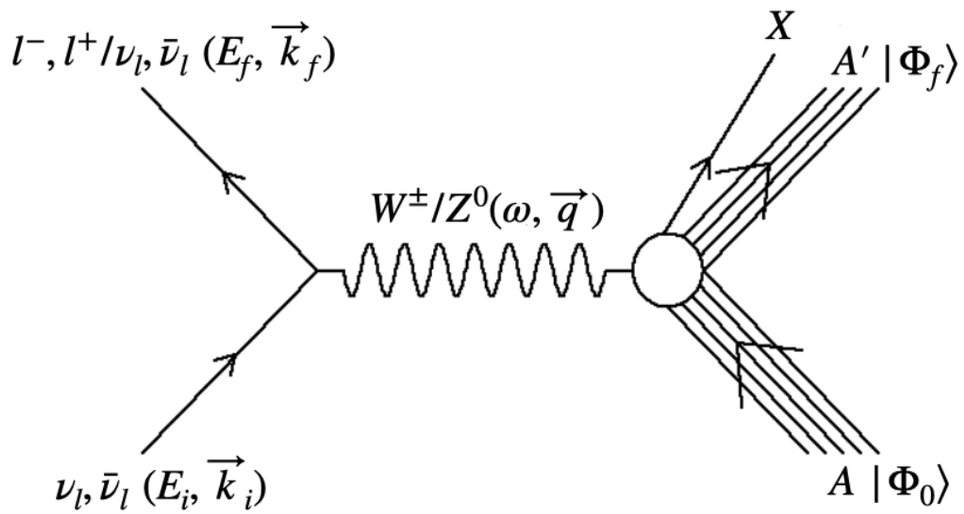

$$\sum_{fi} |\mathscr{M}|^2 \propto \frac{G_F^2}{2} L_{\mu\nu} W^{\mu\nu}$$

Leptonic Tensor: $L_{\mu\nu} = \sum_{fi} (\mathscr{J}_{l,\mu})^\dagger \mathscr{J}_{l,\nu}$

Hadronic Tensor: $W^{\mu\nu} = \sum_{fi} (\mathscr{J}_n^\mu)^\dagger \mathscr{J}_n^\nu$

Transition Amplitude: $\mathscr{J}_n^\mu = \langle \Phi_0 | \hat{J}_n^\mu(q) | \Phi_0 \rangle$

Transition Amplitude: $\mathscr{J}_n^\mu = \langle \Phi_f | \hat{J}_n^\mu(q) | \Phi_0 \rangle$

CEvNS Cross Section and Form Factors

- **Cross section (tree level)*:**

$$\frac{d\sigma}{dT} = \frac{G_F^2}{\pi} M_A \left[1 - \frac{T}{E_i} - \frac{M_A T}{2E_i^2}\right] \frac{Q_W^2}{4} F_W^2(q)$$

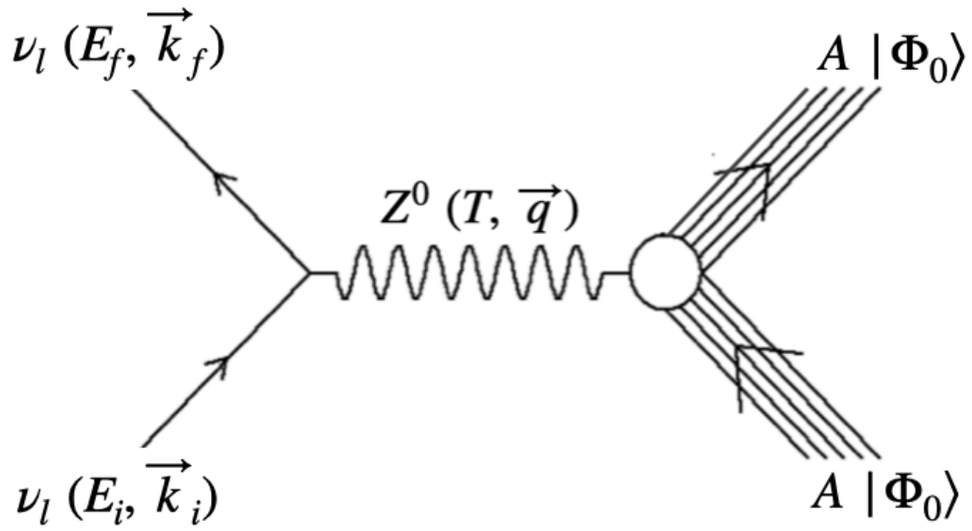

- **Weak Form Factor:**

$$\begin{aligned} Q_W\ F_W(q) &\approx \langle \Phi_0 | \hat{J}_0(q) | \Phi_0 \rangle \\ &\approx \left(1 - 4\sin^2\theta_W\right) Z\ F_p(q) - \ N\ F_n(q) \\ &\approx 2\pi \int d^3r\ \left[(1 - 4\sin^2\theta_W)\ \rho_p(r) - \rho_n(r)\ \right] j_0(qr) \end{aligned}$$

$$T \in \left[0, \frac{2E_i^2}{(M_A + 2E_i)}\right]$$

$$Q_W^2 = [g_n^V N + g_p^V Z]^2$$

*barring radiative corrections, for radiate corrections, see:

O. Tomalak, P. Machado, V. Pandey, R. Plestid, JHEP 02, 097 (2021)

CEvNS Cross Section and Form Factors

- **Cross section (tree level)*:**

$$\frac{d\sigma}{dT} = \frac{G_F^2}{\pi} M_A \left[1 - \frac{T}{E_i} - \frac{M_A T}{2E_i^2}\right] \frac{Q_W^2}{4} F_W^2(q)$$

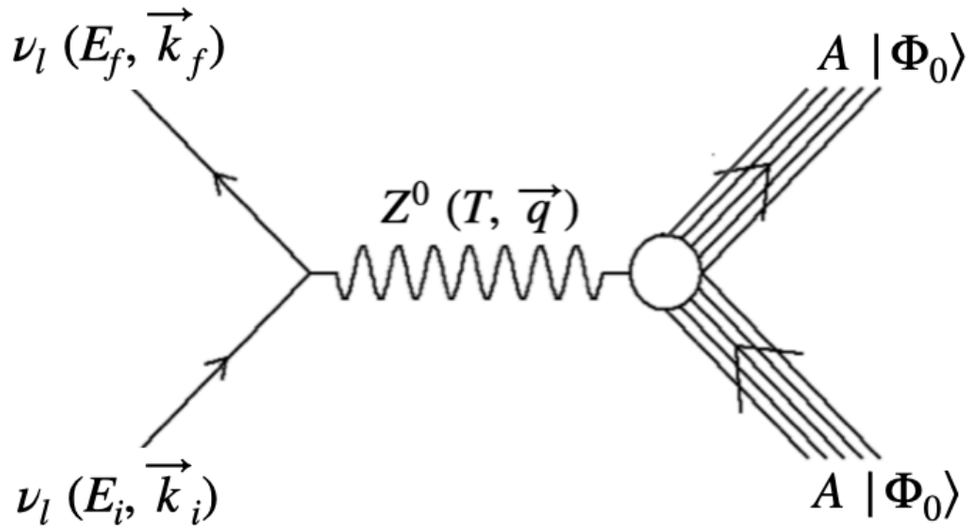

- **Weak Form Factor:**

$$\begin{aligned} Q_W\ F_W(q) &\approx \langle \Phi_0 | \hat{J}_0(q) | \Phi_0 \rangle \\ &\approx \left(1 - 4\sin^2\theta_W\right) Z\ F_p(q) - \ N\ F_n(q) \\ &\approx 2\pi \int d^3r\ \left[(1 - 4\sin^2\theta_W)\ \rho_p(r) - \rho_n(r)\ \right] j_0(qr) \end{aligned}$$

$$T \in \left[0, \frac{2E_i^2}{(M_A + 2E_i)}\right]$$

$$Q_W^2 = [g_n^V N + g_p^V Z]^2$$

Charge density and charge form factor: proton densities and charge form factors are well know through decades of elastic electron scattering experiments.

Neutron densities and neutron form factor: neutron densities and form factors are poorly known. Note that CEvNS is primarily sensitive to neutron density distributions ($1 - 4\sin^2\theta_W \approx 0$).

*barring radiative corrections, for radiate corrections, see:

O. Tomalak, P. Machado, V. Pandey, R. Plestid, JHEP 02, 097 (2021)

CEvNS and PVES Experimental Measurements

- **Electroweak probes** such as parity–violating electron scattering (**PVES**) and **CEvNS** provide relatively model-independent ways of determining weak form factor and neutron distributions.

T. W. Donnelly, J. Dubach and I. Sick,, Nucl. Phys. A 503, 589-631 (1989).

- **CEvNS Cross Section**

$$\frac{d\sigma}{dT} = \frac{G_F^2}{\pi} M_A \left[1 - \frac{T}{E_i} - \frac{M_A T}{2E_i^2}\right] \frac{Q_W^2}{4} F_W^2(q)$$

- **PVES Asymmetry**

$$A_{pv} = \frac{d\sigma/d\Omega_+ - d\sigma/d\Omega_-}{d\sigma/d\Omega_+ + d\sigma/d\Omega_-} = \frac{G_F q^2 |Q_W|}{4\pi\alpha\sqrt{2}Z} \frac{F_W(q)}{F_{ch}(q^2)}$$

- Both processes are described in first order perturbation theory via the exchange of an electroweak gauge boson between a lepton and a nucleus.
- CEvNS: the lepton is a neutrino and a Z^0 boson is exchanged.
- PVES: the lepton is an electron, but measuring the asymmetry allows one to select the interference between the γ and Z^0 exchange.
- As a result, both the CEvNS cross section and the PVES asymmetry depend on the weak form factor $F_W(Q^2)$, which is mostly determined by the neutron distribution within the nucleus.

CEvNS and PVES Experimental Measurements

- **Electroweak probes** such as parity–violating electron scattering (**PVES**) and **CEvNS** provide relatively model-independent ways of determining weak form factor and neutron distributions.

T. W. Donnelly, J. Dubach and I. Sick,, Nucl. Phys. A 503, 589-631 (1989).

- **CEvNS Cross Section**

D. Z. Freedman, Phys. Rev. D 9, 1389-1392 (1974)

"Freedman declared that the experimental detection of CEvNS would be an "act of hubris" due to the associated "grave experimental difficulties".

- **PVES Asymmetry**

- The maximum recoil energy

$$T_{\max} = \frac{E_\nu}{1 + M_A/(2E_\nu)}$$

CEvNS and PVES Experimental Measurements

- **Electroweak probes** such as parity–violating electron scattering (**PVES**) and **CEvNS** provide relatively model-independent ways of determining weak form factor and neutron distributions.
  - **CEvNS Cross Section**

$$\frac{d\sigma}{dT} = \frac{G_F^2}{\pi} M_A \left[1 - \frac{T}{E_i} - \frac{M_A T}{2E_i^2}\right] \frac{Q_W^2}{4} F_W^2(q)$$

COHERENT Collaboration at SNS at ORNL

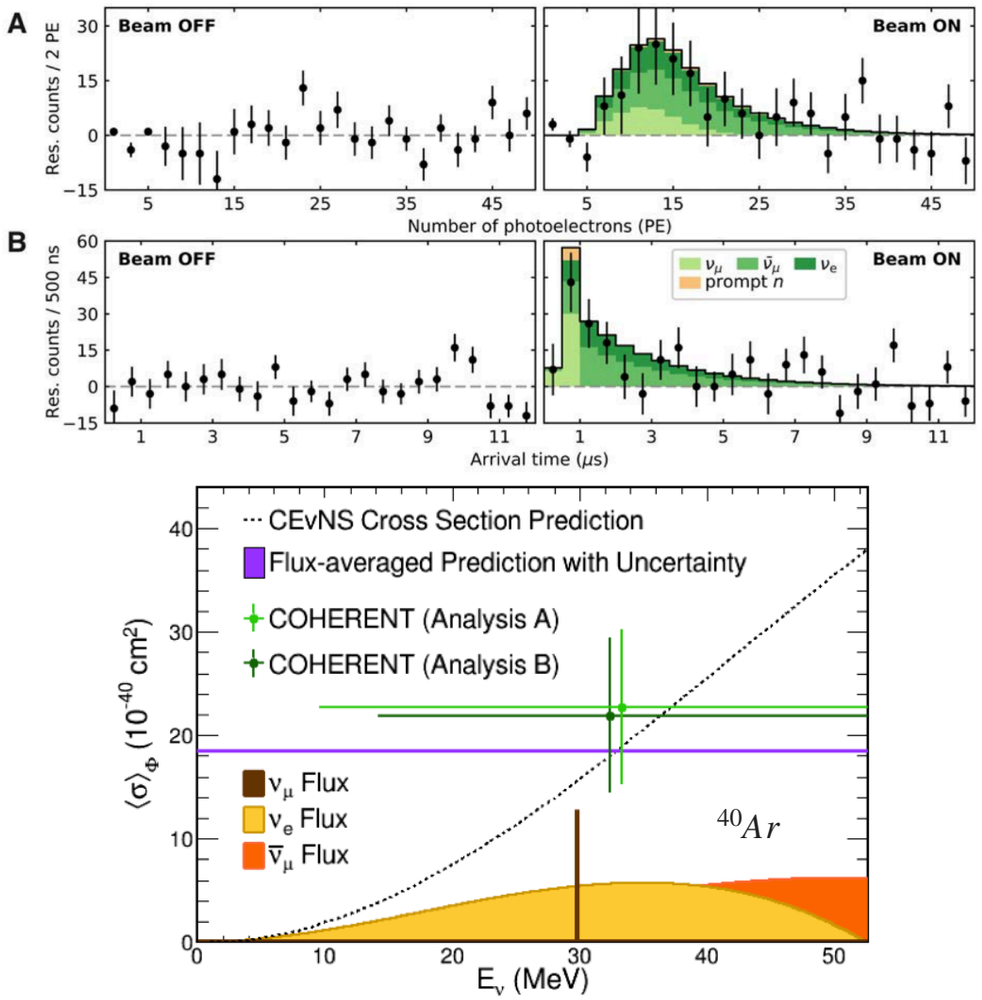

Science 357, 6356, 1123-1126 (2017)
Phys. Rev. Lett. 126, 012002 (2021)

CEvNS and PVES Experimental Measurements

- **Electroweak probes** such as parity–violating electron scattering (**PVES**) and **CEvNS** provide relatively model-independent ways of determining weak form factor and neutron distributions.

  - **CEvNS Cross Section**

$$\frac{d\sigma}{dT} = \frac{G_F^2}{\pi} M_A \left[1 - \frac{T}{E_i} - \frac{M_A T}{2E_i^2}\right] \frac{Q_W^2}{4} F_W^2(q)$$

COHERENT Collaboration at SNS at ORNL

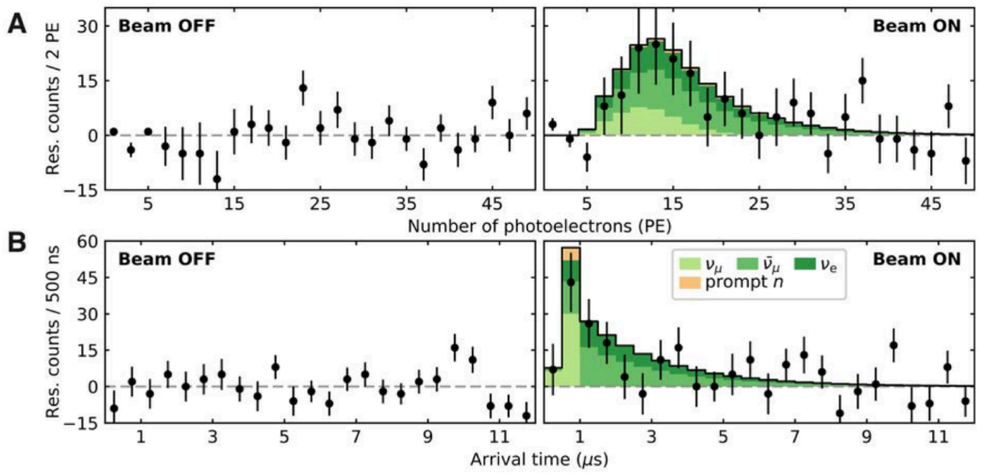

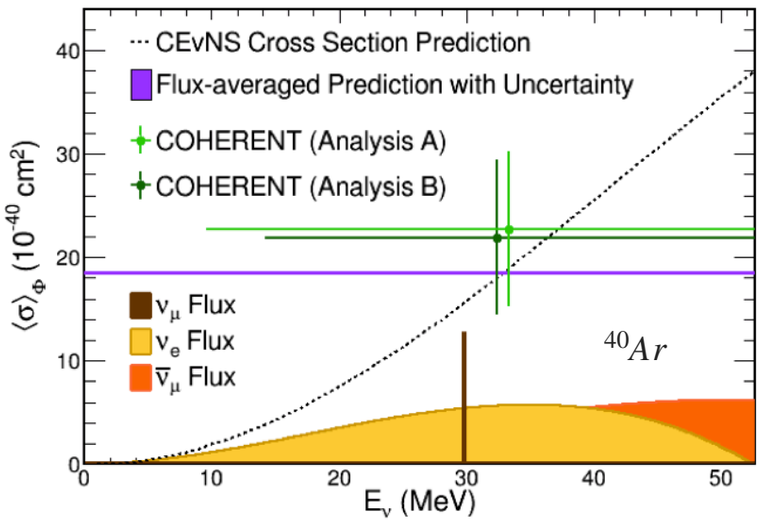

Science 357, 6356, 1123-1126 (2017)
Phys. Rev. Lett. 126, 012002 (2021)

LAr CEvNS detectors

Experiment	Mass (kg)	Distance from source (m)	Dates
CENNS10 (ORNL)	24	27.5	2017 -
CENNS750 (ORNL)	610	27.5	proposed
CCM (LANL)	10,000	20.0	2019 -
PIP2-BD at F2D2 (FNAL)	100,000	20.0	proposed

S. Carey and V. Pandey, 2508.xxxxx [hep-ph]

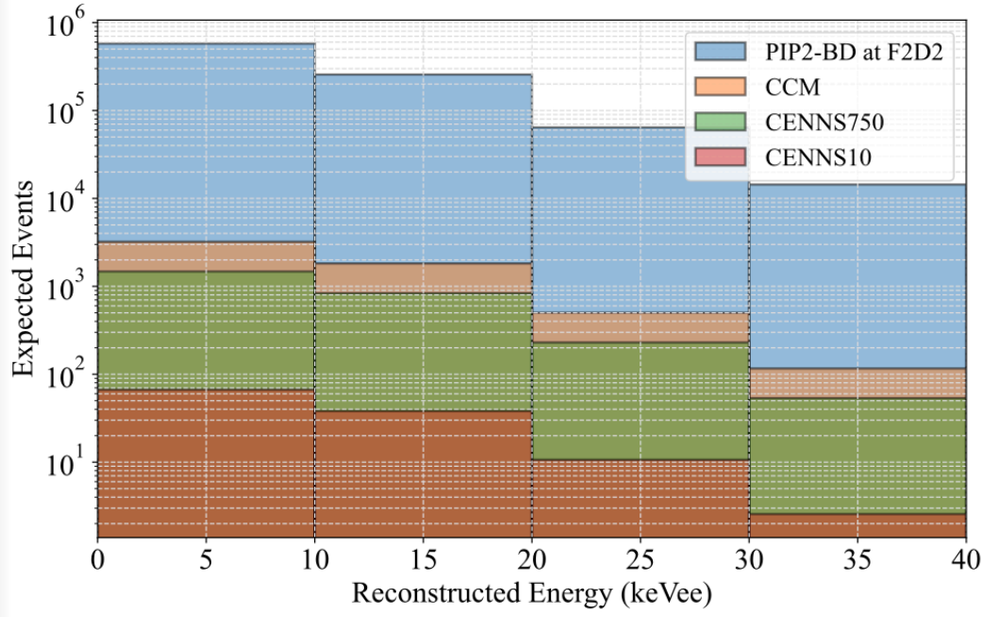

CEvNS and PVES Experimental Measurements

- **Electroweak probes** such as parity–violating electron scattering (**PVES**) and **CEvNS** provide relatively model-independent ways of determining weak form factor and neutron distributions.

• CEvNS Cross Section

$$\frac{d\sigma}{dT} = \frac{G_F^2}{\pi} M_A \left[1 - \frac{T}{E_i} - \frac{M_A T}{2E_i^2}\right] \frac{Q_W^2}{4} F_W^2(q)$$

COHERENT Collaboration at SNS at ORNL

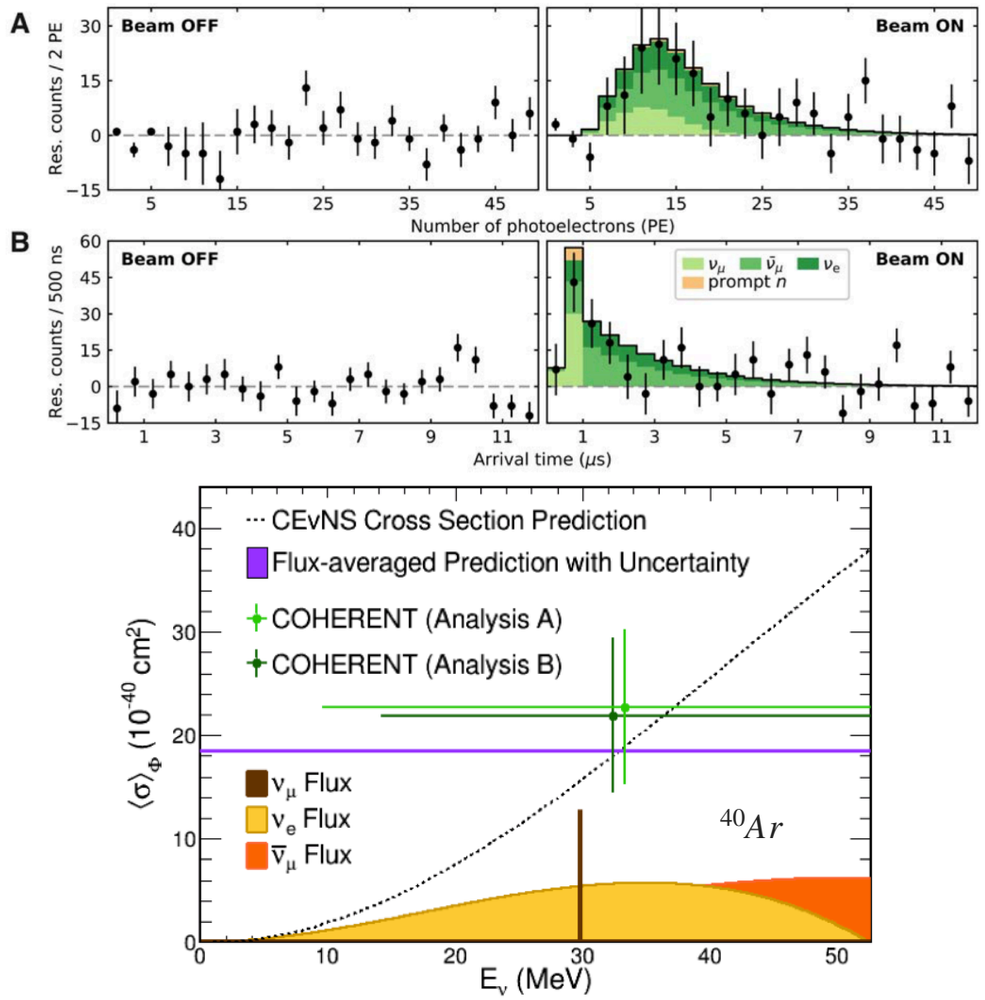

Science 357, 6356, 1123-1126 (2017)
Phys. Rev. Lett. 126, 012002 (2021)

• PVES Asymmetry

▸ The parity violating asymmetry for elastic electron scattering is the fractional difference in cross section for positive helicity and negative helicity electrons.

$$A_{pv} = \frac{d\sigma/d\Omega_+ - d\sigma/d\Omega_-}{d\sigma/d\Omega_+ + d\sigma/d\Omega_-} = \frac{G_F q^2 |Q_W|}{4\pi\alpha\sqrt{2}Z} \frac{F_W(q)}{F_{ch}(q^2)}$$

- Here F_{ch} is the charge form factor that is typically known from unpolarized electron scattering. Therefore, one can extract F_W from the measurement of A_{PV}.

Experiment	Target	q^2 (GeV^2)	A_{pv} (ppm)
PREX	^{208}Pb	0.00616	0.550 ± 0.018
CREX	^{48}Ca	0.0297	
Qweak	^{27}Al	0.0236	2.16 ± 0.19
MREX	^{208}Pb	0.0073	

arXiv:2203.06853 [hep-ex]

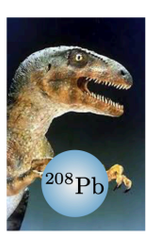

Pb Radius Experiment (PREX)

Calcium Radius Experiment (CREX)

MREX

Mainz Radius Experiment (MREX)
At P2 experimental hall with ^{208}Pb

CEvNS Cross Section Calculations: HF-SkE2

- Nuclear ground state described as a many-body quantum mechanical system where nucleons are bound in an effective nuclear potential.
- Solve Hartree-Fock (**HF**) equation with a Skyrme (**SkE2**) nuclear potential to obtain single–nucleon wave functions for the bound nucleons in the nuclear ground state.
- Evaluate proton and neutron density distributions and form factors

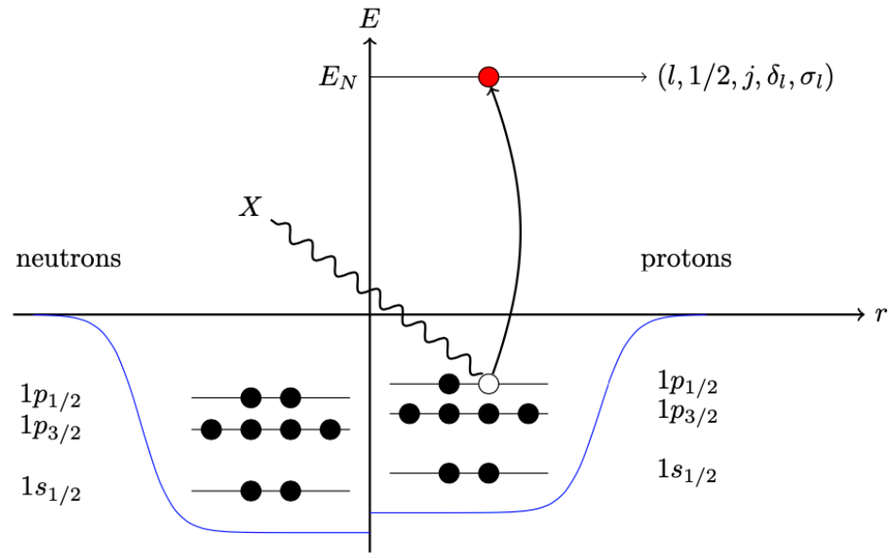

$$\rho_\tau(r) = \frac{1}{4\pi r^2} \sum_\alpha v^2_{\alpha,\tau}\ (2j_\alpha + 1)\,|\,\phi_{\alpha,\tau}(r)\,|^2 \qquad F_\tau(q) = \frac{1}{N}\int d^3r\ j_o(qr)\ \rho_\tau(r)$$

$$(\alpha \in n_\alpha, l_\alpha, j_\alpha)$$

$$(\tau = p, n)$$

CEvNS Cross Section Calculations: HF-SkE2

- Nuclear ground state described as a many-body quantum mechanical system where nucleons are bound in an effective nuclear potential.
- Solve Hartree-Fock (**HF**) equation with a Skyrme (**SkE2**) nuclear potential to obtain single–nucleon wave functions for the bound nucleons in the nuclear ground state.
- Evaluate proton and neutron density distributions and form factors

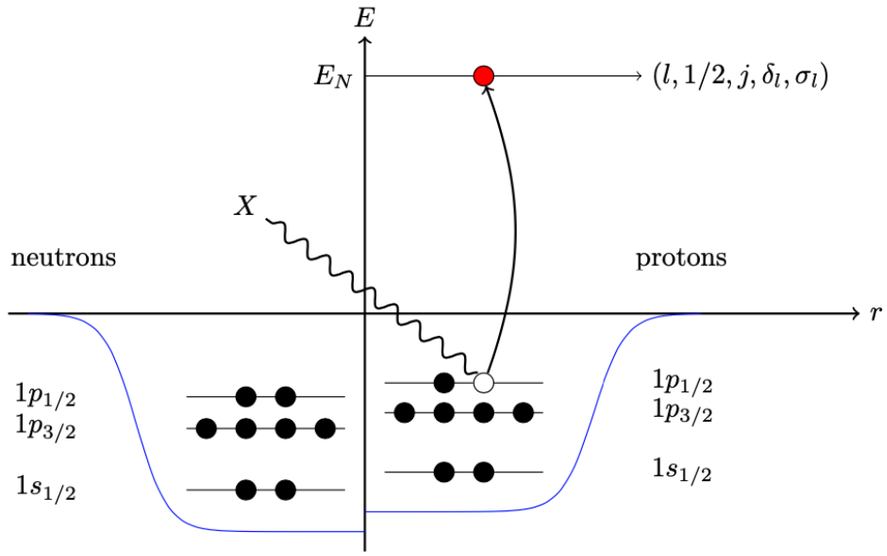

$$\rho_\tau(r) = \frac{1}{4\pi r^2} \sum_\alpha v^2_{\alpha,\tau}\ (2j_\alpha + 1)\,|\,\phi_{\alpha,\tau}(r)\,|^2 \qquad F_\tau(q) = \frac{1}{N}\int d^3r\ j_o(qr)\ \rho_\tau(r)$$

$$(\alpha \in n_\alpha, l_\alpha, j_\alpha)$$

$$(\tau = p, n)$$

Charge Form Factor

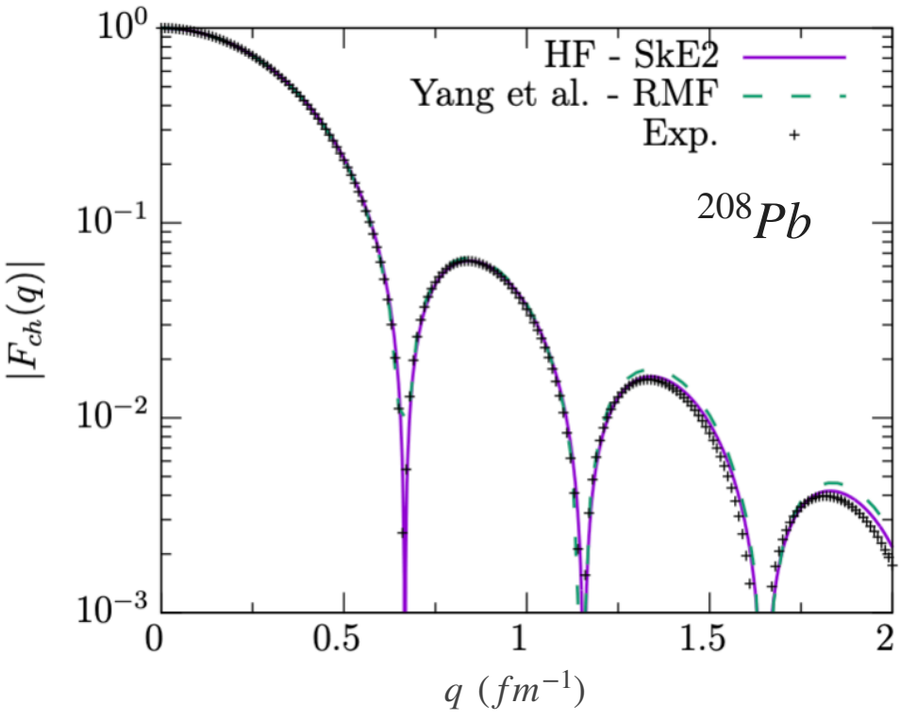

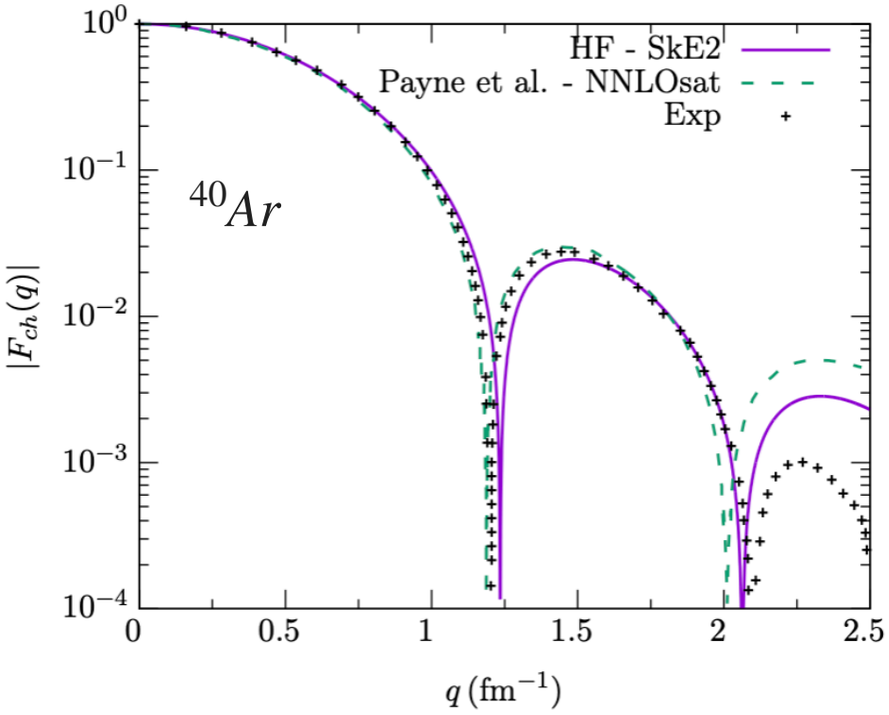

N. Van Dessel, VP, H. Ray and N. Jachowicz, Universe 9, 207 (2023)

Data: H. De Vries, et al., Atom. Data Nucl. Data Tabl. 36, 495 (1987), C. R. Ottermann et al., Nucl. Phys. A 379, 396 (1982)

CEvNS Cross Section Calculations: HF-SkE2

- Nuclear ground state described as a many-body quantum mechanical system where nucleons are bound in an effective nuclear potential.
- Solve Hartree-Fock (**HF**) equation with a Skyrme (**SkE2**) nuclear potential to obtain single–nucleon wave functions for the bound nucleons in the nuclear ground state.
- Evaluate proton and neutron density distributions and form factors

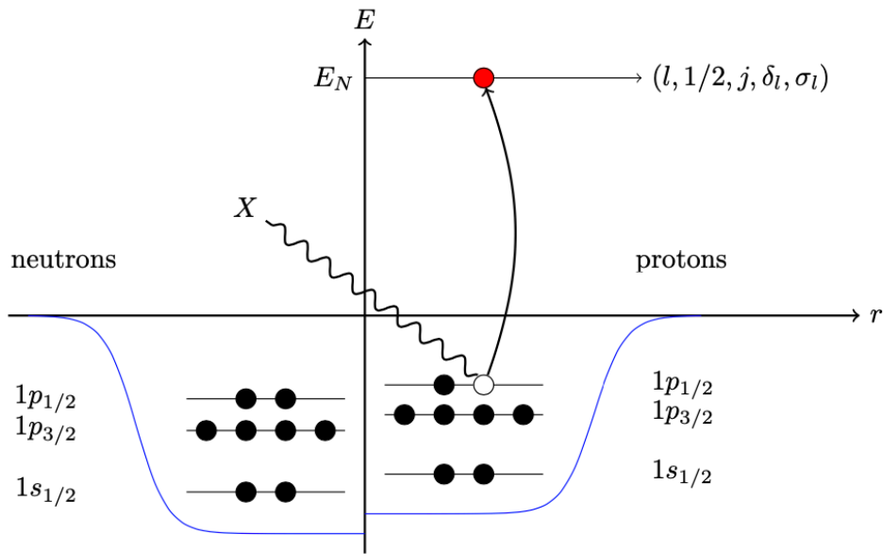

$$\rho_\tau(r) = \frac{1}{4\pi r^2} \sum_\alpha v^2_{\alpha,\tau}\ (2j_\alpha + 1)\,|\,\phi_{\alpha,\tau}(r)\,|^2 \qquad F_\tau(q) = \frac{1}{N}\int d^3r\ j_o(qr)\ \rho_\tau(r)$$

$$(\alpha \in n_\alpha, l_\alpha, j_\alpha)$$

$$(\tau = p, n)$$

Weak Form Factor

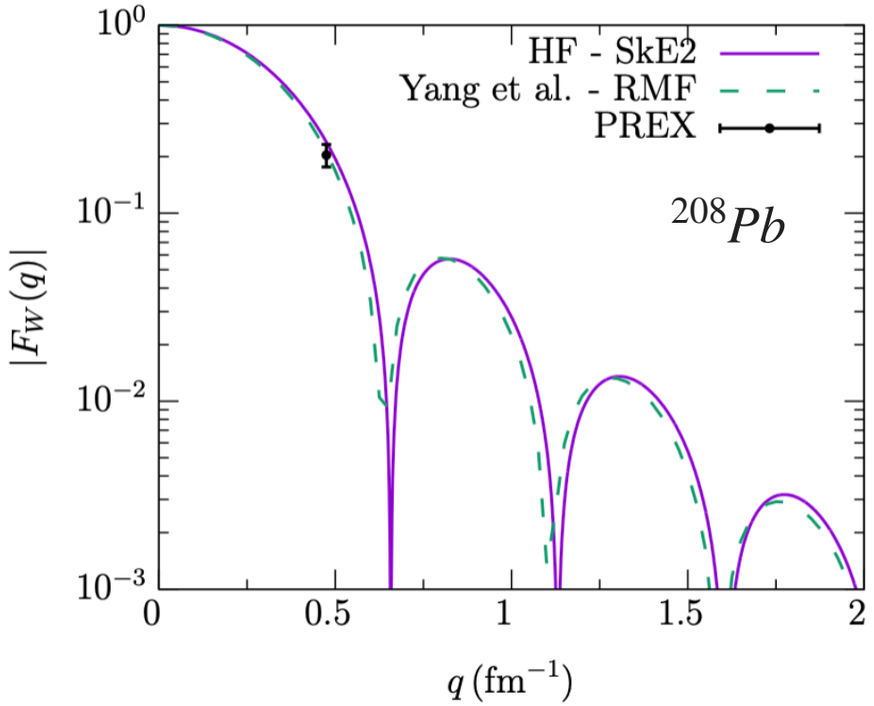

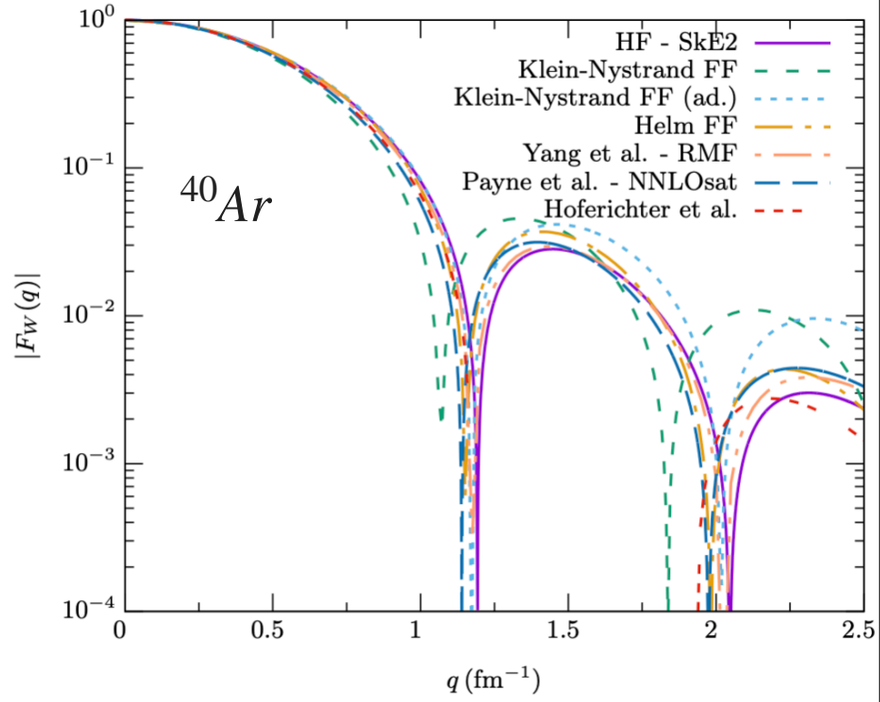

N. Van Dessel, VP, H. Ray and N. Jachowicz, Universe 9, 207 (2023)

Data: S. Abrahamyan et al., Phys. Rev. Lett. 108, 112502 (2012)

CEvNS Cross Section Calculations: HF-SkE2

- Differential cross section on ^{40}Ar, as a function of recoil energy T and scattering angle $\cos\theta_f$.
- The effects of nuclear structure physics are more prominent as the neutrino energy increases.
- Most of the cross section strength lies in the lower-end of the recoil energy and in the forward scattering as the cross section falls off rapidly at higher T (top panels) and higher θ_f values (bottom panels).

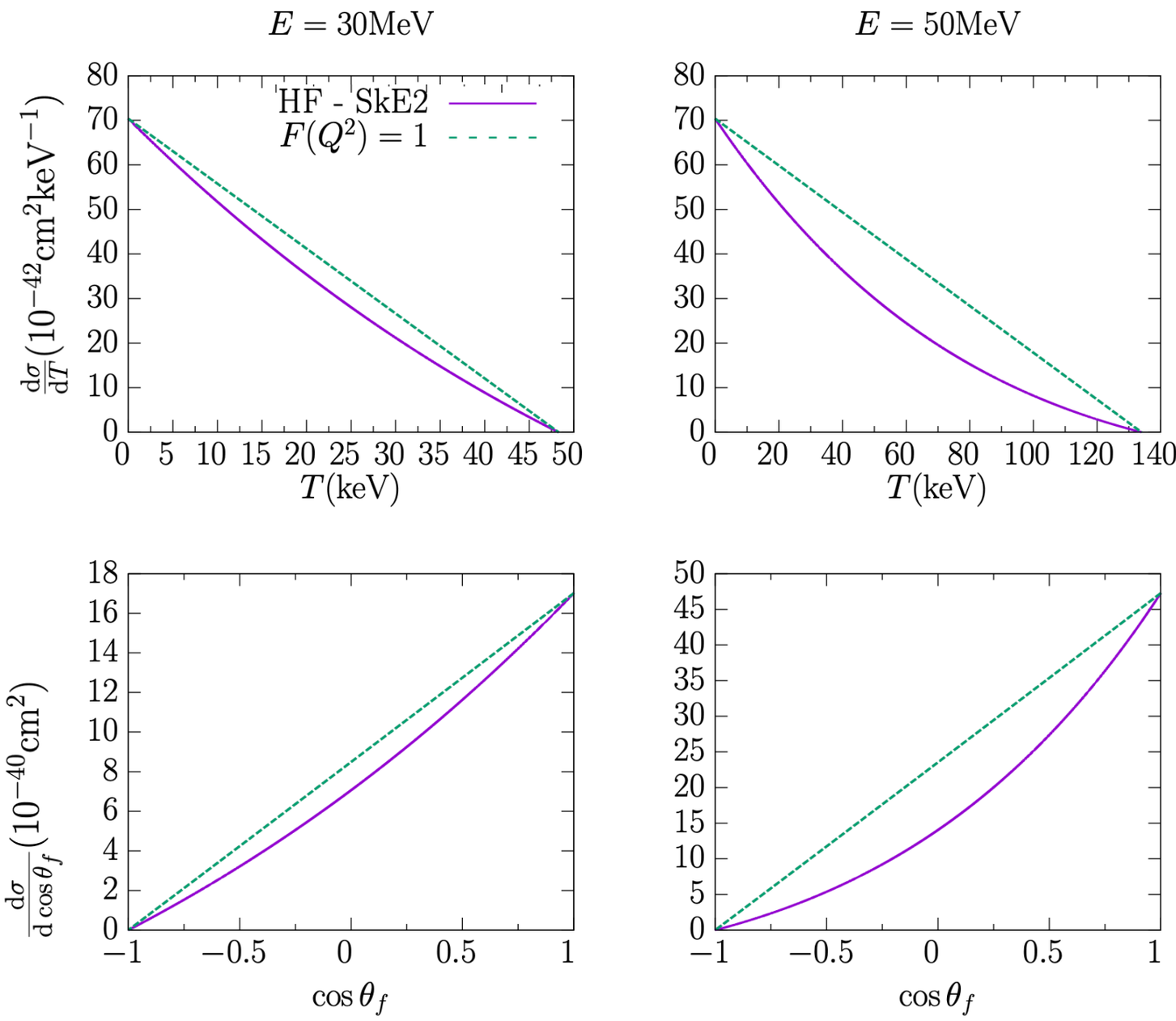

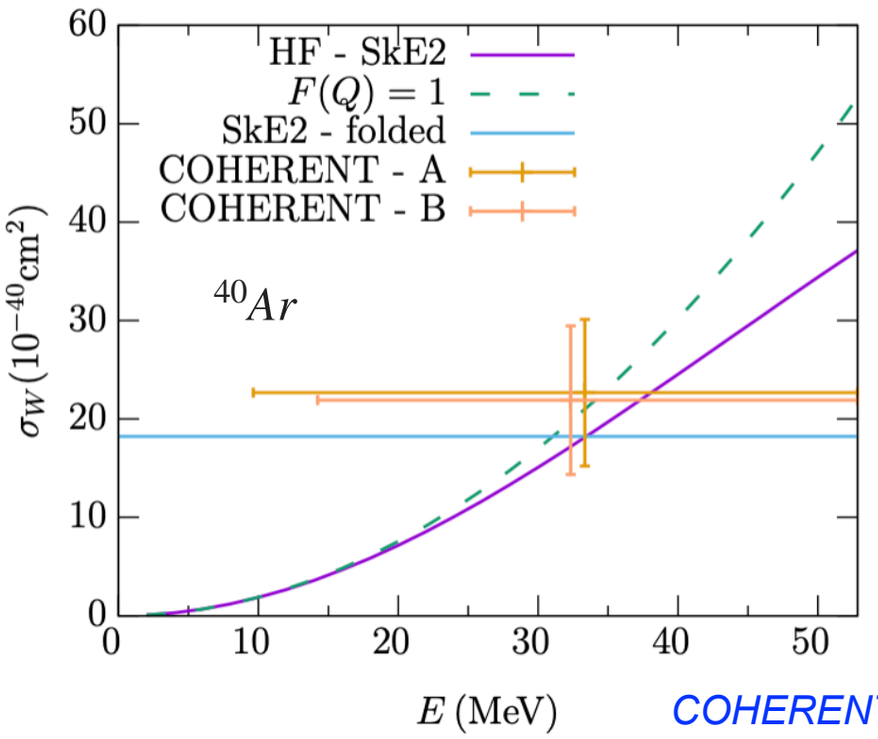

N. Van Dessel, VP, H. Ray and N. Jachowicz, Universe 9, 207 (2023)

COHERENT data: arXiv:2003.10630 [nucl-ex].

CEvNS Cross Section and Form Factors

✱ Only a few percent theoretical uncertainty on the CEvNS cross section!

- Relative CEvNS cross section differences between the results of different calculations.

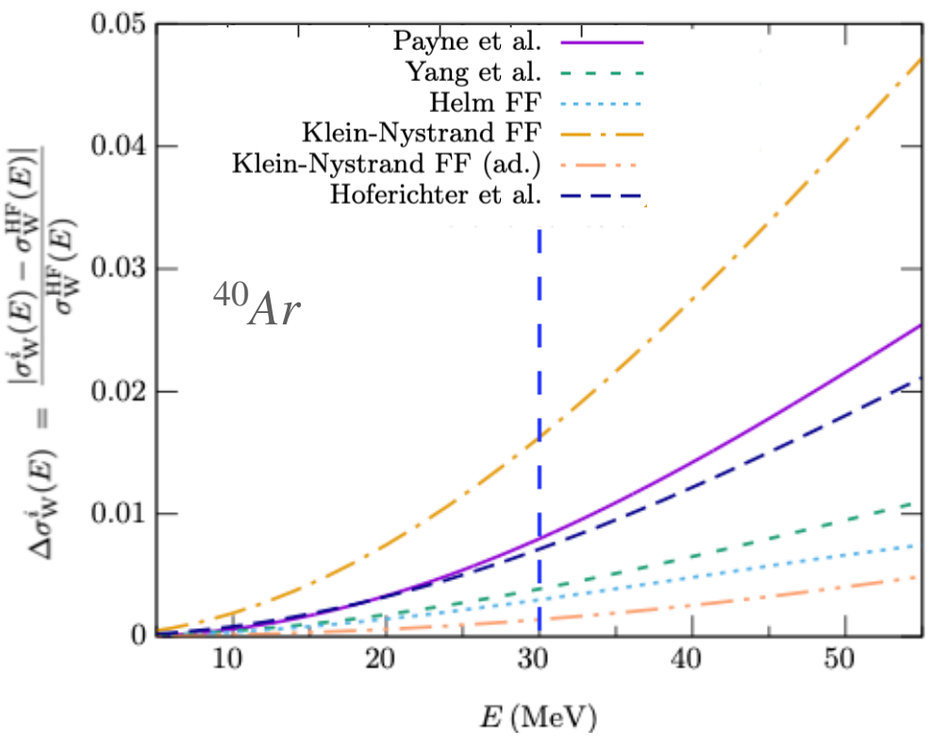

N. Van Dessel, V. Pandey, H. Ray and N. Jachowicz, Universe 9, 207 (2023)

- Relative CEvNS cross section theoretical uncertainty on ^{40}Ar (includes nuclear, nucleonic, hadronic, quark levels as well as perturbative errors):

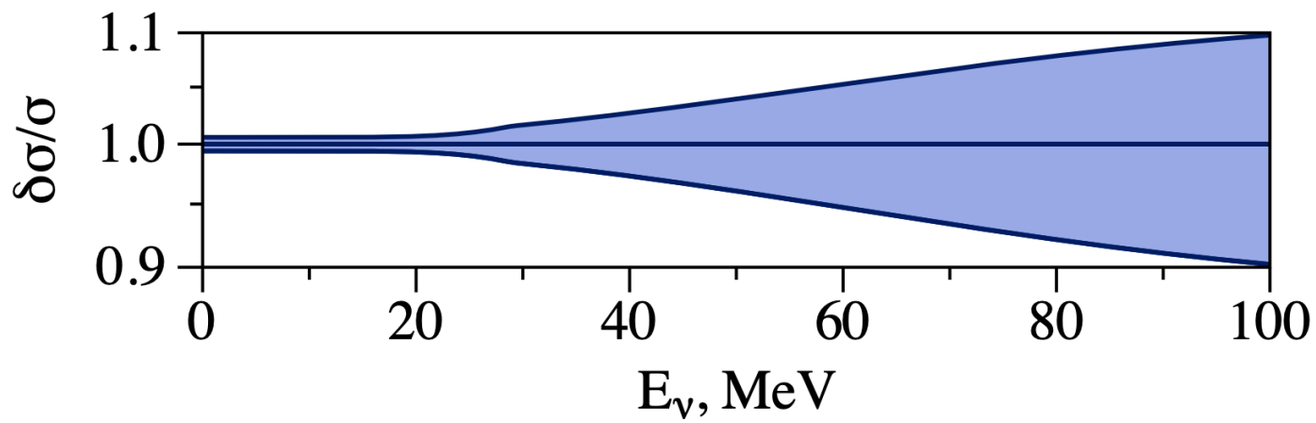

O. Tomalak, P. Machado, V. Pandey, R. Plestid, JHEP 02, 097 (2021)

Yang et al. Phys. Rev. C 100, 054301 (2019)]

Payne et al., Phys. Rev. C 100, 061304 (2019)

Hoferichter et al. [arXiv:2007.08529 [hep-ph]]

CEvNS Cross Section and Form Factors

✱ Only a few percent theoretical uncertainty on the CEvNS cross section!

- Relative CEvNS cross section differences between the results of different calculations.

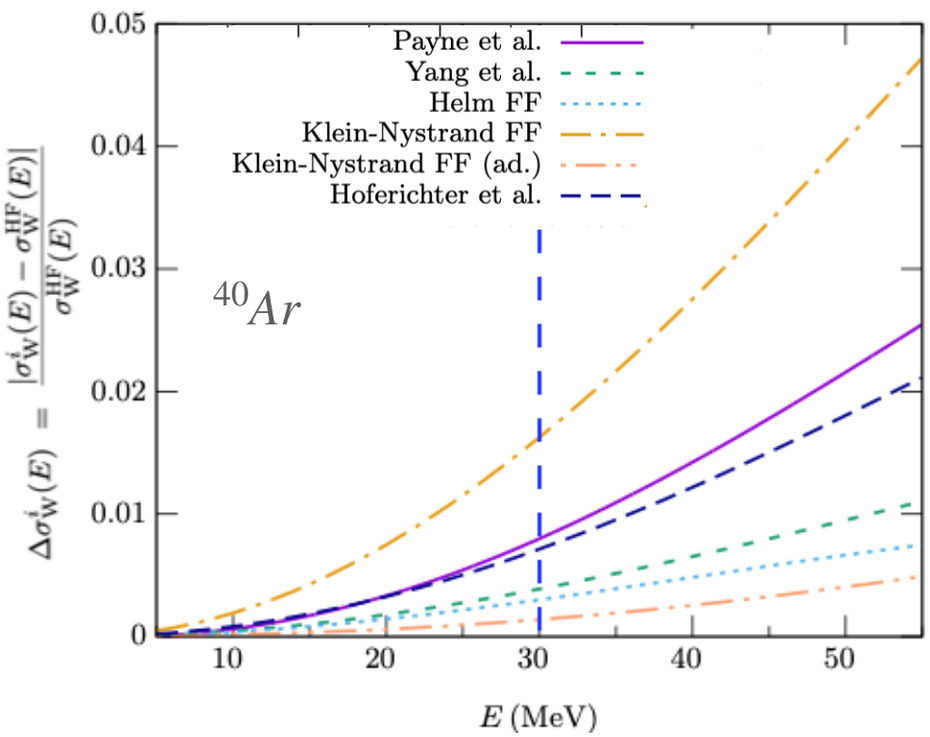

N. Van Dessel, V. Pandey, H. Ray and N. Jachowicz, Universe 9, 207 (2023)

- Relative CEvNS cross section theoretical uncertainty on ^{40}Ar (includes nuclear, nucleonic, hadronic, quark levels as well as perturbative errors):

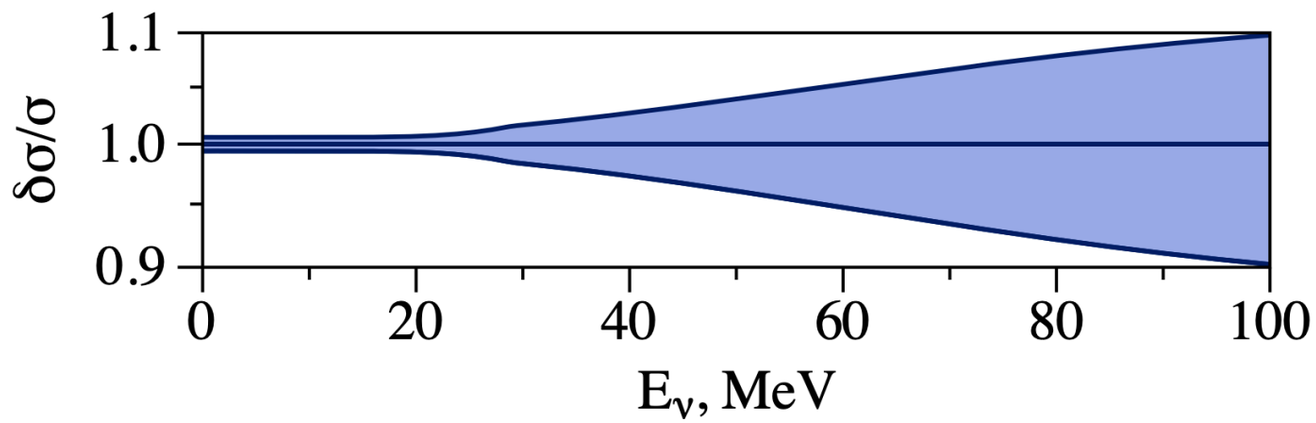

O. Tomalak, P. Machado, V. Pandey, R. Plestid, JHEP 02, 097 (2021)

- Any deviation from the SM predicted event rate either with a change in the total event rate or with a change in the shape of the recoil spectrum → new physics.

- SM expectation of CEvNS cross section have to be know at a precision that allows resolving degeneracies in the standard and non-standard physics observables.

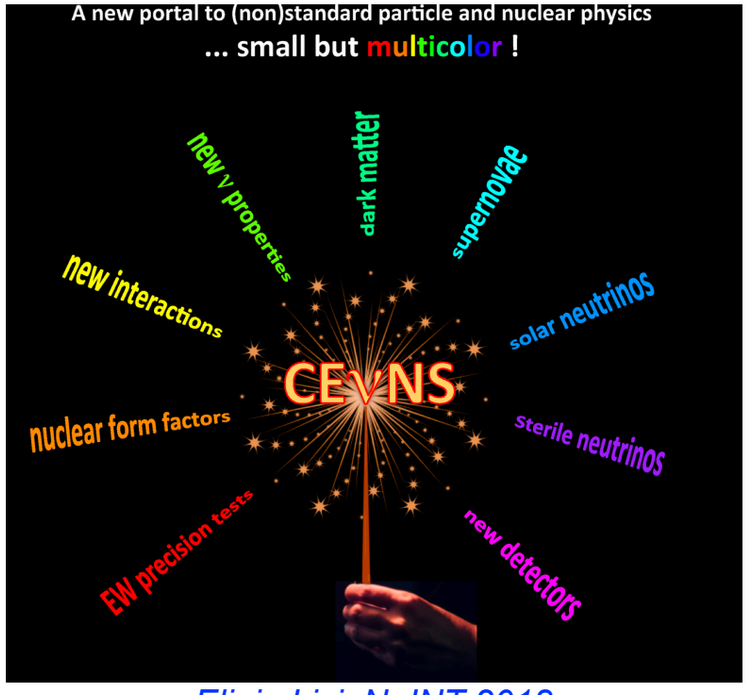

Eligio Lisi, NuINT 2018

Fermilab

CEvNS and New Physics

S. Carey and V. Pandey, 2508.xxxxx [hep-ph]

Experiment	Mass (kg)	Distance from source (m)	Dates
CENNS10 (ORNL)	24	27.5	2017 -
CENNS750 (ORNL)	610	27.5	proposed
CCM (LANL)	10,000	20.0	2019 -
PIP2-BD at F2D2 (FNAL)	100,000	20.0	proposed

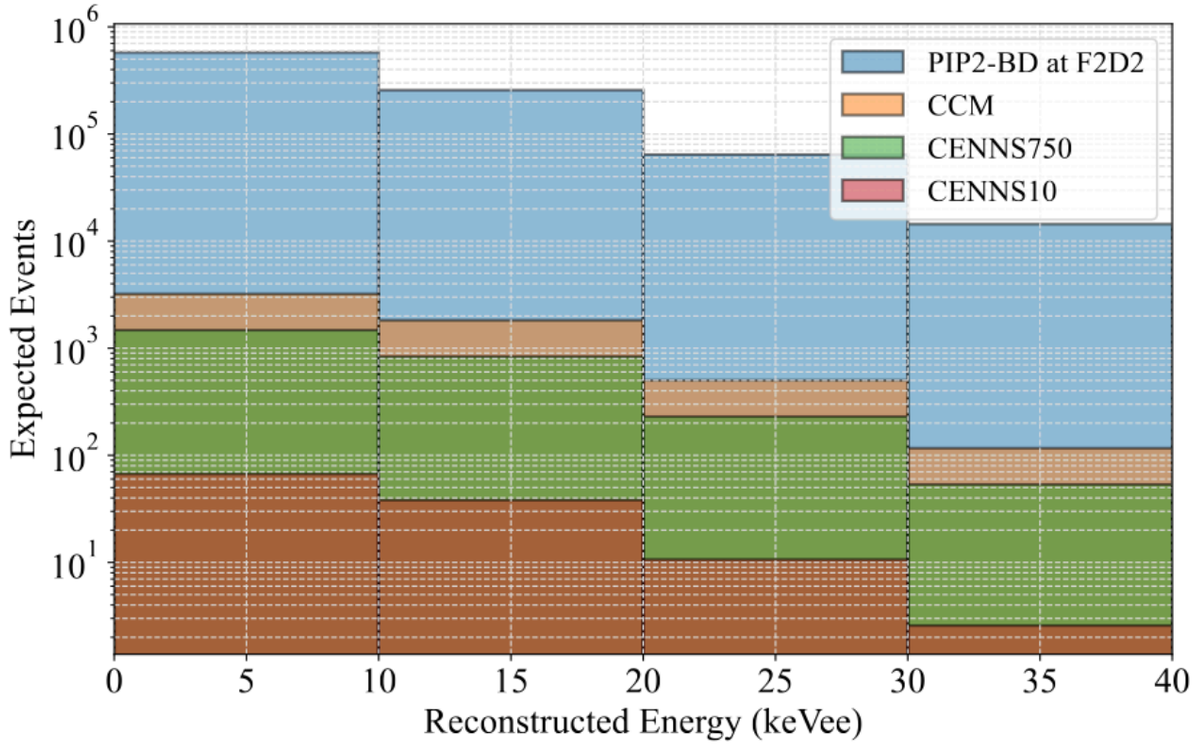

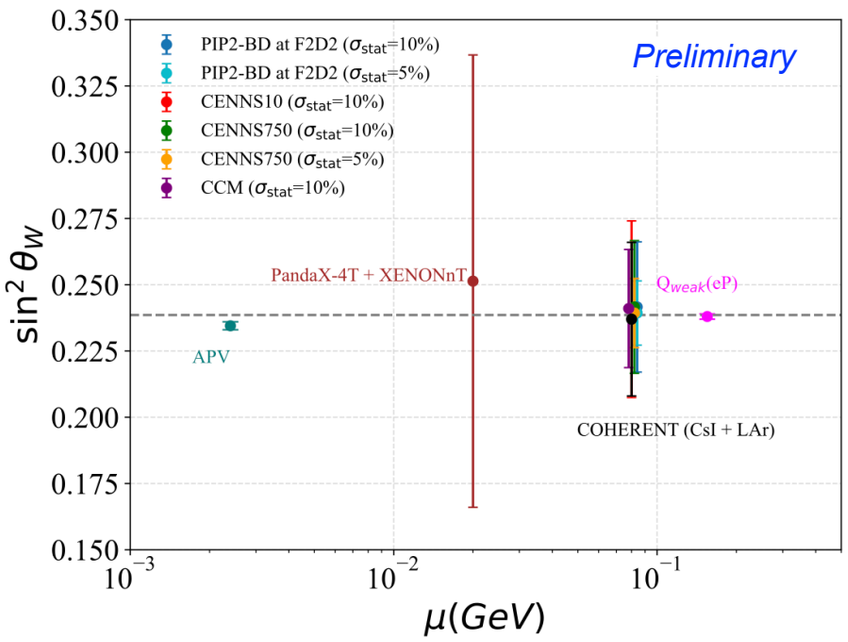

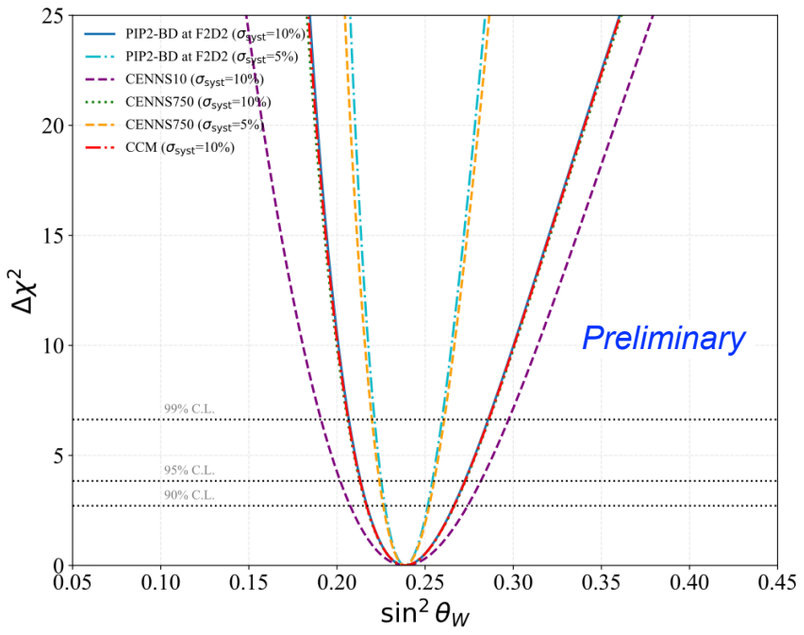

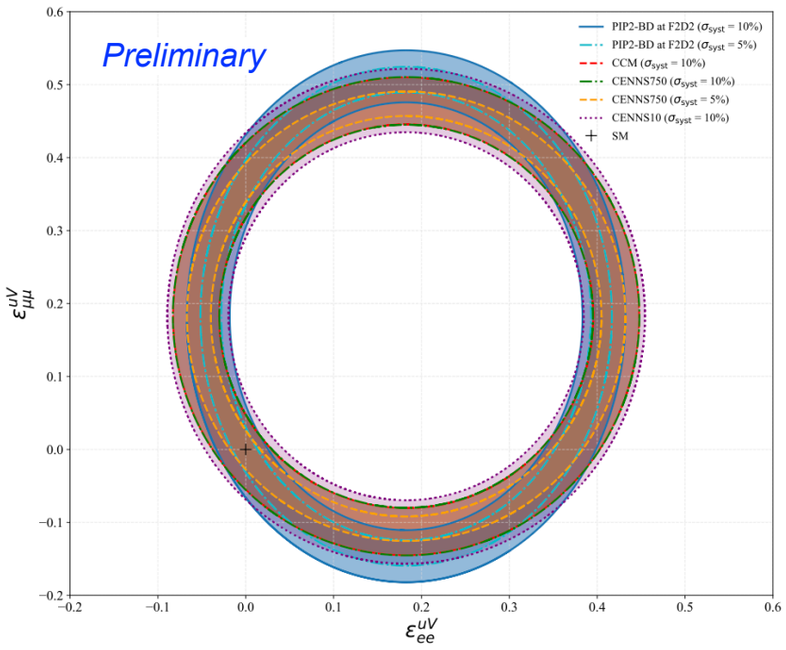

- Does this matter for the GeV scale neutrino program?

10s of MeV Physics in GeV-scale Neutrino Beams

- At forward scattering angles (low momentum transfer), the neutrino-nucleus cross section at GeV-scale energies is impacted by the same nuclear physics effects that are important for the low-energy case more generally.

BNB peak energy ≈ DUNE second oscillation maxima

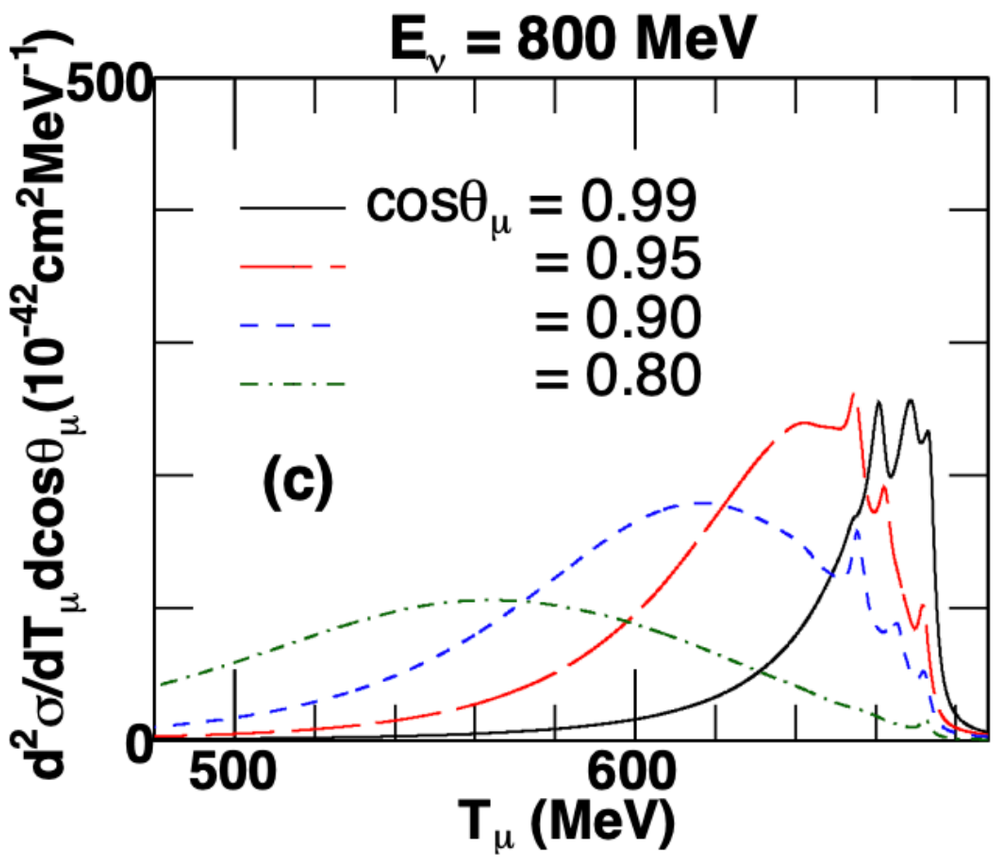

VP, N. Jachowicz, T. Van Cuyck, J. Ryckebusch, M. Martini, Phys. Rev. C92, 024606 (2015)

Folded with BNB ν_μ flux

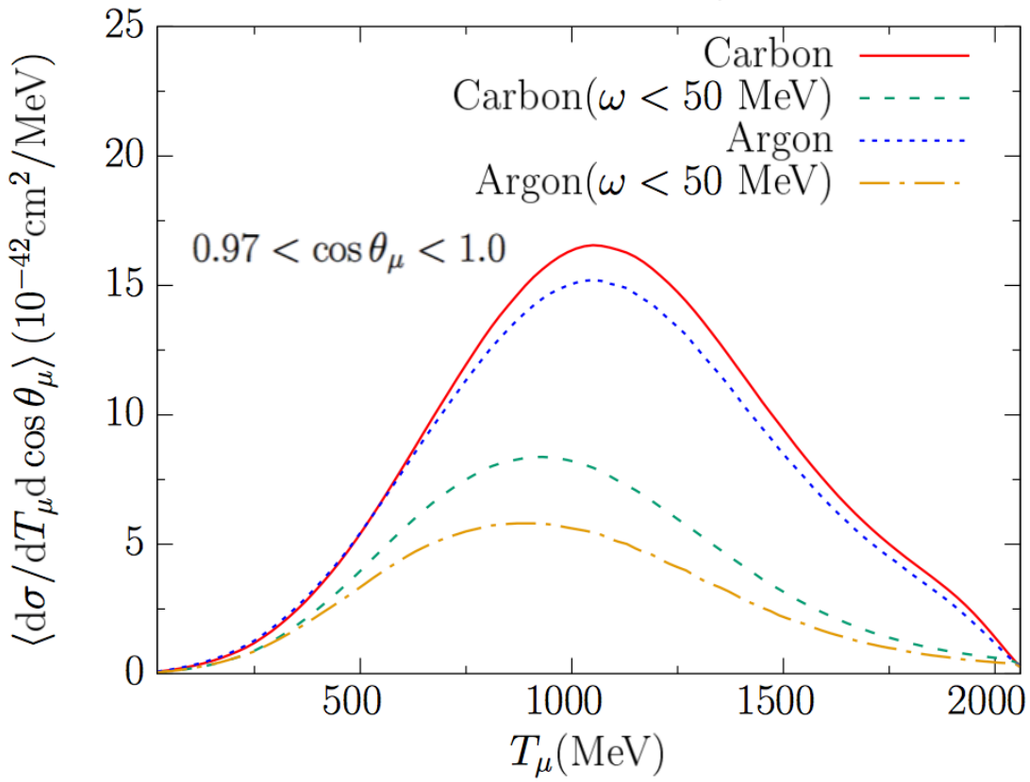

N. Van Dessel, N. Jachowicz, R. González-Jiménez, VP, T. Van Cuyck, Phys. Rev. C97, 044616 (2018).

10s of MeV Physics: Effect on ν_e to ν_μ cross-sections

- At low energy, the ν_e to ν_μ cross-section ratio depends on the details of the nuclear physics.

- Final-state lepton mass impacts the transferred (ω, q) and therefore the nuclear response.

- The muon mass in the final state leads to a larger momentum transfer which shifts the response to larger values.

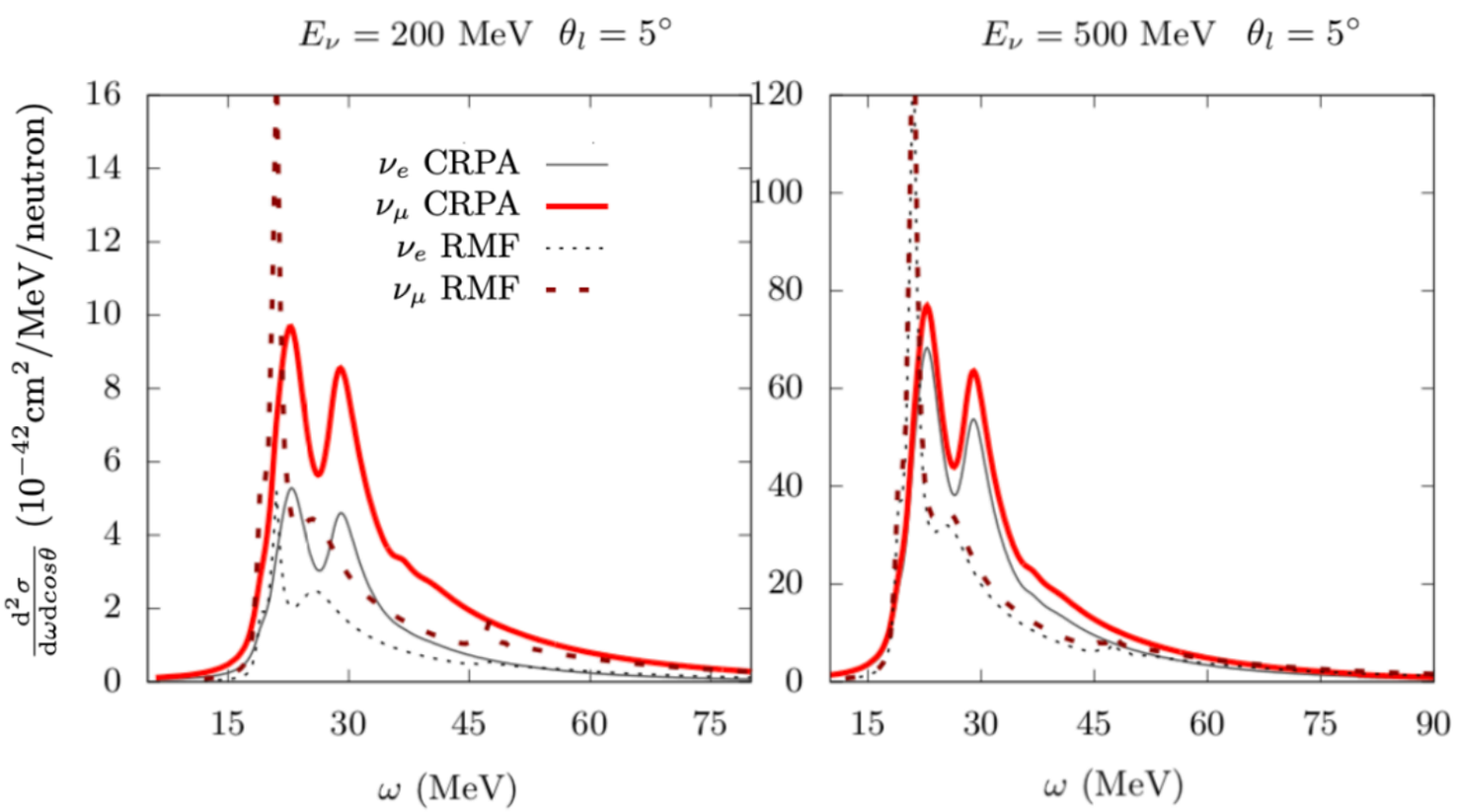

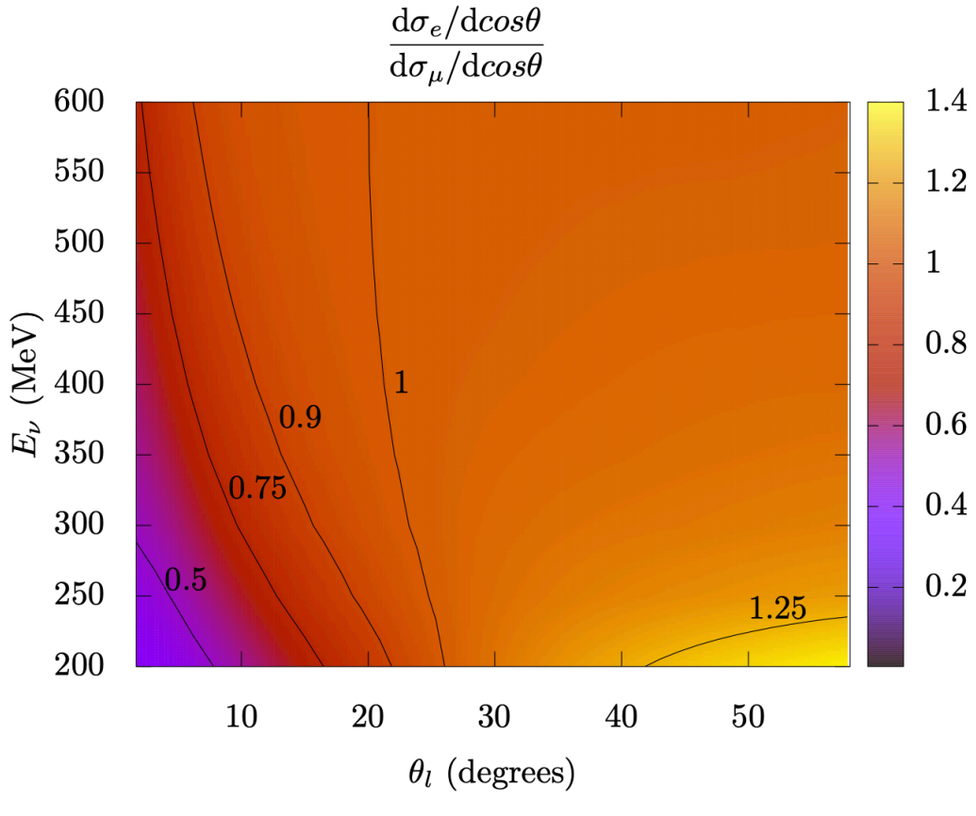

A. Nikolakopoulos, N. Jachowicz, N. Van Dessel, K. Niewczas, R. González-Jiménez, J. M. Udías, V. Pandey, Phys. Rev. Lett. 123, 052501 (2019).

10s of MeV Physics: Effect on ν_e to ν_μ cross-sections

- At low energy, the ν_e to ν_μ cross-section ratio depends on the details of the nuclear physics.

- Final-state lepton mass impacts the transferred (ω, q) and therefore the nuclear response.

- The muon mass in the final state leads to a larger momentum transfer which shifts the response to larger values.

- Exploring this with SBND-PRISM

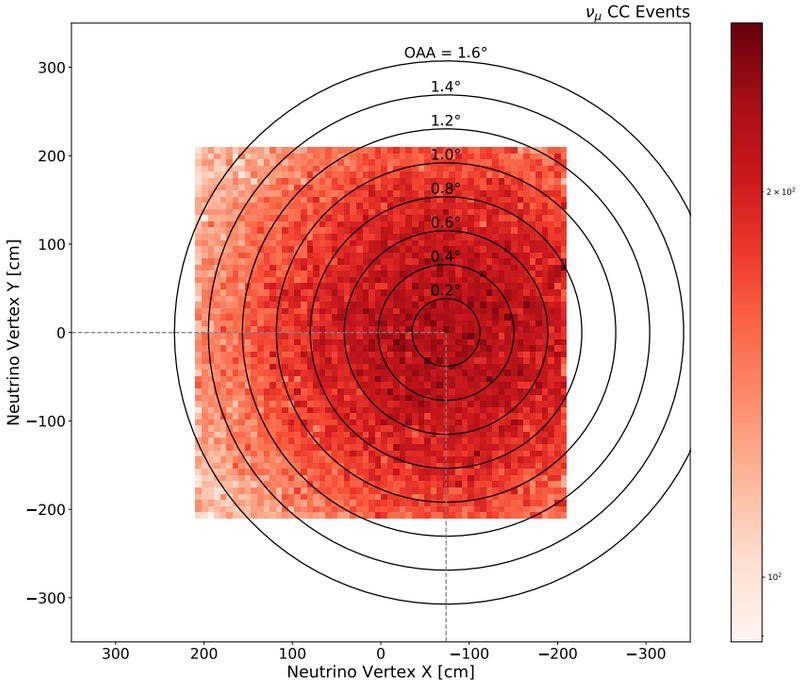

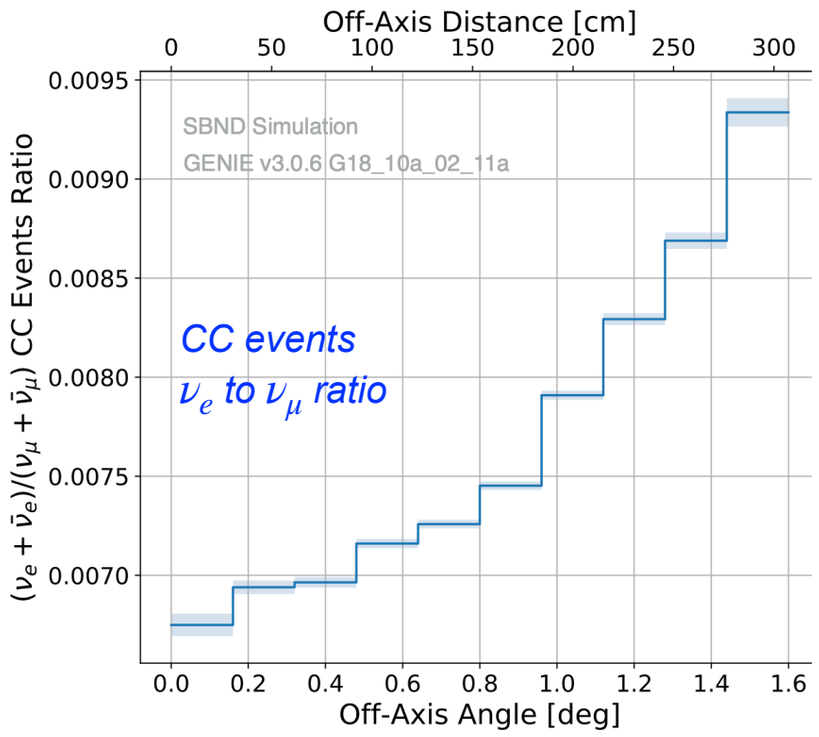

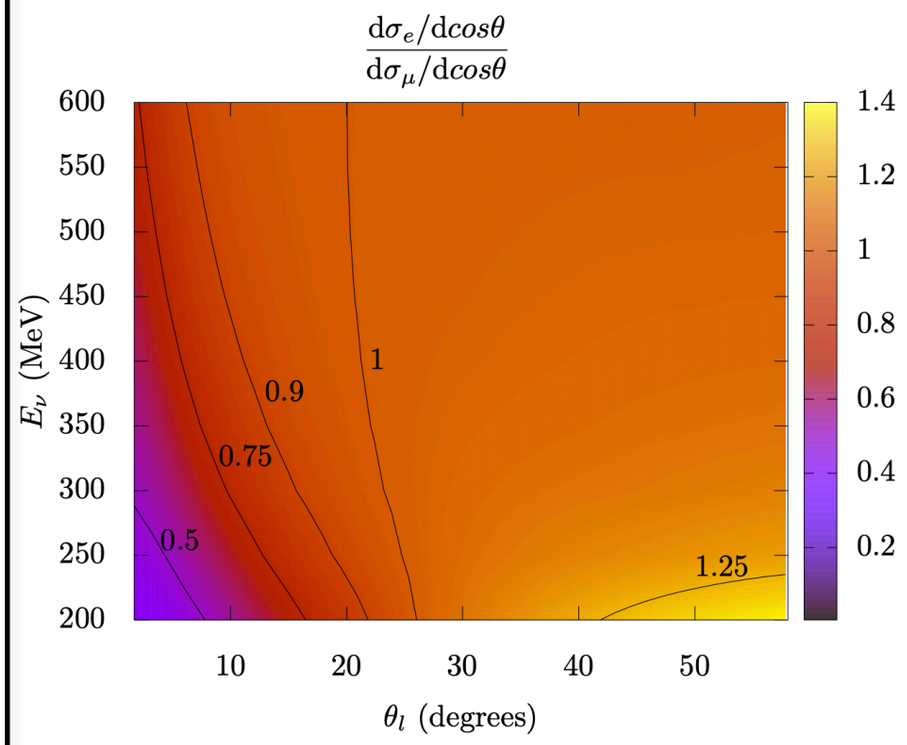

Phys. Rev. Lett. 123, 052501 (2019)

10s of MeV Physics in GeV-scale Neutrino Beams: KDAR Neutrinos

- Mono-energetic KDAR neutrinos at NuMI beam dump (FNAL) and at MLF (JPARC).

$$K^+ \rightarrow \mu^+ \nu_\mu, E_{\nu_\mu} = 236\ MeV$$

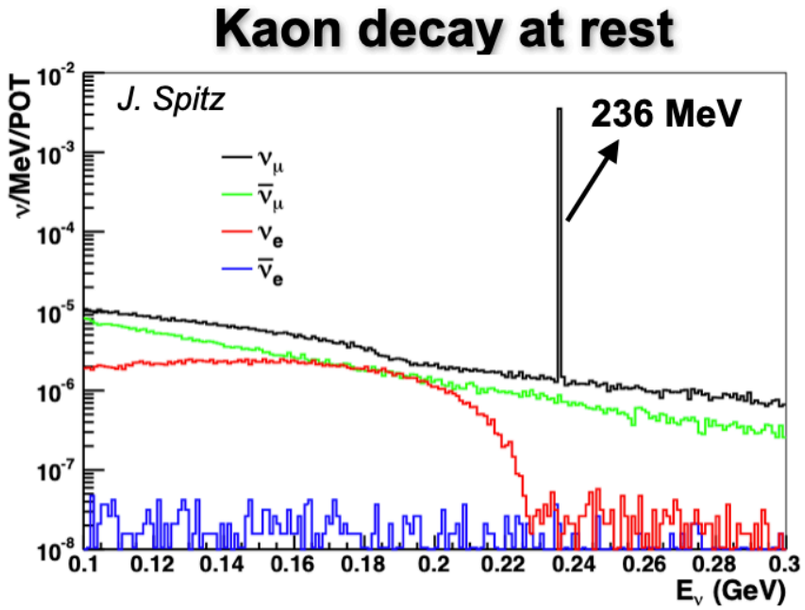

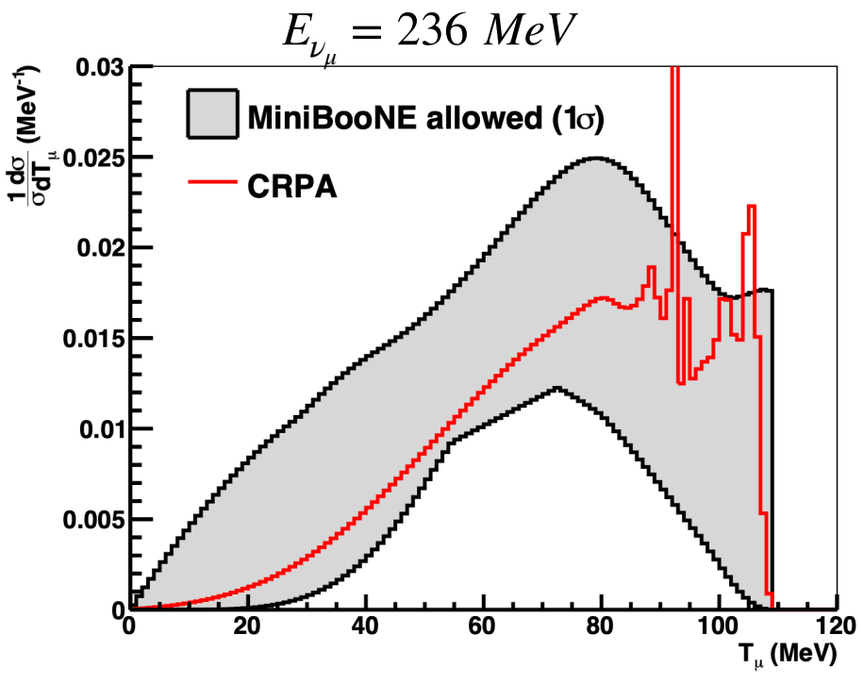

MiniBooNE data: Phys. Rev. Lett. 120, 141802 (2018)

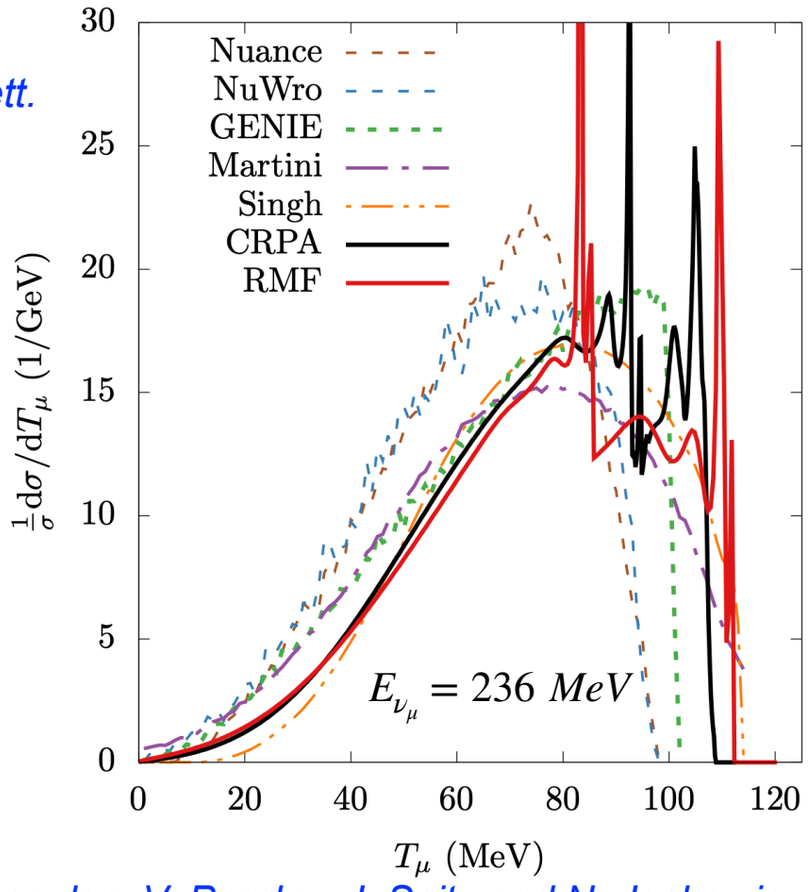

A. Nikolakopoulos, V. Pandey, J. Spitz and N. Jachowicz, Phys. Rev. C 103, 064603 (2021)

10s of MeV Physics in GeV-scale Neutrino Beams: KDAR Neutrinos

- Mono-energetic KDAR neutrinos at NuMI beam dump (FNAL) and at MLF (JPARC).

$$K^+ \rightarrow \mu^+ \nu_\mu,\ E_{\nu_\mu} = 236\ MeV$$

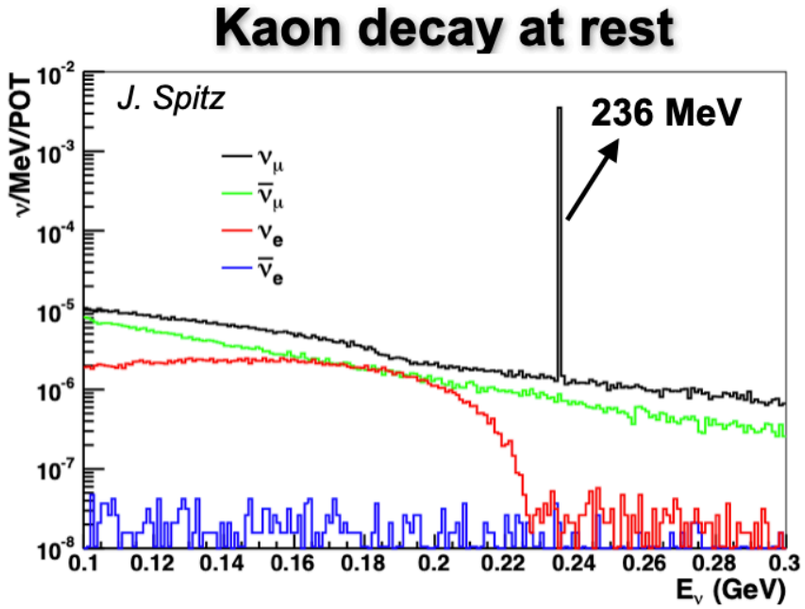

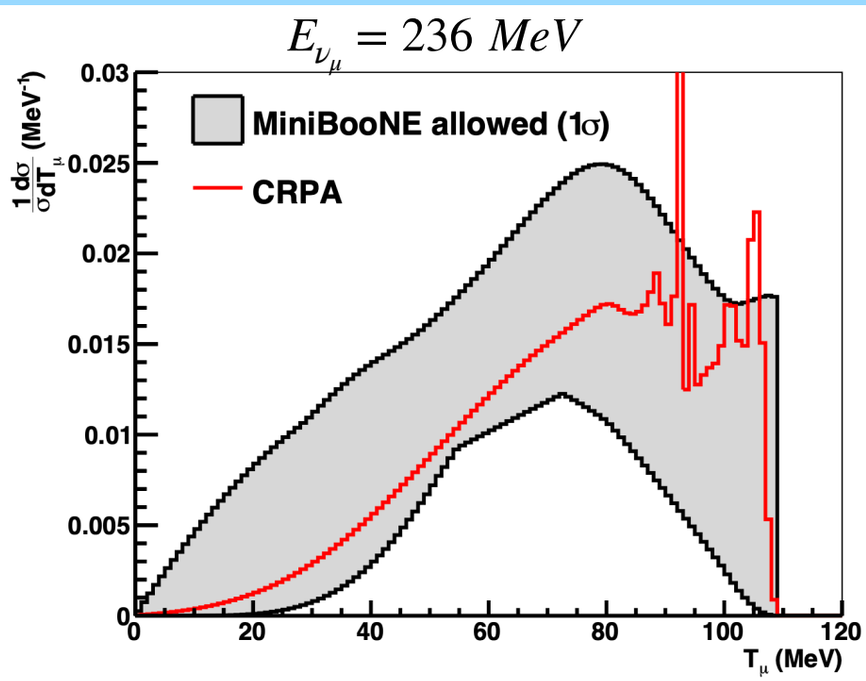

MiniBooNE data: Phys. Rev. Lett. 120, 141802 (2018)

- New Measurement from JSNS^2 at JPARC.

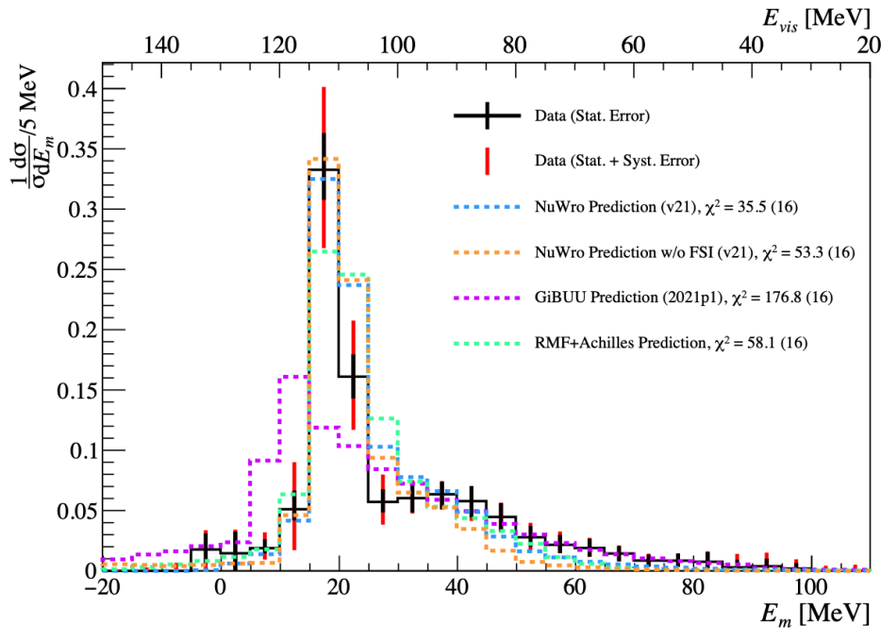

FIG. 4. The KDAR ν_μ CC missing energy, E_m, shape-only differential cross section measurement compared to several neutrino event generator/model predictions. The top x-axis provides the corresponding E_{vis} for each E_m value.

JSNS^2 Collaboration: arXiv:2409.01383 [hep-ex]

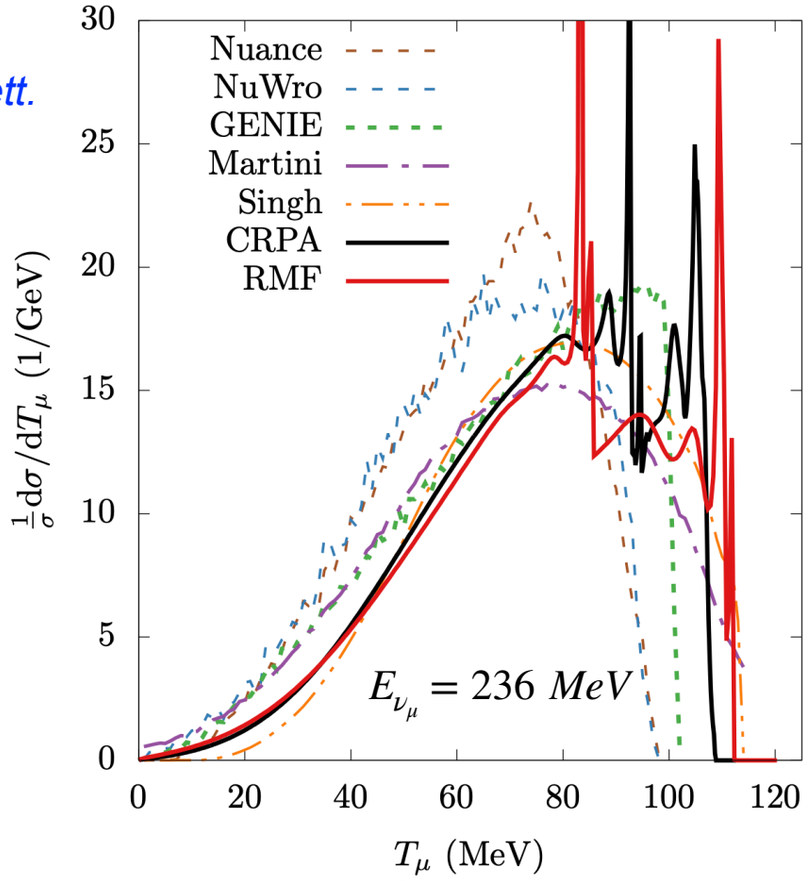

A. Nikolakopoulos, V. Pandey, J. Spitz and N. Jachowicz, Phys. Rev. C 103, 064603 (2021)

Summary

- Interactions of low energy (10s of MeV) neutrinos with the nucleus - elastic (CEvNS) and inelastic - are interesting for studies of various nuclear, neutrino, BSM and astrophysical processes.

- Neutrino-nucleus interactions at these energies are sensitive to neutron radius and weak elastic form factor (CEvNS), and underlying nuclear structure (inelastic).

- Microscopic calculations, future precise measurements of CEvNS cross section and PVES asymmetry measurements will enable precise determination of weak form factor and neutron distributions.

- CEvNS experiments at stopped-pion sources are powerful avenues to measure 10s of MeV inelastic CC and NC neutrino-nucleus cross sections. These measurements will play a vital role in enhancing DUNE's capability of detecting core-collapse supernovae neutrinos.

- Improved cross section estimates will help disentangle potential new physics signals from Standard Model expectations.